A Szilikátipari Tudományos Egyesület lapja

építőanyag

Journal of Silicate Based and Composite Materials

A TARTALOMBÓL:

2023/3

MESSE MÜNCHEN

ceramitec 2024
April 9-12

World's leading trade fair
for the ceramics industry

ceramitec

The meeting point for the ceramics industry
From producers and users to scientists – here, the leading exhibitors from around the world present their entire ceramic production range: machinery, devices, systems, processes, and raw materials. Every branch of the industry is represented, from classic ceramics through industrial ceramics to technical ceramics, powder metallurgy and 3D-printing, additive manufacturing.

The leading trade fair for the ceramics industry

Ceramitec is the meeting point for the ceramics industry. This is where new introductions are presented, information exchanged—and above all, where successful business is conducted.

International flavor

Ceramitec is where the whole world proverbially comes together. 63 percent of exhibitors and 58 percent of visitors come from abroad.

Presence of market leaders

The key players in the industry are always fully represented at ceramitec. They are aware of the value of presenting here—and of making contact with decision-makers.

Innovations

Ceramitec is a skills and technology center and an innovation forum, all in one. This is why ceramitec is always the trade fair for product launches, where all the new innovations are presented.

Innovations to meet market requirements

At ceramitec there are innovative products and applications for industry, research and science—ready for the market and waiting to be discovered.

Complete market overview/ wide range

The whole of the value chain for the ceramics industry is on display at ceramitec. All of the sectors and industries are represented. Every area is represented here at top level.

Top-class conference program gives an informational edge

The conference program always tackles industry-wide topics for the future, including new developments and knowledge. What's more, the presentations also cover special topics and interesting new markets.

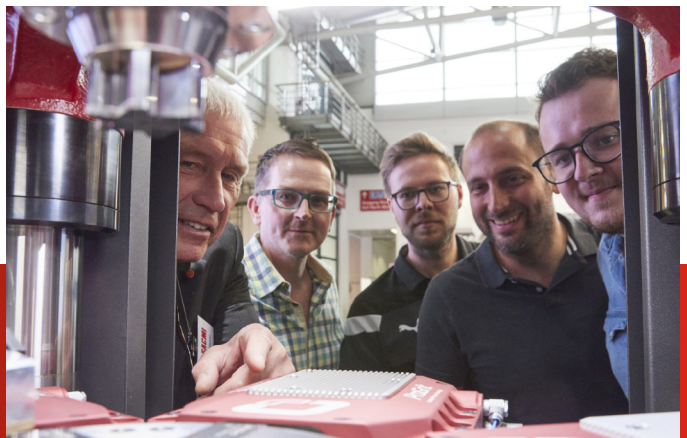

https://ceramitec.com/en/munich

építőanyag

Journal of Silicate Based and Composite Materials

2023/3

TARTALOM

CONTENT

A finomkerámia-, üveg-, cement-, mész-, beton-, tégla- és cserép-, kő- és kavics-, tűzállóanyag-, szigetelőanyag-iparágak szakmai lapja
Scientific journal of ceramics, glass, cement, concrete, clay products, stone and gravel, insulating and fireproof materials and composites

A folyóiratot referálja · The journal is referred by:
ProQuest · Google Scholar · INDEX COPERNICUS INTERNATIONAL · THOMSON REUTERS

A folyóiratban lektorált cikkek jelennek meg.
All published papers are peer-reviewed.
Kiadó · Publisher: Szilikátipari Tudományos Egyesület (SZTE)
Elnök · President: ASZTALOS István
1034 Budapest, Bécsi út 120.
Tel.: +36-1/201-9360 ▪ E-mail: epitoanyag@szte.org.hu
Tördelő szerkesztő · Layout editor: NÉMETH Hajnalka
Címlapfotó · Cover photo: SIMON Andrea

WWW.EPITOANYAG.ORG.HU
EN.EPITOANYAG.ORG.HU

Online ISSN: 2064-4477
Print ISSN: 0013-970x
INDEX: 2 52 50 ▪ 75 (2023) 81–127

Vol. 75, No. 3

Influence of aluminum-containing raw materials on the properties of radio-transparent materials

K. V. BILOHUBKINA ▪ National Technical University "Kharkiv Polytechnic Institute", Ukraine ▪ kari.rindel@gmail.com,
O. Yu. FEDORENKO ▪ National Technical University "Kharkiv Polytechnic Institute", Ukraine ▪ fedorenko_e@ukr.net,
G. V. LISACHUK ▪ National Technical University "Kharkiv Polytechnic Institute", Ukraine ▪ lisachuk @ kpi.kharkov,
R. V. KRYVOBOK ▪ National Technical University "Kharkiv Polytechnic Institute", Ukraine ▪ krivobok491@gmail.com
Artem ZAKHAROV ▪ National Technical University "Kharkiv Polytechnic Institute", Ukraine

Érkezett: 2022. 07. 04. ▪ Received: 04. 07. 2022. ▪ https://doi.org/10.14382/epitoanyag-jsbcm.2023.12

Abstract
The influence of alumina-containing raw materials on the properties and structure of radio-transparent materials (RPM) has been studied. A positive effect of metallurgical and micronized aluminum oxides on physical and technical properties was revealed, namely a significant decrease in the number of closed pores due to an increase in the number of small willemite crystals.
Keywords: celsian, willemite, radio-transparent ceramics, aluminum hydroxide, alumina, dielectric characteristics, pores
Kulcsszavak: celsian, willemite, rádiótranszparens kerámia, alumínium-hidroxid, alumínium-oxid, dielektromos jellemzők, pórusok

Karyna BILOHUBKINA
Ph.D. student, NTU "KhPI", Department of technology of ceramics, refractories, glass and enamels. Specializes in the study of radiotransparent ceramic materials.

Olena FEDORENKO
Doctor of Sciences, full Professor NTU "KhPI". Fields of interests: chemical technology of functional ceramics and protective coatings.

George LISACHUK
Doctor of Sciences, full Professor. Specialist in material sciences of resource saving and energy-saving technologies, new structural ceramic materials and coatings. Head of Research department of NTU "KhPI".

Ruslan KRYVOBOK
Ph.D, Senior researcher. Specialist in material sciences of new special-purpose ceramic materials and coatings. Deputy Head of Scientific and Research Part NTU "KhPI".

Artem ZAKHAROV
Ph.D, Deputy Head of Scientific and Research Part NTU "KhPI". Fields of interests: development and physico-chemical properties of radiotransparent ceramic, functional materials.

1. Introduction

Radio-transparent ceramics are used as a strategically important material in aircraft and rocketry, due to the constant in a wide temperature range of operating frequencies and electrical characteristics, as well as strength, heat resistance and heat resistance.

Aircraft fairing materials support dynamic, vibrational and stationary loads: compression, bending and twisting, sudden changes in temperature (from air level to several hundred degrees per second), hypersonic flows, and in some cases high-intensity infrared, neutron, and other radiation. The structure can significantly affect the functional properties of RPM.

Among the requirements for the quality of raw materials for ceramic radio-transparent materials, the presence of impurities (chemical purity), dispersion and porosity should be highlighted. Therefore, it is necessary to study the effect of raw materials on the sintering temperature for the formation of a given phase composition and obtain the appropriate characteristics. No less promising areas of research are the study of the impact of alumina raw materials of different nature on the phase composition, sintering characteristics and functional properties of radiopaque ceramics.

2. Analysis of literature data and problem statement

In connection with the high requirements for ready-made radio-transparent materials for aircraft and a wide range of their uses, it is important to control structural features, in particular, porosity. Because strength, moisture absorption, and dielectric constant depend on the porosity index.

Minimizing its residual porosity plays a crucial role in obtaining ceramics with high dielectric constant. High values of dielectric constant are observed even for coarse-grained ceramics (with grain sizes from 1.2 to 60 μm) provided that 99% of the theoretical density is reached. At the same time, when the density of ceramics is reduced to ~ 82%, the dielectric constant of samples with an average grain size of up to 1 μm decreases significantly [1].

Fine-grained ceramics has a number of features that are clearly manifested in the field of phase transitions. For example, as the size of the crystallites (areas of coherent scattering) decreases, the microdeformations increase, which can cause suppression of the ferroelectric properties. That is, the dielectric constant and grain size are ambiguous: it is possible that the dielectric properties are suppressed in the presence of small grains in the material. This is confirmed by a study that experimentally showed that the dielectric constant decreases with decreasing grain size [1].

The results of [2] indicate that the degree of porosity of ceramics directly affects the dielectric properties. With increasing porosity, the value of the dielectric constant decreases, while the nature of its frequency dependences does not change. Therefore, by controlling the porosity of the ceramic in the manufacturing process, it is possible to obtain samples with the required dielectric constant for a particular application. The appearance of porosity is significantly influenced by aluminum-containing raw materials and the peculiarities of its sintering.

3. The purpose and objectives of the study

The aim of this work is to determine the effect of the type of alumina-containing raw materials on the phase composition, structure, and properties of radiolucent ceramic materials of celsian-willemite composition, synthesized in the temperature range 1100-1200 °C.

The main task is to characterize the influence of different in structure, the degree of purity of alumina-containing materials on the properties of X-ray contrast material, the choice of optimal raw materials to obtain the desired structure of the source product.

4. Rationale for the choice of thinning additives for research

Improving the quality of technical ceramics is determined by solving the main problem of materials science: dispersion - composition - structure - property. The relationship of these parameters is the basis of modern technologies aimed at obtaining ceramic products with specified performance properties, which is of paramount importance in increasing the competitiveness of products.

The vast majority of industrial brands of domestic alumina are characterized by a predominant aggregate size of 30-40 μm in the presence of particles with a maximum size of up to 150 μm. Such materials cannot be used in the production of densely sintered ceramics without prior grinding (brand GK - alumina non-metallurgical) or without prior heat treatment (brand G-00 - metallurgical alumina) and subsequent fine grinding. Currently, leading foreign producers of alumina-containing raw materials (Alcoa Industrial Chemical, USA; Alcan Bauxite and Alumina Aluminum Pechiney, France; Almatis GmbH, Germany) offer a wide range of ready-to-use alumina, which differ in calcination temperature, content α-Al_2O_3 and impurities, the presence or absence of mineralizers, the degree of dispersion, the specific surface area, and others [3, 4].

In view of the above, it is of interest to study the effectiveness of the use of micronized alumina and aluminum hydroxide as alternative aluminum-containing materials.

5. Materials and methods

During the research, aluminum-containing materials were used to obtain celsian-willemite ceramics: alumina grade G-00, alumina ST3000SDP, aluminum hydroxide (Alcoa Industrial Chemical, USA; Alcan Bauxite and Alumina Aluminum Pechiney, France; Almatis GmbH, Germany).

The most widely used method for obtaining alumina is Bayer's method [5], which consists in obtaining a solution of sodium aluminate by the interaction of natural bauxite with a solution of sodium hydroxide. The resulting sodium aluminate solution is purified from impurities, and after appropriate treatment, pure aluminum hydroxide is isolated, from which alumina is obtained by calcination in rotary kilns at a temperature of 1150 - 1200 °C. As aluminum hydroxide is an intermediate in the production of alumina, it is the same raw material available in Ukraine as alumina and is produced by the same manufacturers.

Alumina ST3000 SDP is a new development of the company Alcoa Industrial Chemicals (now Almatis GmbH). It is made of alumina ST3000 SG (ground in a ball mill with the addition of 0.06 - 0.12 wt% MgO in a spray dryer), especially for parts with a polished surface, such as pump valves, pistons, shut-off valves for hot and cold water mixers, etc. The sintering temperature recommended by the manufacturer is 1600 °C.

According to petrographic analysis, aluminum hydroxide brand GD00 consists of colorless, transparent aggregates of spherulites, consisting of lamellar crystals. Aggregates are represented by hydrargillite, have a complex round, round-polygonal, rectangular shape. Unit size: maximum - 130 μm, single - up to 190 μm, which prevails 40 ÷ 80 μm [7].

Determination of the apparent density, water absorption and open porosity of the experimental samples was performed by hydrostatic weighing in water on samples of ceramic materials weighing from 50 to 80 g.

Samples in the form of tablets with a diameter of 20 mm and a height of 3 mm were used to determine the dielectric constant and the tangent of the dielectric loss angle. The measurements were performed on an automated device (Tangent-3M), designed to measure the characteristics of the dielectric loss in the range 0.0001 to 1 at a range of operating voltages between 0 and 270 V.

The phase composition of the test samples was determined using the method of X-ray phase analysis (X-ray diffraction) using a DRON-3M diffractometer with CuKβ radiation and a nickel filter under standard operating conditions. The American ASTM 1527 21 file was used to identify phases [6].

Studies of the morphology of the developed ceramic materials were performed by scanning electron microscopy on a microscope JSM-6390LV (Jeol, Japan) in the mode of secondary electrons. The study was subjected to chipping of materials, which allowed to assess the features of its structure more objectively (because the fault reveals defective areas of the sample).

Total shrinkage is determined by changes in linear dimensions after firing. Shrinkage is determined on tiles measuring 100×100×10 mm.

Hardness was tested using the Rockwell method. According to this method of hardness measurement, the depth of penetration into the test material of the diamond pyramid is found.

6. Results and discussion

Using the method of X-ray analysis, it was determined that the main contribution to the formation of micropores is made by aluminum hydroxide of a hydrargillite structure as a result of the removal of constitutional water and the rearrangement of the crystal lattice under the influence of heat treatment with the formation of porous fine-grained aggregates with a highly developed surface, consisting of single-crystal particles of corundum.

Thus, this study confirm the feasibility of using aluminum hydroxide to intensify the solid-phase synthesis of aluminosilicates, in particular $SrAl_2Si_2O_8$ $BaAl_2Si_2O_8$ and sintering ceramics, which are of considerable interest for the technology of ceramic RPM.

The paper investigates metallurgical alumina brand G-00, as well as alternative aluminum-containing raw materials (micronized alumina brand ST3000 SDP, and aluminum hydroxide brand GD-00), which are of interest in terms of intensification of structure and phase formation of ceramic RPM based on barium anornurite), and other aluminosilicates.

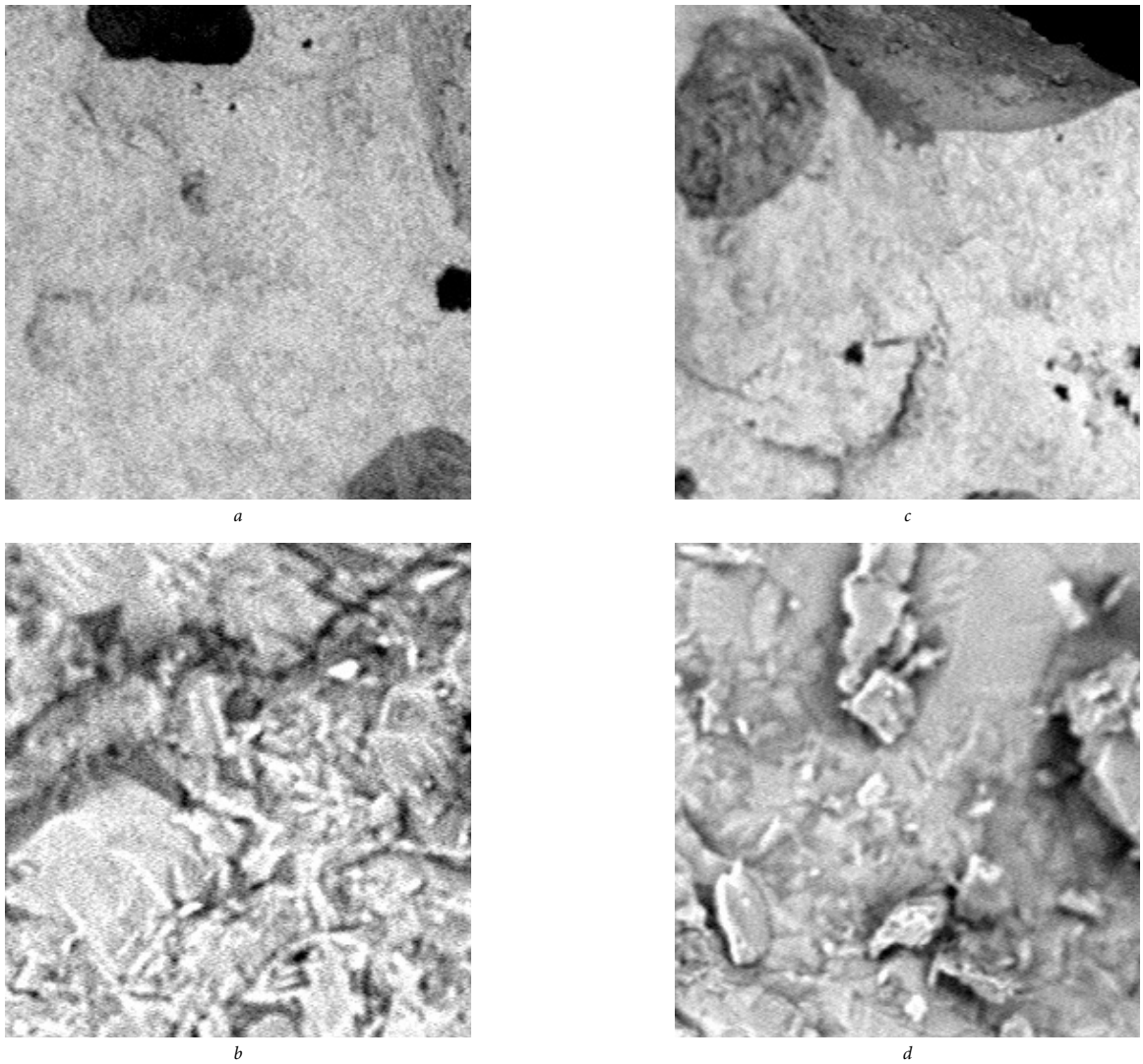

a *c*

b *d*

Fig. 1 SEM images of test samples with magnification of ×250 Sample I (a), Sample II (c), and magnification of ×2000 Sample I (b), Sample II (d)
1. ábra A próbatestek SEM felvételei 250-szeres nagyítással I. minta (a), II. minta (c), 2000-szeres nagyítással I. minta (b), II. minta (d)

Material	The content of components, wt. %		
	Sample I	Sample II	Sample III
Novoselivsky sand	30.05	30.10	28.66
Zinc whitewash	34.11	34.17	32.54
Barium carbonate	21.16	21.19	20.18
Alumina metallurgical G-00	14.67	-	-
Alumina micronized ST3000SDP	-	14.54	-
Aluminum hydroxide GD-00	-	-	18.62

Table 1 Batch composition of the samples
1. táblázat A minták összetétele

The data obtained as a result of differential thermal and petrographic analysis indicate the feasibility of using alternative aluminum-containing materials to intensify low-temperature synthesis of celsian.

The compositions of raw material mixtures (*Table 1)* are calculated, in which the aluminum-containing component is represented by different raw materials: metallurgical alumina G – 00 (I), micronized alumina CT3000SDP (II) and aluminum hydroxide GD – 00 (III).

Properties are shown in *Table 2*, all samples fully comply with the norms of dielectric properties for radiolucent ceramics (dielectric loss tangent $tg\delta$ = 10-2 ... 10-5, dielectric constant ε <10). Sample I has zero total porosity and water absorption, but has the highest total shrinkage (6.05%). According to the obtained data, it is expedient to use both G-00 metallurgical alumina and CT3000SDP micronized alumina for further research.

As can be seen from the microphotographs of *Figs. 1a, 1c* taken at a magnification of 250×, ceramic samples I and II, have a crystalline homogeneous structure without visible defects (cracks) and foreign inclusions. Both materials are characterized by the presence of closed pores, mostly spherical in shape. The pore size varies in a wide range: from 4 μm to 207 μm. The preferred pore size is ~25 μm.

Sample	Properties								
	General shrinkage L_{gen}, %	Imaginary density ρ, g/cm^3	Water absorption W, %	Total porosity *Pt*, %	Dielectric constant, ε	Tangent of the dielectric loss angle, tgδ	Rockwell hardness, HRA	Vickers Hardness, HV	Strength limit of compression σ_{ct}, MPa
I	6.05	2.99	0	0	2.85	0.0076	74	471	1520
II	2.35	2.99	0.18	0.54	3.11	0.0044	72	435	1405
III	5.83	2.88	0.6	1.74	2.46	0.0091	56	180	610

Table 2 Properties of samples fired 1200 °C
2. táblázat 1200 °C-on égetett minták tulajdonságai

The compared microphotographs indicate that the use of micronized alumina (sample II) can reduce the closed porosity of the material by reducing the pore size. Photographs of the microstructure of the samples at high magnification (× 2000) are more informative. The obtained data indicate that in comparison with sample I obtained using metallurgical alumina, the structure of sample II containing micronized alumina is fine-crystalline. In *Fig. 1b* and *1d*, it can be seen that the inner surface of the pores is covered with small crystalline neoplasms. The difference in the shape and size of the crystals is also noticeable. In both samples there are lamellar crystals with a size of 22.4×11.4 μm (for example, barium aluminate) and needle crystals of 15.75×0.55 μm (celsian). Finely divided willemite crystals up to 1.70×1.14 μm in size form clusters between larger crystals, which contributes to the compaction of the material.

The effect of different types of aluminum-containing raw materials on the main properties of radiotransparent ceramic materials based on the BaO - ZnO - Al_2O_3 - SiO_2 system was studied.

It is established that all samples obtained using the developed masses meet the requirements for RPM on electrophysical characteristics. Due to the maximum level of sintering at a firing temperature of 1200 °C (water absorption W = 0 - 0.5%, open porosity Pv = 0 - 1.74%) the received materials belonging to densely sintered ceramics are characterized by high indicators of durability and hardness.

Microscopic studies showed the presence of closed porosity. The positive effect of using CT3000SDP micronized alumina is noted by the reduction in the number of pores due to the increase in the number of small willemite crystals. In general, the work solves the problem of obtaining ceramic radiopaque materials and studying their properties depending on the phase composition and structure.

7. Conclusions

Raw material compositions containing different types of aluminum-containing raw materials were developed: metallurgical alumina brand G-00, micronized alumina brand ST3000 SDP and aluminum hydroxide brand GD-00.

It is established that the materials fired at a temperature of 1200 °C are characterized by the maximum level of sintering (W = 0-0.5%, P = 0-1.74%) and completely satisfy requirements to radio-transparent materials on electrophysical characteristics. ε = 2.08 - 3.85, $tg\delta$ = (0.0091-0.0755) · 10^{-2}. Samples of ceramics obtained using metallurgical alumina G – 00 predominate in terms of the level of physical and mechanical properties and σ_{st} = 1529 MPa).

The microstructure of the samples has a high density, but in the materials obtained in the laboratory there are closed pores, mostly spherical in shape with an average size of ~25 μm, the number of which decreases when using micronized alumina.

References

[1] Shalgunov S.I. Fiberglass for radio-transparent fairings and shelters / S.I. Shalgunov, A.H. Trofimov, VI Sokolov // Application of composite materials in civil and military aircraft construction: scientific. Conference. August 24, 2009: abstracts - Andreevka, 2009 ISBN: 5-03-003541-9

[2] Sarkisov P.D. The current state of issues in the field of technology and production of sitals based on aluminosilicate systems. Sklassov, l. A. Orlova, NV Popovich, NE Shcheglova, Yu. E. Lebedeva, DV Grashchenkov // All materials - 2011. - № 8. ISBN 0-916094-04-9.

[3] Stalemate. 6677261 USA, IPC7 C 04 B 35/10, C 04 B 35/195. Alumina-bound high strength ceramic honeycombs / Addiego William P., Magee Cecilia S. (USA); Applicant and Patent Owner of Corning Inc. - № 10/210674; declared 31.07.2002; publ. 13.01.2004 - 6 p.

[4] Application 19747387 EPV, IPC7 C 04 B 35/10, F 28 D 17/02. Alumina honeycomb structure, method for manufacture of the same, and heat-strong honeycomb structure using the same / Nippon Furnace Kogyuo K.K., Kasai Yoshiyuki, Harada Takashi, Umeha Kzuhiko, Mori Isao and oth. (USA); Applicant and patentee "NGK Insulators Ltd, NKK Corp." - № 01965581.0; declared 12.09.2001; publ. 09.07.2003 –10 c.

[5] Klimenko LP, Solovyov SM, Nord GL Technology Systems: A Textbook. - Mykolaiv: Moscow State University named after Petro Mohyla, 2007. 231-250p. ISBN 978-617-692-166-0

[6] American Society for Testing Materials: Diffraction Date Cards and Alphabetical and Grouped Numeral Index for X - Paradise Diffraction Date. - Philadelphia, 1997

[7] Kushchenko, K.I.,Corundum catalyst carrier for steam conversion of hydrocarbons: autoref. Dis... Cand. technical Sciences: 05.17.11 / K.I. Kushchenko; National Technical University "Kharkiv Polytechnic Institute". - Kh., 2009. - 20 p.

Ref.:
Bilohubkina, K. V. – **Fedorenko**, O. Yu. – **Lisachuk**, G. V. – **Kryvobok**, R. V., – **Zakharov**, A.V.: *Influence of aluminum-containing raw materials on the properties of radio-transparent materials*
Építőanyag – Journal of Silicate Based and Composite Materials, Vol. 75, No. 3 (2023), 84–87. p.
https://doi.org/10.14382/epitoanyag-jsbcm.2023.12

Performance of rubber bituminous asphalt mixes at hot and warm production temperatures

Kornél ALMÁSSY ▪ Budapest University of Technology and Economics
Domonkos KOCH ▪ Budapest University of Technology and Economics
Érkezett: 2023. 05. 30. ▪ Received: 30. 05. 2023. ▪ https://doi.org/10.14382/epitoanyag-jsbcm.2023.13

Abstract
In the production of asphalt mixtures, the possibility of recycling rubber grits has appeared for decades. A rubber bituminous mixture appearing as a special Hungarian patent greatly reduced the viscosity problems of rubber bitumen mixtures, resulting in a bitumen type that is easily transportable and does not require special equipment, The asphalt mechanical properties of the MOL rubber bituminous mixture are excellent both in the field of plastic deformation, cold behavior, and fatigue properties, so they are real competitors to polymer-modified bituminous mixtures. New research possibilities have emerged for use at reduced production temperatures, as a so-called WMA asphalt mix, in which case the first experimental – wheel tracking and cold behavior test - results are also encouraging.
Keywords: rubber grid, rubber bitumen mixture, WMA mixture, asphalt mixture performance
Kulcsszavak: gumiőrlemény, gumi bitumen keverék, WMA keverék, aszfaltkeverék teljesítmény

Kornél ALMÁSSY
Associate professor at the Department of Highway and Railway Engineering, Faculty of Civil Engineering, Budapest University of Technology and Economics. Director of Hungarian Museum of Architecture and Monument Protection Documentation Center. Field of interest: asphalt technology, road building and maintenance, transportation planning and monument protection.

Domonkos KOCH
Ph. D student at the Department of Highway and Railway Engineering, Faculty of Civil Engineering, Budapest University of Technology and Economics. Engineer of the Hungarian Concession Infrastructure Development Plc. Field of interest: asphalt technology, road building and maintenance, statistical analysis.

1. Introduction

The use of rubber bituminous binder, i.e., rubber-modified bitumen, has been present in asphalt production for decades. The purpose of rubber bitumen is twofold, since on the one hand it aims to recycle tire waste and, on the other hand, it seeks to use the beneficial properties of rubber during mixing with bitumen. However, its spread was not a complete breakthrough in the asphalt industry, which may be due to problems of production technology, quantity and quality. At the same time, rubber bitumen developed by the Hungarian Oil Industry Company (MOL) eliminated and reduced production technology problems to an acceptable extent, resulting in rubber-modified bitumen whose use in asphalt mixtures rivals the mechanical properties of polymer-modified bituminous asphalt mixes. Asphalt mixes made with domestic MOL rubber bitumen have appeared on the expressway network since last year, not only for wear layer installations, but also for bonding and base layer applications. Due to the increased energy costs, the application possibilities of asphalts made at reduced production temperatures have come to the fore again, accordingly, it is also possible to produce moderately warm asphalt mixtures in the production of rubber bituminous asphalt mixes. The purpose of publishing this article is to briefly summarize the most important asphalt mechanical experiences of mixtures made with rubber bitumen developed in Hungary and to discuss the production possibilities of moderately warm mixtures.

2. Production technologies of rubber bitumen

Advances in manufacturing technology have made it possible to recycle tyre materials (shredering). By refining grinding technologies, the tyre's main components could now be separated into rubber groats, steel and fabric. The technologies developed for the use of rubber powder are now widespread, in a very simple way the literature distinguishes between the so-called dry and wet process and their technologically modified versions. The addition of rubber granules and grits to asphalt mixtures appeared already in the 1950s and 60s in the USA and Sweden [2]. In addition to cold technologies (pressed glued rubber mats), experiments have been conducted since the 1960s to explore the application possibilities of warm technologies. MacDonald's experiments have already aimed to turn rubber-doped bitumen into rubber bitumen, i.e., to increase the rate of use from 3% to a minimum of 15% [3].

An engineer from Arizona thought it was worth mixing the rubber grist with bitumen and letting the two materials react with each other for about 1 hour, because in this case we get a new material with engineered advantageous properties. He named the material rubber asphalt, and the process is called the "water process" in scientific language.

In the dry process, rubber ground is added to the heated mineral additive, and only then mixed with bitumen during the preparation of asphalt. In this case, the rubber powder must be activated beforehand to achieve optimal particulate swelling. In the wet process, the rubber grist is first mixed with bitumen and then mixed with the stone frame. During the wet process, bitumen contains the aromatic douching oils necessary for the activation of rubber. Already early rubber bitumen studies showed that the grain size of the rubber groats, the mixing temperature and the duration of mixing are closely related to the properties of the final product [2]. The swelling and subsequent dissolution of crumb rubber can be demonstrated through rheological characteristics, e.g., the change in viscosity (*Fig. 1*) [3].

Due to its high viscosity, rubber bitumen produced by wet process requires a special asphalt recipe and asphalt production conditions, moreover, it requires a special mineral framework

for the manufacture of the mixture. Despite the difficulties, asphalts and built asphalt roads mixed with the use of rubber bitumen produced in this way resulted in significant quality and durability improvements compared to asphalts and roads manufactured with normal road construction bitumen [3].

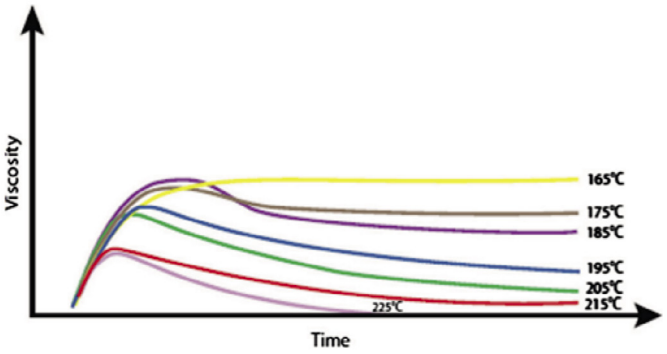

Fig. 1 Change of rubber bitumen viscosity as a function of blending temperature and duration
1. ábra A gumibitumen viszkozitásának változása a keverési hőmérséklet és idő függvényében

3. Modified wet process, or MOL technology

The joint research and development activities of MOL and the University of Pannonia in the field of rubber bitumens started in the early 2000s. The objective was to produce a rubber bitumen product that has the advantages of already known rubber bitumen products but eliminates or at least reduces to an acceptable extent the problems of their production and/or use, and it was also an important goal to make the new production technology feasible in the oil refinery. This will make it possible that the production of rubber bitumen does not require a special rubber-bitumen mixing plant at the site of asphalt production, and the product is transported, used in asphalt manufacturing and road construction similarly to polymer-modified bitumens. As a result of the successful research and development activity, a patent-protected technology and product (HU226481) was developed [4]. The technology described by the patent is the so-called "technology". Modified wet process and the manufactured product is chemically stabilized rubber bitumen [4]:

- In the first technological step of the modified wet process, the rubber grist is added to high-temperature bitumen (210-250 °C) and subjected to intensive stirring, resulting in swelling and partial dissolution of the rubber grit.
- In the next technological step, during mixing at a lower temperature (140-180 °C), the partially dissolved rubber powder is stabilized, and the split carbon-sulfur and sulphur-sulfur bonds are partially rebuilt (revulcanized).
- A multifunctional, self-developed and manufactured additive is also used in MOL, which improves the dissolution of rubber grits in bitumen and the compatibility of the rubber-bitumen system, and on the other hand, due to its viscosity reducing function, it also plays a significant role in improving the applicability of the product (pumpability at asphalt mixing stations, atomization, compressibility).

The complete dissolution of the rubber powder does not take place even during the modified wet process developed by MOL and the University of Pannonia, as complete dissolution would be at the expense of the quality of the manufactured product. 50-60% by weight of the rubber grist used dissolves, so a significantly higher proportion than in the previously applied wet rubber bitumen production technologies. Polymers that enter bitumen by the dissolution of rubber as active modifying agents improve the properties of bitumen. The undissolved rubber grains, swollen by the binding of the oily components of bitumen, partially retain their elastic properties. As a consequence, the fatigue and low-temperature properties of the binder improve, which also results in a significant improvement in the quality of asphalt [5].

4. Experience and tests of rubber bitumen installation in Hungary

Rubber bituminous test sections were already built in Hungary before 2010 on a test basis, and the first laboratory asphalt mechanical tests started during this period.

The opening of MOL's rubber bitumen manufacturing plant in Zalaegerszeg created a new opportunity for the production of rubber bitumen mixtures, and since 2012 rubber bituminous asphalt mixtures have been integrated into Hungarian road technical regulations. Between 2012 and 2021, more than 110 km of road sections made using rubber bituminous asphalt mixture were created or renovated in Hungary. On the affected road sections, they were typically built mostly in wear and bonding layers, but after 2018 the base layers were also built with rubber bitumen mixtures (RMB), and from this year these modern mixtures were also installed on some Hungarian expressways.

Budapest University of Technology and Economics' (BUTE) Department of Highway and Railway Engineering has been involved in the investigations of RMB almost since the beginning of the development. Tests have already been carried out on mixtures made according to the previous technical specification in 2009, with encouraging results. The asphalt mechanical properties (fatigue, resistance to deformation, etc.) of the RMB mixture have been shown to be superior to those made with conventional road construction bitumen; some of its characteristics were found to be close to, and sometimes even precede those of polymer-modified bitumen binder (PMB) asphalt mixes.

It is clear that rubber bitumen is not a competitor to conventional asphalt mix, but to polymer-modified bituminous mixture. It is becoming clear that the cold-side behavior and fatigue resistance are significantly better when comparing rubber bituminous mixtures with polymer-modified bituminous mixtures, in the case of plastic deformation – and so far, this has been confirmed by the small number of triaxial tests – there is no significant difference between the two mixtures, and the stiffness test results favor PMB mixtures.

The researchers of BUTE's Department of Highway and Railway Engineering compared the traditional, polymer-modified and rubber-bituminous asphalt track structures built with an unbound base structure using the dimensioning procedure of the road structure, and the results concluded that under the same load conditions, asphalt thicknesses up to 1.5 cm thinner than PMB mixtures may be sufficient to withstand loads [5].

Type of asphalt mechanical test	Normal asphalt mix	Polymer modified asphalt mix	Rubber bituminous asphalt mix
Wheel tracking test	+	++	++
Fatigue resistance test	+	++	+++
IT-CY stiffness test	+	+++	++
Cold behaviour test	+	++	+++
Note: The difference between the + signs represent the positions of the test results of each mixture relative to each other			

Fig. 2 Comparison of asphalt mechanical tests carried out over the last ten years for each type of mixture (+++: indicates best performance) [6]
2. ábra Az elmúlt tíz évben az egyes keveréktípusokon elvégzett aszfaltmechanikai vizsgálatok összehasonlítása (+++: a legjobb teljesítményt jelzi) [6]

5. Rubber bitumen as moderately warm asphalt

The production temperature of hot mix asphalt mixes (HMA) is between 160 °C and 180 °C. Various viscosity reduction processes can be used to produce „Warm Mix Asphalt" (WMA) between 100 °C and 150 °C and semi-warm asphalt mixtures between 60 °C and 100 °C [7]. The purpose of the high temperature is to temporarily reduce the viscosity of bitumen enough to coat the grains and be transported to the work area for installation. At the same time, the viscosity of bitumen can be reduced by various processes, foaming, or by adding chemical and organic substances.

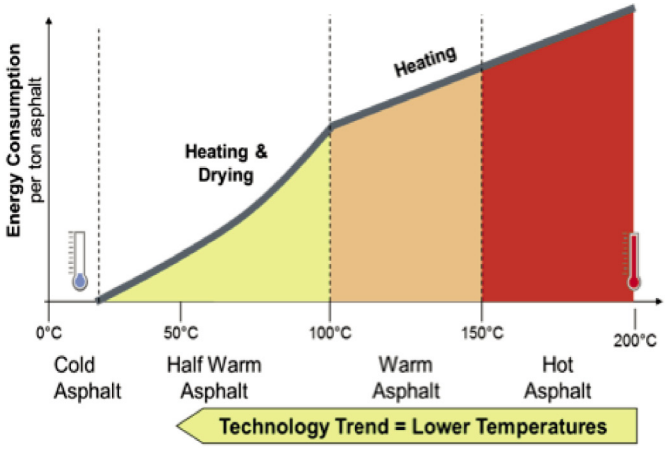

Fig. 3 Types of asphalt depending on production temperature: cold asphalt, half warm asphalt, warm asphalt, and hot asphalt [7]
3. ábra Az aszfalt típusai a gyártási hőmérséklettől függően: hideg aszfalt, félig meleg aszfalt, meleg aszfalt és forró aszfalt [7]

By reducing the viscosity of bitumen, WMA mixtures can be produced at temperatures up to 30-60 °C lower than conventional asphalt. Thus, by reducing the energy required for heating, direct fuel savings of up to 30-50% can be achieved, which can be easily and immediately realized during asphalt production. Another important aspect is that the coating of the aggregate frame with bitumen is not damaged and thus its compactability is not inferior to WMA asphalt compared to conventional asphalt mixes [8].

International research has also proven that by adding an additional organic or chemical additive, it is possible to create a mixture that meets the mechanical properties of the original rubber bituminous asphalt mix as WMA asphalt, since the modulus values of indirect tensile stress, wheel track formation resistance and elasticity practically did not differ in the case of the WMA mixture compared to the „normal" rubber bituminous mixture representing the reference mixture [9]. A Spanish study looked at how the WMA-RMB mixture performed. Four mixtures were tested, the control mixture was made with bitumen PMB 45-80-65 and the rubber bituminous mixture was made with 20% by weight of rubber powder added to bitumen 70/100. During the WMA process, a paraffinic organic substance (Sasobit) and a surface activating chemical additive (Zycotherm®®) were used. The mixture itself was BBTM 11A, produced at different temperatures. Based on the stiffness measurements carried out according to EN 12697-26, rubber bituminous mixtures performed better than polymeric mixtures at all test temperatures except chemical additive mixtures, with paraffin additive achieving best results. The wheel tracking test result of this mixture was practically identical to that of the PMB mixture [5, 10].

As a moderately warm asphalt mix, the rubber bituminous mixture developed by MOL was also tested in spring 2023. Two types of WMA additives were used mixed with RMB:

- GMB: wax (paraffin) type additive containing 2339-B/22 WMA additive-1, has a viscosity reducing effect at high temperatures, thereby reducing the temperature of asphalt mixing. However, when cooled to 50-70 °C, there is no softening effect, it brings about the quality parameters of the unadditive binder or asphalt, possibly it may have a stiffness/modulus increasing effect in the range of the road surface usage temperature.
- 2340-B/22: GMB containing WMA additive-2: surfactant, the mechanism of action of which is that bitumen wets the mineral more easily by reducing surface tension. As a result, at lower temperatures, rock wetting, that is, asphalt mixing, can be carried out.

In addition to the mixture with the two additives, two reference mixtures were prepared, a rubber bituminous AC 16 binding course (mF) (RMB 45/80-55 reference) and a polymer-modified AC 16 binding course (mF) (PMB 25/55-65 reference) mixture. The two reference mixtures were mixed according to MSZ EN 12697-35 and compacted at 170 °C, but the two WMA additive mixtures were mixed 20 °C lower.

Experiments were carried out to determine wheel traces (MSZ EN 12697-22 /9.3.2.) and cold behaviour, i.e., cracking temperatures, on the above-mentioned mixtures. Based on the results, it can be clearly seen that the surface-active additive

rubber bituminous mixture mixed at a temperature lower than 20 °C gave the same results in terms of plastic deformation resistance as the reference PMB and RMB mixtures (*Fig. 4*).

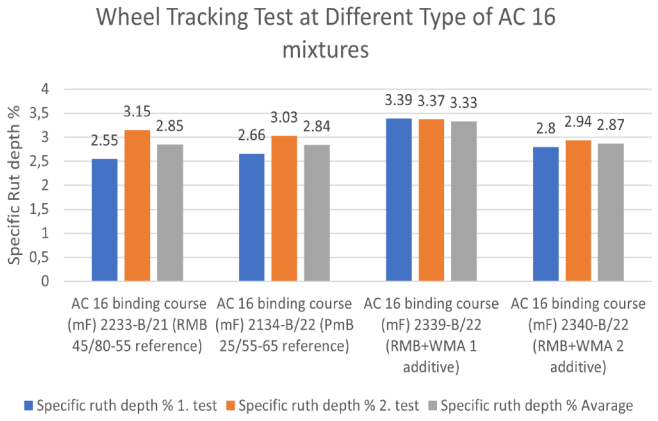

Fig. 4 Wheel tracking properties of rubber bituminous and "conventional" mixtures with WMA additive
4. ábra Gumi bitumenes és "hagyományos" keverékek keréknyomképződési tulajdonságai WMA adalékanyaggal

In terms of cracking temperature, the same mixture prepared with an active surface additive exceeded the cracking temperature result of the PMB reference mixture and yielded the level of the reference RMB mixture (*Fig. 5*).

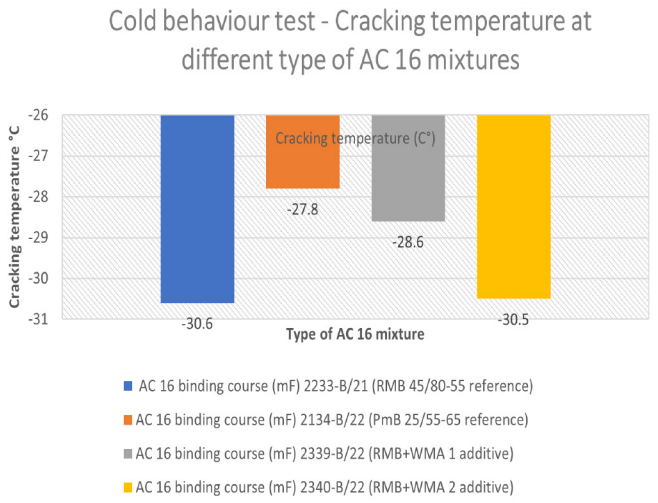

Fig. 5 Cracking temperature of rubber bituminous and "conventional" mixtures with WMA additive (Cold behavior)
5. ábra Gumi bitumenes és "hagyományos" keverékek repedési hőmérséklete WMA adalékkal (hideg viselkedés)

6. Conclusion

The use of rubber bitumens has been present in road construction for almost 50 years. Despite the beneficial properties, the application of the material could not spread to the desired extent, mainly due to manufacturing technology problems. MOL's chemically stabilized rubber bitumen product has successfully eliminated these technological problems of production and transportation and has created a favorable material that can be successfully used as a binder for any asphalt mix. In recent years, numerous asphalt mechanical tests have proven the application of domestically developed rubber bitumen, and rubber bituminous mixtures have finally appeared on the expressway network as well. In the current situation, in order to spread rubber bitumen domestically and internationally, it is necessary to examine how the scope of application of rubber bitumen can be extended.

Based on the test results presented above and international examples, it would be worthwhile to examine the possibility of using rubber bitumen in the case of WMA asphalts as well, and further studies should be carried out on the application of rubber bituminous mixtures in the binding and upper base layers regarding the overall track structure behavior.

References

[1] D. I. Hanson - K. Y. Foo - E. R. Brown -R. Denson: "Evaluation and characterization of a rubber-modified hot mix asphalt pavement," Transportation Research Record, no. 1436, pp. 98–107, 1994.
[2] Zanzotto, L. and G.J. Kennepohl (1996): Development of Rubber/Asphalt Binders by Depolymerization/Devulcanization of Scrap Tires in Asphalt, Transport Research Report 1530, TRB. pp. 51-58.
[3] D Lo Presti: Recycled Tyre Rubber Modified Bitumens for road asphalt mixtures: A literature review, Construction and Building Materials, 49, 863–881, 2013
[4] HU 226481, Bíró, Sz. – Bartha, L. – Deák, Gy. – Geiger, A.: Chemically stabilized asphalt rubber compositions and a mechanochemical method for preparing the same, 2009
[5] Gáspár L. - Tóth Cs. - Primusz P. - Almássy K. – Hunyadi D.- Szentpéteri I.: A hazai GmB kötőanyagú útpályaszerkezeti rétegek komplex viselkedési értékelése, KTI Közlekedéstudományi Intézet és BME Út és Vasútépítési Tanszék Vizsgálati Jelentés, 2019
[6] Almássy K. – Geiger A.: Gumibitumen alkalmazások a nagyvilágban - A MOL gumibitumen helyzete nemzetközi összehasonlításban, Az Aszfalt újság, XXVIII year 2020/2 vol pp. 33-39. , 7 p. (2020)
[7] https://eapa.org/warm-mix-asphalt/
[8] Tóth Cs.: LEA® – alacsony energiatartamú aszfaltkeverék, Útügyi Lapok, 2014. 2. évf. 3.szám.
[9] C. Akisetty: Evaluation of Warm Asphalt Additives on Performance Properties of CRM Binders and Mixtures, Civil Engineering. Clemson University, Clemson, USA (2008)
[10] Miguel Sol-Sánchez - Ana Jiménez del Barco Carrión - Ana Hidalgo-Arroyo - Fernando Moreno-Navarro - Leticia Saiz - María del Carmen Rubio-Gámez, Viability of producing sustainable asphalt mixtures with crumb rubber bitumen at reduced temperatures, Construction and Building Materials Volume 265, 30 December 2020

Ref.:
Almássy, Kornél – **Koch**, Domonkos: *Performance of rubber bituminous asphalt mixes at hot and warm production temperatures*
Építőanyag – Journal of Silicate Based and Composite Materials, Vol. 75, No. 3 (2023), 88–91. p.
https://doi.org/10.14382/epitoanyag-jsbcm.2023.13

Case study evaluation of selected binder course asphalt concrete used in road construction in Nigeria

Roland Kufre ETIM ▪ Department of Civil Engineering, Akwa Ibom State University, Ikot Akpaden, Nigeria ▪ rolandetm@aksu.edu.ng
Kenneth Edet ANDEM ▪ Department of Marine Engineering, Maritime Academy of Nigeria, Oron, Akwa Ibom State, Nigeria
Paul YOHANNA ▪ Department of Civil Engineering, University of Jos, Plateau State, Nigeria
David Ufot EKPO Department of Civil Engineering, Akwa Ibom State University, Ikot Akpaden, Nigeria
Ini-Obong Nnah STEPHEN ▪ Department of Civil Engineering, Akwa Ibom State University, Ikot Akpaden, Nigeria

Érkezett: 2023. 05. 30. ▪ Received: 30. 05. 2023. ▪ https://doi.org/10.14382/epitoanyag-jsbcm.2023.14

Abstract
This study evaluates asphalt concrete (binder course) being one of the components of flexible pavement to determine the quality grade of asphalt used in construction in line with the Nigeria General specification (NGS). Compacted binder course samples were collected from three selected asphalt plants in Akwa Ibom State and subjected to bitumen extraction, Marshall Stability and flow test. Characterization of materials was carried out in line with requisite standard and specification for binder course. Statistical data analysis tool (minitab and Microsoft excel 2013) was used to validate the relationship between bitumen content and other related variables. The results indicate that more than 95 % samples satisfied the requirement of Marshall Stability, flow and bitumen content, based on the NGS for roads. The results of multiple regression models and analysis of variance as well as the relationship between the experimental and predicted outcome of bitumen content indicate that stability and flow cannot be used in predicting the optimum bitumen content yields. Also, the relationship between bitumen content and other related Marshall variables show that these variables should be carefully monitored during Marshall Stability for optimum design. The scan electron microscopy results revealed voids in compacted specimen. This study has shown that microanalysis through SEM is significant and should be incorporated into pavement evaluations in addition to conventional material characterization and various physical and mechanical quality control tests.
Keywords: asphalt binder course, bitumen content, stability, flow, scan electron microscopy, statistical evaluations
Kulcsszavak: aszfalt kötőanyag réteg, bitumentartalom, stabilitás, folyás, pásztázó elektron-mikroszkópia, statisztikai kiértékelések

Roland K. ETIM
is a lecturer in the Department of Civil Engineering, Akwa Ibom State University, Ikot Akpaden, Nigeria. His research interest is in the field of Geotechnical and Geo-Environmental Engineering, Sustainable cleaner environment, Civil engineering materials and pavement condition survey/evaluation. He has published a number of scholarly articles in high impact Journals and conference proceedings. He is a registered Engineer with COREN and a Corporate Member of Nigeria Society of Engineers.

Kenneth E. ANDEM
is a Lecturer in the Department of Marine Engineering, Maritime Academy of Nigeria, Oron, Akwa Ibom State, Nigeria. He has done and published a number of scholarly articles in areas of Corrosion, Materials characterization, Materials Modification and General Corrosion of offshore concrete. He is a member of Materials Society of Nigeria (MMSN).

Paul YOHANNA
is a lecturer in the Department of Civil Engineering, University of Jos, Nigeria. He has done and published a number of scholarly research articles in areas of sustainable geotechnical and highway materials.

David U. EKPO
is a lecturer in Akwa Ibom State University. He is a registered Engineer with COREN and a corporate member of the Nigeria Society of Engineers. He has a Master's degree in Civil Engineering with specialization in Geotechnical and Geo-environmental Engineering. He has published scholarly articles in Geotechnical and Geo-environmental Engineering.

Ini-obong N. STEPHEN
is a Graduate Engineer of Civil Engineering, Akwa Ibom State University. She is currently undergoing a MSc. Degree programme in Civil Engineering (Geotechnical Engineering) at University of Uyo. She is a Member of Nigeria Society of Engineers.

1. Introduction

Road construction and infrastructure is one of the biggest capital investments of many countries world over. This is a critical sector which is generally known to automatically boost the economy of many countries. With the consistent public outcry in raising the infrastructural deficit in Nigeria, road construction is now in the exclusive list of government priority at all levels. Without a well-maintained road system, the transportation infrastructural needs of the public, businesses, industries and government cannot be met [1]. Road transportation provides vital links between spatially separated facilities which enables social contact and interaction between man and the environment [2]. However, premature failure and subsequent deteriorations of road pavement due to poor qualities of binder course amongst other factors have hampered the socio economic activities of many economies. Therefore, with regard to the paramount importance of road network in the economic development, safety and social cohesion of each country, it is important to continually assess the quality of materials that is used in road construction.

Asphaltic concrete is one of the vital materials in pavement construction. It is a composite material made up of aggregates, binder and filler materials which is commonly used in providing a stable surface area on highways of road surface, parking lots and runways of airport [3]. Asphalt plays a vital role in global transportation infrastructure and drives economic growth and social well-being in developed as well as developing countries [4]. An average asphalt pavement consists of the road structure above the formation level which include unbound and bituminous bond materials. This gives the pavement the ability to distribute the loads of traffic before it arrives at the formation level. About 95 % of roads in Nigeria are surfaced with asphalt concrete composite. Amongst other factors, bitumen content in this composite is one of the significant parameters that could affect the sustainability and durability of road sections. Binder course is one of the layers of pavement structure and its plays a very significant role in protecting the underlying layers (sub-base and subgrade) in the complete cross section of a road pavement structure. The quality of asphalt concrete

for binder course in road structure depends on the bitumen content amongst other material quality and factors which is key to the durability and sustainability of the underlying sub base and sub grade layers.

Asphaltic concrete mix design and their engineering properties form an essential part for all asphaltic concrete mixture. An asphaltic concrete is designed, produced and placed in order to obtain desirable properties which include; stability, durability, flexibility, fatigue resistance, skid resistance, impermeability and workability. In Akwa Ibom State, huge investments have and still being made by government on the construction of new roads and rehabilitation of existing ones [5]. However, most of these roads are considered unsafe for vehicular movement, extend travel time due to premature development of potholes, cracks and various signs of pavement distresses. This situation has called for investigation on road pavement materials used in construction of roads in Akwa Ibom State. This is with the aim of ensuring that road pavements are in serviceable condition within its design life. The durability of a cross section of a road pavement is a function of the sub-structure material (sub-grade and sub-base). The reliability of these materials either in its natural or modified form might not be unconnected with some of their engineering behavior in terms of plasticity, CBR and UCS [6-20, 35-43]. Several studies have been conducted on the qualities of materials used in pavement construction and general assessment of infrastructural quality in Akwa Ibom State. Ilori [21] reported the suitability of naturally occurring aggregates as sub base and subgrade construction materials in Akwa Ibom State and concluded that 85 % of the sample materials satisfied the AASTHO and US Army criteria upon particle size distribution, plasticity index, liquid limit and California Bearing Ratio value. Similarly, Osunkunle et al. [22] presented that asphaltic concrete produced in southwestern Nigeria conform to the specifications of the Federal Ministry of Works and that the quality and quantity of bitumen and aggregates used for production were satisfactory. They went further to revealed that despite the strict adherence to specification standard, roads were subjected to severe pressure as a result of increased vehicular traffic which contribute to pavement failures. In conclusion, they recommended that regular laboratory analysis must be conducted to ensure that asphalt concrete produced conform to the acceptable standards. Akinleye and Tijani [23] also carried out a study to assess the quality of asphalt concrete used in south west Nigeria. They reported that the comprehensive assessment revealed non conformity of asphalt concrete samples to the Federal Ministry of Works specification. They further concluded that the use of poorly graded mineral aggregates, poor and inadequate bitumen content resulted in the mixture having poor stability, flow and excess voids. A considerable amount of literature has been published on the utilization of asphalt as a road pavement material. However, it seems little attention has been paid to Akwa Ibom state, because of the limited published report.

Consequently, it is important to investigate the quality of asphaltic concrete used in the construction sector so as to appraise the situation of incessant failure of flexible pavement as reported [22, 23]. Whilst there are various ranges of test associated with various sections of a road pavement, this study will only consider the testing of materials for binder course section of a road pavement. Based on hands-on practical data established from some of the tests, far reaching results have been obtained in specific areas. However, some of these outcomes have not been made available to public domain for purpose of scientific validation from the various findings. Thus the need to report such investigations as case study situation for Akwa Ibom state becomes necessary as it would reflect the true quality of binder course asphalt used in road construction as well as contribute to the existing report. Also, morphological investigation through scanning electron microscopy further gives impetus to the outcome of this study thus closing the gap and shortfall in previous study reported for case of wearing course asphalt in same region [34].

Various modelling techniques are used in predicting different factors or variable in asphaltic concrete. Wang et al. [24] predicted the stress of asphalt concrete using multiple linear regression. Bala et al. [25] proposed a model which yields good predicted results for optimum binder content using stability and flow results obtained from Marshall Stability results. Kim and Kim [26] used the regression analysis to develop a performance prediction model. Also, prediction models developed from properties of asphalts material was realized from well-built investigational outcome using statistical regression method [27 - 29]. Baldo et al. [30] used artificial neural networks (ANN) and predicted the numerical-mechanical behaviour of asphalt concretes for road pavement. Also, the use of simple statistical applications has become necessary to validate or appraise laboratory data in civil engineering [6 - 20]. Therefore, the use of multilinear regression model would be essential to evaluate large laboratory results obtained from stability test of binder asphaltic concrete. In the light of the foregoing, this paper present an overview of the simple multiple regression application carried out for selected asphalts concrete production plants in Akwa Ibom state, as part of evaluations study on Marshall Stability investigation and material characterisation for the production of asphaltic concrete bound for binder course level.

Developing effective predictive equations for any reasonable variable that offers a major role in Marshall Stability investigation are fundamental to the outcome of optimum design of asphaltic concrete. Although lack of adequate data or sample size has made it almost impossible to use conventional statistical modelling tools/package such as simple regression Kajner et al. [31]. However, the use of large sample size obtained from eliminating inconsistent results due to laboratory errors addresses the lack of adequate data or sample size which has made its almost impossible to use conventional statistical modelling tools/package. The trust of this study is based on the fact that larger data mining from variables in Marshall stability investigation was obtained within a longer space of time and the out of range results which are inconsistent due to experimental error were rejected in this study. Although simple linear regression is an assured solution used in a number of studies to coherently permits clear decision and proffer solutions, this study seeks to test the adequacy, robustness and usability of simple multiple linear regression in determination of optimum binder content.

2. Materials and methods

2.1 Materials

The bitumen, aggregate and asphaltic concrete for binder course were sourced from major three asphalt plant in Akwa Ibom state, Nigeria. Although the batch of production were based on satisfactory established optimum design that meet the requirement of asphaltic concrete according to NGS [32] was adopted by each of the production plant. The characterization of bitumen and aggregate materials was done to ascertain that quality according to specification was maintained throughout the study.

2.2 Methods

Samples of materials used in asphaltic concrete production were collected from three different asphalt plants during production and on information that they are for binder course. Preliminary investigation on bitumen (penetration and softening points tests) and aggregates (fine and coarse) used in each asphalt production was carried out. Asphaltic concrete was collected from three asphalt plants labelled as A, B, and C and their corresponding samples of binder course was labelled as sample 1 to 12. Samples was analyzed for bitumen extraction, sieve analysis, Marshal Stability and flow according to related standards (*Table 1*).

Test	Standard
Bitumen	
Penetration test	AASHTO D T 49
Softening point	ASTM D36-95
Flash point	AASHTO D T-48
Aggregates/Asphalt Concrete	
Aggregates (Fine and coarse)	ASTM C127/C128
Specific gravity (bituminous mixture)	ASTM 2041
Los Angeles Abrasion test	ASTM C131/ EN 1097-8
Flakiness index	EN 933-3
Aggregate crushing value ACV	BS 812-114
Bitumen extraction	ASTM D2172
Marshall stability	ASTM D1669
Sieve analysis	ASTM C136

Table 1 Test and standard of testing used
1. táblázat Az alkalmazott vizsgálati szabvány

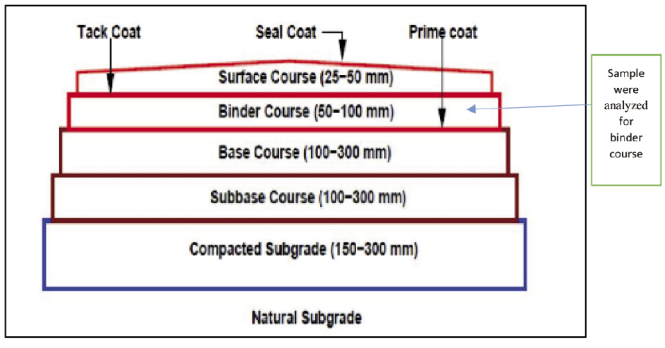

Fig. 1 Typical layers of conventional flexible pavement includes seal coat, surface or wearing course, tack coat, binder course, prime coat, base course, sub-base course, compacted subgrade, and natural subgrade
1. ábra A hagyományos rugalmas burkolat tipikus rétegei közé tartozik a tömítőréteg, a felület vagy a kopóréteg, a tapadóréteg, a kötőanyagréteg, az alapbevonat, az alapréteg, az aljzatréteg, a tömörített aljzat és a természetes aljzat

This test was carried out for twelve-month duration to span throughout a calendar year of both wet and dry weather conditions. The minimum of three samples of binder course asphalt were adopted. The result is collated and compared with general specifications for roads and bridges from Federal Ministry of Works and Housing to make necessary recommendations. Tests results (Marshall Stability) was confirmed for consistency based on specifications of NGS [32]. The various units of a flexible pavement of a road structure is shown by the cross section of *Fig. 1*. The bottom structure is the natural formation ground level also known as the natural subgrade while the top most layer is called the wearing course or surface course with seal coat followed by the second from top (binder course).

2.2.1 Formulation of regression model

The simple multiple study focused on the development of a model to predict the bitumen/binder content (optimum) in asphalt concrete for binder course pavements. The data used in the analysis were obtained from the laboratory study of several batches of asphaltic concrete production for the various selected companies. The guidelines of Agunwamba [33] were followed in formulation of regression models and with strict adherence to the principle of asphalt mix design. The bitumen content in an asphaltic concrete is usually an intricate component for optimum and satisfactory design of asphalt concrete. Bitumen content is therefore modelled for the selected asphalt plants denoted by A, B and C. Data used in this study were result of laboratory study obtained from several batches of asphalt production from the said plant. In this study, asphalt produced for binder course of a road pavement is assumed to meet Marshall Stability optimum mix design according to NGS [32] specification. Throughout the study, the condition of the laboratory was kept and sustained at room temperature. All other factors were assumed unchanged with regard to the study in consideration. The behaviours of bitumen content (optimum) in asphaltic concrete for the various asphalt plant were then modelled using the concept of multiple linear regression association with twelve data points. The twelve data point is a function of minimum of three average values that were observed to be very close to each other.

2.2.2 Bitumen content regression model

Independent variable (Y) identified as optimum bitumen content (B_{opt}) was achieved based on identified independent variables x_1 and x_2 as stability (S) and flow (F), respectively. The mode of compaction and other associated conditions of laboratory are kept constant. The general formula for multilinear regression is presented as:

$$Y = a + bx_{1(i)} + Cx_{2(i)} + \varepsilon \quad (1)$$

Where $Y = B_{opt}$; $x_{1(i)}$ =stability, S; $x_{2(i)}$ = flow, F;

a, b and c are constants called regression constants. i = 1, 2, 3,...n data points for asphalt plants A, B and C respectively. ε = zero random erratic error due to level of accuracy with which the laboratory investigation was achieved. *Eq. 1* is the linear form for selected three variables associated with the prerequisite needed for quality and sustainable pavement structure based on accumulated laboratory study. For the set of populated data points results and reducing the sum of least square results, the constant as well as coefficient of regression (a, b and c) are determined using Microsoft 2013 excel tools.

This implies that $B_{opt} = a + bF_{(i)} + cS_{(i)}$; i = 1,2,3,…,n (2)

Additional statistical tool was deployed to check the adequacy of the models. The experimented and predicted responses from linear model were paired and then subjected to ANOVA (single factor).

3. Results and discussion

3.1 Characterization of materials used

Characterization of materials used in this study is shown in *Table 2* for bitumen. The penetration test of bitumen at 25°C for the three samples clearly show that all samples had penetration above 60/70 penetration value allowable in FMW [32] general specification for road construction in tropical climate like Akwa Ibom State.

Test	A	B	C	Specified limit by NGS
Penetration test	60	62	64	60-70 at 25°C
Specific gravity	1.01	1.02	1.01	1.01-1.05 at 25°C
Softening point	50°C	49° C	48° C	48-50°C
Flash point	254	253	252	250 °C

Table 2 Characteristic properties of bitumen
2. táblázat A bitumen jellemző tulajdonságai

Aggregate properties	Asphalts concrete site			Specified limits NGS
	D	E	G	
Gs (Coarse aggregate)	2.68	2.68	2.68	-
Gs (fine aggregate)	2.64	2.67	2.67	-
Average % passing 75 um sieve	93	94	95	≥ 75 %
Los Angeles Abrasion test, %	16	17	21	≤ 25 %
Aggregate crushing value ACV, %	21	22	22.5	≤ 30 %
Flakiness index %	19	21	20	≤ 35 %

Table 3 Properties of aggregate used for asphalt production
3. táblázat Az aszfaltgyártáshoz használt adalékanyagok tulajdonságai

The test measures the hardness or consistency of bituminous material. The outcomes of this test confirms that the bitumen is soft which may be accredited to the existence of dilutants. During asphalt production, bitumen is heated to reduce it viscosity, hence the presence of dilutants will vaporize thus reducing the amount of bitumen content in the mixture and may subsequently leads to raveling which will result in premature failure of pavement. The result of softening point values for the three samples. The test is carried out to ascertain the temperature at which the bituminous materials attain a certain viscosity level. Bitumen softening point should be higher than the hottest day temperature of the study area otherwise bitumen may sufficiently soften and result in bleeding and development of ruts. In the study area, the average hottest temperature is about 26.7 °C and the softening point for all the three samples were above 48 °C. The conformity of the softening values with the standard specification indicate an asphalt concrete with increase resistance to permanent deformation (the standard). The ductility test of bitumen samples indicates a mean ductility value that is above 100 cm. The minimum recommended value specified by general specification for roads and bridges is 100 cm. It is important that bituminous material forms ductile film around the aggregates which serve as a binder. Bitumen without sufficient ductility, renders pervious pavement surface and leads to development of cracks. The properties of aggregates tested for the three selected sites as presented in *Table 3* indicate satisfactory limit as asphaltic road material specified in FMW general specification [32].

3.2 Sieve analysis

The gradation of the aggregate sizes for the three samples are obtainable in *Fig. 2*. However, for samples A, B and sample C obtained from the three asphalt plants show that the three specimens lie on a smooth curve within the envelope. Poor particle size distribution of aggregates utilized in asphalt mixture plays a major role in the stability and stiffness of the binder layer.

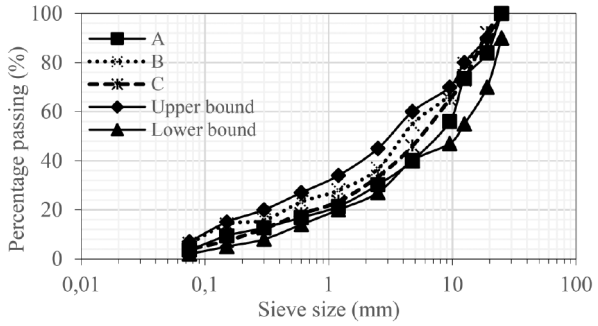

Fig. 2 Typical gradation of aggregates from binder course from site A, B and C
2. ábra Az A, B és C helyszínről származó kötőanyagból származó aggregátumok tipikus osztályozása

3.3 Asphalt concrete properties for binder course

The properties of asphalt concrete phase of binder course quality that meet the basic requirement and purpose for the region of study is controlled and tied to the relevant limit as per Nigeria general specification shown in *Table 4*. The results of the selected asphalt plants A, B and C are presented in *Table 5*. The results of each samples revealed the following engineering properties of asphalt; marshal stability (S), flow (F), bitumen content (BIT), voids in total mixture (VIM) and voids filled with bitumen (VFB). It is expected that asphalt concrete from the three asphalt plant can withstand traffic load without getting cracked. The results also suggest that failure in pavement structure which have been often said to be associated with the quality of asphaltic concrete may not be entirely accurate as it were. While the writer notes that quality of asphalt could be compromised for financial gains and inducement, poor material handling/ preparation etc., it is also relevant to note that failure in service could be due to poor and or inefficient compaction of sub grade and subbase structure, excessive wheel load greater than expected traffic design, poor drainage condition etc. This suggests why continued research into deficient soil improvement for subgrade and sub-base structure of road construction and hydraulic bound material are reported [13 – 20, 35-43] and are continuously given attention. The results in this study indicate that the bitumen content ranged from 4.50 to 5.40, 4.80 to 5.60 and 4.50 to 5.20 for asphalts A, B and C, respectively. Also, the stability and flow result were observed to be satisfactory and in line with the quality of asphalt specified in NGS [32] for binder course layer.

Properties	Standards as per NGS
Bitumen content, BIT (%)	4.5 - 6.5
Stability, S (kN)	≥3.5 KN
Flow, F (mm)	2 - 6
Voids in total mix, VIM (%)	3 -8
Voids filled with bitumen, VFB (%)	65 -72

Table 4 Standard of asphalt concrete of binder course
4. táblázat Kötőanyagréteg aszfaltbeton szabványa

Specimen (binder course)	BIT (%)	VIM (%)	VMA (%)	VFB (%)	S (kN)	F (mm)
A1	5.40	3.18	16.11	66.02	14.62	3.18
A2	5.40	3.24	16.18	65.68	14.49	3.24
A3	4.90	3.65	16.22	65.33	16.10	3.65
A4	5.00	3.41	16.37	65.11	15.24	3.41
A5	5.40	3.22	16.63	66.13	14.44	3.22
A6	4.70	3.82	16.33	64.95	17.79	3.82
A7	4.90	3.38	16.26	63.22	15.08	3.38
A8	4.50	3.80	15.84	65.45	18.38	3.80
A9	5.20	3.27	15.92	64.00	14.70	3.27
A10	4.80	3.36	16.03	62.27	15.37	3.36
A11	5.30	3.35	16.14	65.67	14.78	3.35
A12	4.60	4.05	16.44	66.19	18.08	4.05
B1	5.60	4.92	11.48	66.32	16.15	4.92
B2	5.80	4.57	11.48	66.83	15.62	4.57
B3	5.40	4.51	15.21	70.50	17.60	4.51
B4	5.50	4.11	16.15	70.17	15.43	4.11
B5	5.20	4.26	15.09	66.71	15.03	4.26
B6	4.90	4.62	16.22	65.78	14.86	4.62
B7	5.10	4.66	15.81	70.29	14.97	4.66
B8	4.90	4.52	15.51	65.23	14.81	4.52
B9	4.80	4.86	15.66	70.66	14.73	4.86
B10	5.30	4.07	15.77	66.82	15.24	4.07
B11	5.10	4.72	16.48	71.51	14.95	4.72
B12	5.30	4.14	16.60	69.67	15.24	4.14
C1	4.80	2.90	16.07	65.05	14.95	2.90
C2	5.10	3.10	16.41	67.47	15.24	3.10
C3	4.60	3.20	16.78	65.24	14.65	3.20
C4	4.70	2.70	16.33	63.99	14.76	2.70
C5	4.50	3.15	16.67	63.43	14.49	3.15
C6	5.00	3.18	16.26	66.04	15.43	3.18
C7	4.90	3.34	16.82	64.66	15.19	3.34
C8	5.20	3.52	16.22	65.32	15.51	3.52
C9	4.80	3.16	16.74	63.17	15.03	3.16
C10	5.20	2.95	16.07	67.95	15.43	2.95
C11	4.90	3.45	17.56	65.27	15.19	3.45
C12	4.80	3.51	16.82	62.63	14.97	3.51

BIT=Bitumen content in total weight of mix; VIM=Void in the mix; VMA=Void in total mix dry aggregate; VFB=Void filled with bitumen, S=stability, F=Flow

Table 5 Analysis of asphalt concrete (binder course)
5. táblázat Az aszfaltbeton elemzése (kötőszerkezet)

3.4 Morphological properties of binder course asphalt

The morphological structure of selected batch of binder course asphalt were studied using scan electron microscope. Test specimens for SEM was obtained from compacted asphalt. Scan electron images evaluated from selected specimen A1, A4 and A9 of production plant A show a clear morphology of aggregates with bitumen coated on all particle sizes (*Fig. 3a-c*). Similarly, morphology of selected specimen B1, B4 and B9 of production plant B revealed aggregates and other constituent material are well batched such that aggregates are uniformly coated in the bituminous mix that show a relative dense structure (*Fig 4a-c*).

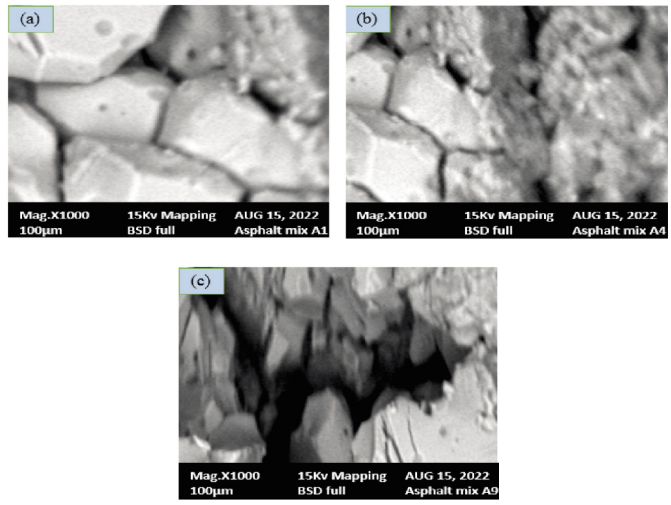

Fig. 3 Structural morphology of asphalt concrete collected from selected of asphalt plant A of: (a) A1, (b) A4 and (c) A9, batch productions
3. ábra Az A aszfaltüzemből gyűjtött aszfaltbeton szerkezeti morfológiája: a) A1, b) A4 és c) A9 gyártásnál

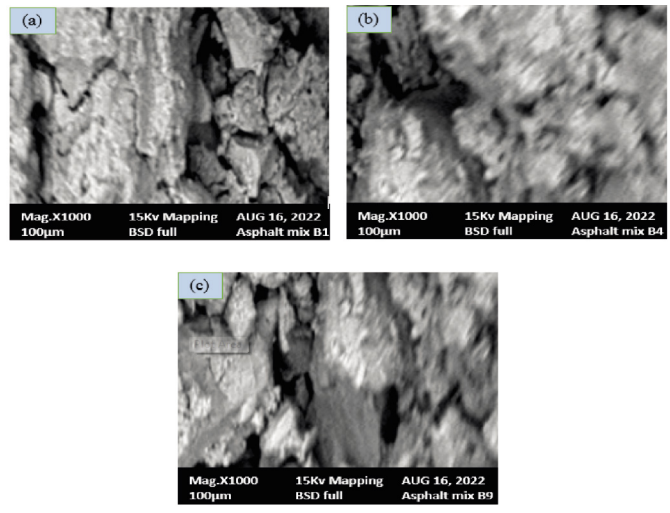

Fig. 4 Structural morphology of asphalt concrete collected from selected of asphalt plant B of: (a) B1, (b) B4 and (c) B9, batch productions
4. ábra A B aszfaltüzemből gyűjtött aszfaltbeton szerkezeti morfológiája: a) B1, b) B4 és c) B9 gyártásnál

Similar morphology is observed for selected specimen C1, C4 and C9 of production plant C (*Fig. 5a-c*). However, it is obvious that insignificant pore spaces were observed in all structures (A, B and C). This might not be unconnected with inadequate compaction of specimen. It can said that, the micrograph has

clearly exposed the inefficiency of poor/faulty mechanical roller used by contractors and or poor placement and compaction protocol of materials. This scenario if not checked can eventually led to moisture percolation and consequent failure of other layers and collapse of the entire pavement. This study has further shown that microanalysis through SEM of high resolution configuration and other microanalysis should be incorporated into pavement quality control in addition to conventional material characterization and sundry physical and mechanical quality control tests.

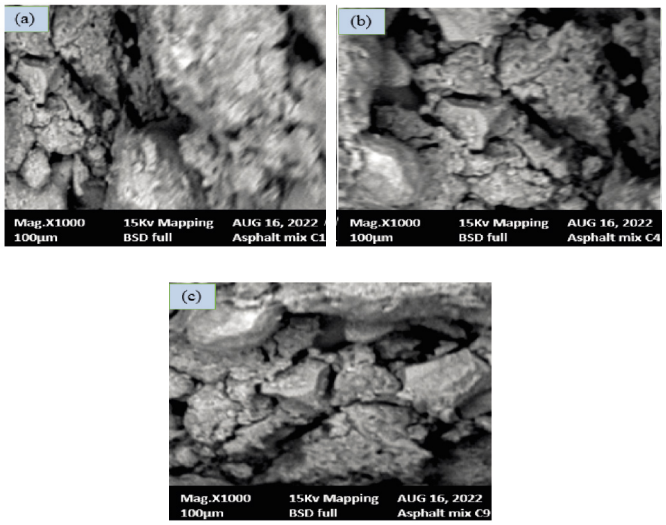

Fig. 5 Structural morphology of asphalt concrete collected from selected of asphalt plant C of: (a) C1, (b) C4 and (c) C9, batch productions
5. ábra A C aszfaltüzemből gyűjtött aszfaltbeton szerkezeti morfológiája: a) C1, b) C4 és c) C9 gyártásnál

3.5 Regression statistics

The results of simple multiple linear regression for optimum binder content (independent variable) on bitumen extraction test for binder and wearing course specimens from the three asphalts plants are shown in *Eq. 1* to *3*. The linear relation between the laboratory and predicted values did not show adequacy as R-squared were less than 0.95 (*Fig. 6*). Non-linear relationship could prove better although that is not considered in this study.

$$B_{opt.A} = 8.181 - 0.1723S_A - 0.1319F_A \quad (3)$$

$$B_{opt.B} = 2.941 + 0.2198S_B - 0.2405F_B \quad (4)$$

$$B_{opt.C} = -5.114 + 0.6829S_c - 0.0947F_c \quad (5)$$

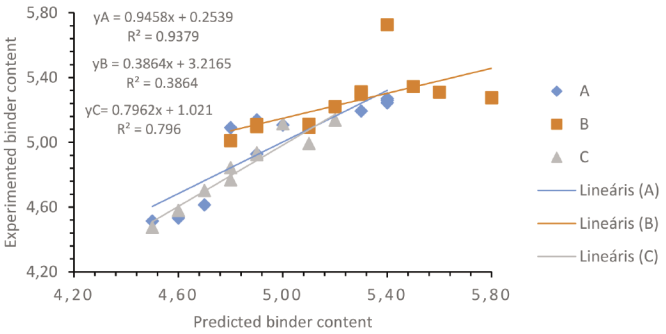

Fig. 6 Relationship between predicted and experimented binder content
6. ábra A várható és a kísérleti kötőanyag-tartalom közötti kapcsolat

Sample description	Y_{exp}	Y_{pred}	Abs. error	Percentage error
A1	5.40	5.24	0.0290	2.90
A2	5.40	5.26	0.0262	2.62
A3	4.90	4.93	0.0055	0.55
A4	5.00	5.11	0.0213	2.13
A5	5.40	5.27	0.0240	2.40
A6	4.70	4.61	0.0184	1.84
A7	4.90	5.14	0.0486	4.86
A8	4.50	4.51	0.0032	0.32
A9	5.20	5.22	0.0034	0.34
A10	4.80	5.09	0.0604	6.04
A11	5.30	5.19	0.0202	2.02
A12	4.60	4.53	0.0148	1.48
B1	5.60	5.31	0.0521	5.21
B2	5.80	5.27	0.0906	9.06
B3	5.40	5.73	0.0603	6.03
B4	5.50	5.34	0.0284	2.84
B5	5.20	5.22	0.0037	0.37
B6	4.90	5.10	0.0403	4.03
B7	5.10	5.11	0.0022	0.22
B8	4.90	5.11	0.0428	4.28
B9	4.80	5.01	0.0438	4.38
B10	5.30	5.31	0.0023	0.23
B11	5.10	5.09	0.0018	0.18
B12	5.30	5.30	0.0009	0.09
C1	4.60	4.58	0.0044	0.44
C2	5.10	4.99	0.0212	2.12
C3	4.60	4.58	0.0044	0.44
C4	4.70	4.70	0.0004	0.04
C5	4.50	4.48	0.0055	0.55
C6	5.00	5.11	0.0227	2.27
C7	4.90	4.93	0.0071	0.71
C8	5.20	5.14	0.0123	1.23
C9	4.80	4.84	0.0089	0.89
C10	5.20	5.14	0.0124	1.24
C11	4.90	4.92	0.0050	0.50
C12	4.80	4.77	0.0065	0.65

Table 6 Predicted and measured binder content values
6. táblázat A kötőanyag-tartalom előrejelzett értékei és mért értékei

The experimented results and predicted responses of optimum bitumen content shown in *Table 6* indicate that error ranged from 0.32 to 6.04, 0.09 to 9.06 and 0.04 to 2.12 for A, B and C, respectively. Further statistical tool is set up to check the adequacy of the models. The variables in experimented and predicted results are paired and then subjected to t-test (paired two sample for means) and ANOVA (single factor). Two conditions hypothesis namely; null and alternative hypothesis were used to interpret the t-test and single factor ANOVA. The null hypothesis states that there is no significant difference between the experimental results and predicted outcome of optimum binder content. Similarly, the alternative hypothesis is the reverse of the null hypothesis and of course implies that

there is a significant difference between the experimental test and predicted outcome of optimum binder content results, which does not reflect a good prediction tool

Anova: Single Factor						
Summary						
Groups	Count	Sum	Average	Variance		
Yexp	12	60.1	5.008333	0.106288		
Ypred.	12	60.10405	5.008671	0.084644		
ANOVA						
Source of Variation	SS	df	MS	F	P-value	F crit
Between Groups	6.83E-07	1	6.83E-07	7.16E-06	0.997889	4.301
Within Groups	2.100255	22	0.095466			
Total	2.100256	23				

Table 7 Analysis of variance: Single factor for A
7. táblázat Varianciaelemzés A esetén

Anova: Single Factor						
Summary						
Groups	Count	Sum	Average	Variance		
Yexp	12	62.9	5.241667	0.091742		
Ypred.	12	62.89899037	5.241583	0.035445		
ANOVA						
Source of Variation	SS	df	MS	F	P-value	F crit
Between Groups	4.25E-08	1	4.25E-08	6.68E-07	0.999355	4.30095
Within Groups	1.399062	22	0.063594			
Total	1.399062	23				

Table 8 Analysis of variance: Single factor for B
8. táblázat Varianciaelemzés B esetén

Anova: Single Factor						
Summary						
Groups	Count	Sum	Average	Variance		
Yexp	12	58.3	4.858333	0.055379		
Ypred.	12	58.18428	4.84869	0.052812		
ANOVA						
Source of Variation	SS	df	MS	F	P-value	F crit
Between Groups	0.000558	1	0.000558	0.010314	0.920026	4.30095
Within Groups	1.190102	22	0.054096			
Total	1.19066	23				

Table 9 Analysis of variance: Single factor for C
9. táblázat Varianciaelemzés C esetén

However, from the anova results on the experimental and predicted results of A (*Table 7*), if F cal > F crit, then the model is adequate and significat in prediction of dependent variable. Consequently, the result has shown that F cal = 7.16E-06 and F crit = 4.301 thus F crit > F cal. Which indicates that the difference between the observed results and the model outcome values was not significant and cannot be considered effiecient or effective. Hence the model can be said to be inadequate for use in predicting the binder content for an optimum asphalt design mixture. Similarly, the results of B1 to B12 and C1 to C12 (*Table 6*) and corroborated with ANOVA (*Table 8* and *9*) follow the same trend as inadequacy is achieved. The implication of this study lies in the fact that multiple linear regression model cannot be used in prediction of optimum binder content for binder course grade of asphalt.

3.6 Correlation statistics

The results of correlation statistics with their respective p-values are presented in *Table 10-15*. Correlation statistic results for binder and wearing courses for the respective asphalt plants considered in this study were analyzed based on significant variables that were obtained during Marshall Stability investigation. These variables are BIT, VIM, VMA, VFB, S, and F representing bitumen content in total weight of mix, void in the mix, and void in total mix dry aggregate, void filled with bitumen, stability and Flow, respectively. It was observed that that BIT for site A, B and C which were correlated with (VIM, VMA, VFB, S, and F) shows changing correlations. For A, high negative values correlations were observed between BIT and VIM (-0.863; $P < 0.05$); S (-0.892; $P < 0.05$); F (-0.863; $P < 0.05$) while low correlations were observed between BIT and VMA (0.152; $P>0.05$) and VFB (0.259; $P > 0.05$) (See *Table 10*). For site B, varying correlations were observed between BIT and VIM (-0.214; $P > 0.05$); VMA (-0.676; $P < 0.05$) VFB (0.067; $P>0.05$); S (0.557; $P>0.05$) and F (-0.214; $P>0.05$) (See *Table 11*). And lastly for C, the correlations of BIT and VIM (0.189; $P>0.05$); VMA (-0.353; $P>0.05$); VFB (0.699; $P < 0.05$); S (0.960; $P < 0.05$) and F (0.189; $P>0.05$) is presented in *Table 12*. Detailed P-values results are shown in *Tables 13, 14* and *15*. The outcome of this analysis shows VIM, S and F significantly influence the BIT of site A, VIM for site B and VFB and S for site C. Therefore, these variables must be strictly monitored so as to achieve the best optimum bitumen content for design of asphalt concrete.

	BIT	VIM	VMA	VFB	S	F
BIT	1					
VIM	-0.863	1				
VMA	0.152	0.091	1			
VFB	0.259	0.188	0.377	1		
S	-0.892	0.957	-0.067	0.152	1	
F	-0.863	1	0.091	0.188	0.957	1

Table 10 Pearson correlation matrix for bitumen content; site A
10. táblázat Pearson korrelációs mátrix a bitumentartalomra vonatkozóan; A

	BIT	VIM	VMA	VFB	S	F
BIT	1					
VIM	-0.214	1				
VMA	-0.676	-0.400	1			
VFB	-0.067	0.055	0.428	1		
S	0.577	0.028	-0.367	0.148	1	
F	-0.214	1	-0.400	0.055	0.028	1

Table 11 Pearson correlation matrix for bitumen content; site B
11. táblázat Pearson korrelációs mátrix a bitumentartalomra vonatkozóan; B

	BIT	VIM	VMA	VFB	S	F
BIT	1					
VIM	0.189	1				
VMA	-0.353	0.553	1			
VFB	0.699	-0.217	-0.385	1		
S	0.960	0.299	-0.243	0.596	1	
F	0.189	1	0.553	-0.217	0.299	1

Table 12 Pearson correlation matrix for bitumen content; site C
12. táblázat Pearson korrelációs mátrix a bitumentartalomra vonatkozóan; C

	BIT	VIM	VMA	VFB	S	F
BIT	0					
VIM	0.000	0				
VMA	0.636	0.779	0			
VFB	0.417	0.558	0.227	0		
S	0.000	0.000	0.835	0.637	0	
F	0.000	0.000	0.779	0.558	0.000	0

Table 13 P-values (Pearson) for bitumen content; site A
13. táblázat P-értékek (Pearson) a bitumentartalomra; A

	BIT	VIM	VMA	VFB	S	F
BIT	0					
VIM	0.505	0				
VMA	0.016	0.198	0			
VFB	0.835	0.866	0.165	0		
S	0.049	0.931	0.240	0.646	0	
F	0.505	0.000	0.198	0.866	0.931	0

Table 14 P-values (Pearson) for bitumen content; site B
14. táblázat P-értékek (Pearson) a bitumentartalomra; B

	BIT	VIM	VMA	VFB	S	F
BIT	0					
VIM	0.556	0				
VMA	0.260	0.062	0			
VFB	0.011	0.497	0.216	0		
S	0.000	0.346	0.446	0.041	0	
F	0.556	0.000	0.062	0.497	0.346	0

Table 15 P-values (Pearson) for bitumen content; site C
15. táblázat P-értékek (Pearson) a bitumentartalomra; C

4. Conclusions

The study on analysis of binder course asphalt grade used in pavement construction clearly revealed that asphalt concrete from all the asphalt plants met the requirements for bitumen content, stability and flow when compared to requirements of NGS for roads and bridges. The aggregates gradation obtained from the study asphalt locations are well graded and falls within the grading envelope. The results of bitumen penetration, softening point and ductility tests were all satisfactory. The stability and flow results were satisfactory and within the acceptable quality control boundary for acceptability in line with NGS. This study has shown that microanalysis through SEM can be incorporated into pavement evaluations in addition to conventional material characterization and various physical and mechanical quality control tests. Also, there should be strict supervision of laying temperature of asphalt as well as the compaction temperature. Asphalt compaction thickness must conform to design provision and asphalt pavement surface should be subjected to adequate drainage condition to avoid failure cause by ingress of moisture. The study has shown that stability and flow not efficient as independent variables in prediction of optimum bitumen content for binder course asphalt concrete. The study recommends that extensive data mining from several asphalt plants not covered in this study be carried out in future work and a general predicting model developed and validated using robust statistical tool and or smart optimization techniques. Regardless of the assuring solution of simple multiple linear regression in a number of studies which in most cases clearly permits strong decision, this study confirmed an hitherto establish conventional result in asphalt mix design principle that optimum bitumen content cannot be derived by multiple linear regression of independent mechanical properties of flow and stability.

References

[1] Tri B, Hisashi, K. Safety and security improvement in public transportation based on public perception in developing countries. IATSS Research. 2006; 30(1): 86-100.

[2] Adedotum SB, Ogundalunsi DS, Oyeniyi AS. Assessment of road transport infrastructure in Osogbo, Osun State. WIT Transactions on the Built Environment. 2016; 16(4): 61-72.

[3] Eme DB, Nwaobakata C. Effect of low density polyethylene as bitumen modifier on some properties of hot mix asphalt. Nigerian Journal of Technology. 2019; 3(8):1-7.

[4] Ivanova E, Masarova J. Importance of road infrastructure in the economic development and competitiveness. Economics and Management. 2013; 18(2): 4 – 34.

[5] Umoren V, Sule RO, Eni, DD. Assessment of some road infrastructural variables in Akwa Ibom State, Nigeria. Ethiopian Journal of Environmental Studies and Management. 2011; 4(2): 83 – 87.

[6] Osinubi KJ, Eberemu AO, Yohama P, Etim RK. Reliability estimate of compaction characteristics of iron ore tailings treated tropical black clay as road pavement sub-base material. In; American society of Civil Engineering, Geotechnical Special publication. 2016; NO. 271, 855-864. http://dx.doi.org/10.1061/9780784480144.085

[7] Sani JE, Yohanna P, Etim RK, Osinubi KJ, Eberemu AO. Reliability evaluation of optimum moisture content of tropical black clay treated with locust bean waste ash as road pavement sub-base material. Geotechnical and Geological Engineering Springer. 2017 http://link.springer.com/article/10.1007/sl0706-017-0256-2

[8] Bassey OB, Attah IC, Ambrose EE, Etim RK. Correlation between CBR Values and Index Properties of Soils: A Case Study of Ibiono, Oron and Onna in Akwa Ibom State. Resources and Environment. 2017; 7(4): 94-102. http://dx.doi.org/ 10.5923/j.re.20170704.02

[9] Moses G, Etim RK, Sani, JE, Nwude M. Desiccation effect of compacted tropical black clay treated with concrete waste. Leonardo Electronic Journal of Practices and Technologies. 2018; 33: 69-88.

[10] Sani JE, Etim RK, Joseph A. Compaction behaviour of lateritic soil–calcium chloride mixtures. Geotechnical and Geological Engineering. Springer Nature Switzerland. 2019; 37:2343-2362. https://doi.org/10.1007/s10706-018-00760-6

[11] Attah IC, Etim RK, Sani JE. Response of oyster shell ash blended cement concrete in sulphuric acid environment. Civil and Environmental Research. 2019; 11(4): 62–74. http://dx.doi.org/10.7176/CER/11-4-07

[12] Moses G, Etim RK, Sani JE, Nwude M. Desiccation-induced volumetric shrinkage characteristics of highly expansive tropical black clay treated with groundnut shell ash for barrier consideration. Civil and Environmental Research. 2019; 11(8): 58–74. http://dx.doi.org/10.7176/CER/11-8-06

[13] Etim RK, Attah IC, Eberemu AO, Yohanna P. Compaction behaviour of periwinkle shell ash treated lateritic soil for use as road sub-base construction material. Journal of GeoEngineering, Taiwan Geotechnical Society. 2019; 14(3): 179-190. http://dx.doi.org/10.6310/jog.201909_14(3).7

[14] Attah IC, Agunwamba JC, Etim RK, Ogarekpe NM. Modelling and predicting of CBR values of lateritic soil treated with metakaolin for road material. ARPN Journal of Engineering and Applied Sciences. 2019; 14(20): 3606 – 3618.

[15] Attah IC, Etim RK. Experimental investigation on the effects of elevated temperature on geotechnical behaviour of tropical residual soils. Springer Nature Applied Sciences. Springer Nature Switzerland AG. 2020. https://doi.org/10.1007/s42452-020-2149-x

[16] Etim RK, Attah IC, Yohanna P. Experimental study on potential of oyster shell ash in structural strength improvement of lateritic soil for road construction. International Journal of Pavement Research Technology, Chinese Society of Pavement Engineering, Springer Nature Singapore. 2020. https://doi.org/10.1007/s42947-020-0290-y

[17] Attah IC, Etim RK, Alaneme GU, Bassey OB. Optimization of mechanical properties of rice husk ash concrete using Scheffe's theory. Springer Nature Applied Sciences. Springer Nature Switzerland AG. 2020. https://doi.org/10.1007/s42452-020-2727-y

[18] Attah IC, Etim RK, Usanga IN. Potentials of cement kiln dust and rice husk ash blend on strength of tropical soil for sustainable road construction material. In book of abstract: 2nd International Conference on Sustainable Infrastructural Development, ICSID. Centre for Research, Innovation and Discovery, Covenant University, Canaan Land, Ota, Nigeria. July 27 – 28, 2020; 84

[19] Sani JE, Yohanna P, Etim RK, Attah IC, Bayang F. Unconfined compressive strength of compacted lateritic soil treated with selected admixtures for geotechnical applications. Nigerian Research Journal of Engineering and Environmental Sciences. 2019; 4(2): 801-815.

[20] Yohanna P, Ibrahim UA, Etim RK. Compaction behaviour of black cotton soil treated with selected admixtures: A statistical approach. Premier Journal of Engineering and Applied Sciences. Publication of Nigerian Society of Engineers, Ibadan Branch. 2020; 1(1): 35 – 44.

[21] Ilori A. Evaluation of naturally occurring aggregates as sub-base and subgrade construction materials in Akwa Ibom State, Southeastern Nigeria. International Journal of Geotechnical and Geological Engineering. 2016; 3(4):621-634.

[22] Osunkunle A, Yusuf I, Ako T, Abolarin J. Assessment of engineering properties of asphaltic concrete produced in South Western Nigeria. Webs Journal of Science and Engineering Application. 2016; 5(1): 41-48.

[23] Akinleye MT, Tijani MA. Assessment of quality of asphalt concrete used in road construction in South West Nigeria. Nigerian Journal of Technology Development. 2017; 14(2): 51 – 54.

[24] Wang X, Feng J, WanG H, Hong S, Zheng S. Stress regression analysis of asphalt concrete deck pavement based on orthogonal experimental design and interlayer contact. IOP Conference Series: Materials Science and Engineering. 2018; 322, 042026 https://doi:10.1088/1757-899X/322/4/042026

[25] Bala N, Napiah M, Kamaruddin I. Application of multivariable regression models for prediction of composite nanosilica/polymer asphalt mixture OBC. International Journal of GEOMATE. 2018; 14(45): 202-209. https://doi.org/10.21660/2018.45.94051

[26] Kim SH, Kim N. (2006) Development of performance prediction models in flexible pavement using regression analysis method. KSCE Journal of Civil Engineering. 2006; 10(2): 91–96.

[27] Laurinavi˘cius A, Oginskas R. Experimental research on the development of rutting in asphalt concrete pavements reinforced with geosynthetic materials. Journal of Civil Engineering and Management. 2006; 12(4): 311–317.

[28] Shukla PK, Das A. A re-visit to the development of fatigue and rutting equations used for asphalt pavement design. International Journal of Pavement Engineering. 2008; 9(5): 355–364.

[29] Asifur Rahman ASM, Mendez Larrain MM, Tarefder RA. Development of a nonlinear rutting model for asphalt concrete based on Weibull parameters. International Journal of Pavement Engineering. 2017; 1–10.

[30] Baldo N, Manthos E, Pasetto M. Analysis of the mechanical behaviour of asphalt concretes using artificial neural networks. Advances in Civil Engineering. 2018. https://doi.org/10.1155/2018/1650945

[31] Kajner L, Kurlanda M, Sparks GA. Development of Bayesian regression model to predict hot-mix asphalt concrete overlay roughness. Transportation Research Record. 1995, 1539: 125 -131

[32] Nigerian General Specification, Roads and Bridges Works. Federal Ministry of Works and Housing, Lagos, Nigeria. 1997

[33] Agunwamba JC. Engineering mathematical analysis. De-Adroit Innovation, Enugu, Nigeria. 2007; Chap 16 and 17. ISBN 978-8137-08-3

[34] Etim RK, Usanga IN, Ekpo DU, Attah IC. (2022) Material characterization and statistical evaluation of properties of hot mix asphalt concrete (HMAC) used in wearing course of road pavement; Southern Nigeria. Építőanyag – Journal of Silicate Based and Composite Materials. 74(5): 204-213. https://doi.org/10.14382/epitoanyag-jsbcm.2022.30

[35] Etim, RK. Ekpo DU, Ebong UB, Usanga IN. (2021) Influence of periwinkle shell ash on the strength properties of cement-stabilized lateritic soil. International Journal of Pavement Research Technology, Chinese Society of Pavement Engineering, Springer Nature Singapore https://doi.org/10.1007/s42947-021-00072-8

[36] Etim RK, Attah IC, Ekpo DU, Usanga IN. (2021) Evaluation on Stabilization Role of Lime and Cement in Expansive Black Clay - Oyster Shell Ash Composite. Transportation Infrastructure Geotechnology. https://doi.org/10.1007/s40515-021-00196-1

[37] Etim RK, Ekpo DU, Etim GU, Attah IC (2021) Evaluation of lateritic soil stabilized with lime and periwinkle shell ash (PSA) admixture bound for sustainable road materials. Innovative Infrastructure Solutions. https://doi.org/10.1007/s41062-021-006650-z

[38] Etim RK, Ekpo DU, Attah IC, Onyelowe KC. (2021) Effect of micro sized quarry dust particle on the compaction and strength properties of cement stabilized lateritic soil. Cleaner Materials, Elsevier https://doi.org/10.1016/j.clema.2021.100023

[39] Attah IC, Etim RK, Ekpo DU, Onyelowe KC**.** (2021) Understanding the impacts of binary additives on mechanical and morphological response of ameliorated soil for road infrastructures. Journal of King Saud University-Engineering Sciences, Elsevier https://doi.org/110.1016/j.jksues.2021.12.001

[40] Sani JE, Moses G, Etim RK, Wilson UN, Babatunde AO. (2022) Stabilization of lateritic soil with cement and treated sisal fibre. *ACTA TECHNICA CORVINIENSIS – Bulletin of Engineering*. Vol.1: pp 41-47.

[41] Attah IC, Etim RK, Ekpo DU, Usanga, IN (2022) Effectiveness of cement kiln dust-silicate based mixtures on plasticity and compaction performance of an expansive soil Építőanyag – Journal of Silicate Based and Composite Materials. 74(4): 144–149. https://doi.org/10.14382/epitoanyag-jsbcm.2022.22

[42] Yohanna P, Kanyi MI, Etim RK, Eberemu AO, Osinubi KJ (2021) Experimental and Statistical Study on Black Cotton Soil Modified with Cement–Iron Ore Tailings. FUOYE Journal of Engineering and Technology (FUOYEJET). 6(1): 117-122. http://dx.doi.org/10.46792/fuoyejet.vAiB.C

[43] Alaneme GU, Attah IC, Etim RK, Dimonyeka MU. (2021) Mechanical properties optimization of soil-cement kiln dust mixture using extreme vertex design. International Journal of Pavement Research Technology, Chinese Society of Pavement Engineering, https://doi.org/10.1007/s42947-021-00048-8

Ref.:
Etim, Roland Kufre – **Andem**, Kenneth Edet – **Yohanna**, Paul – **Ekpo**, David Ufot – **Stephen**, Ini-Obong Nnah: *Case study evaluation of selected binder course asphalt concrete used in road construction in Nigeria*
Építőanyag – Journal of Silicate Based and Composite Materials, Vol. 75, No. 3 (2023), 92–100. p.
https://doi.org/10.14382/epitoanyag-jsbcm.2023.14

Reinforcing effect of MWCNT derivatives on glass/epoxy and carbon/epoxy composites perpendicular to the fiber direction

Hamed NAZARPOUR-FARD ▪ Department of Chemistry, Faculty of Sciences, Lorestan University, Khoram-Abad, Iran ▪ Nazarpour.ha@lu.ac.ir
Mohammad Hosain BEHESHTY ▪ Department of Composites, Iran Polymer and Petrochemical Institute, Tehran, Iran

Érkezett: 2023. 03. 13. ▪ Received: 13. 03. 2023. ▪ https://doi.org/10.14382/epitoanyag-jsbcm.2023.15

Hamed NAZARPOUR-FARD
Ph.D in polymer science, Department of Chemistry, Faculty of Sciences, Lorestan University, Khoram-Abad, Iran. His research interests include polymer characterization, composites and nanocomposites.

Mohammad Hosain BEHESHTY
Professor in polymer composites, Department of Composites, Iran Polymer and Petrochemical Institute, Tehran, Iran. His research interests include polymer composites, nanocomposites, resins and adhesive.

Abstract
In the current study, the nano-composites of unidirectional carbon and glass fiber reinforced-epoxy resin with multi-walled carbon nanotubes (MWCNTs) were separately prepared by hand lay-up and hot pressing of fiber epoxy prepregs. Three types of MWCNT derivatives (parent-CNT, low carboxylated CNT (LCCNT) and higher carboxylated CNT (HCCNT)) were dispersed into the epoxy resin/fiber composites. The improved mechanical properties observed in the three component composites could be attributed to the uniform dispersion of CNTs in epoxy/fiber matrices, nanosize of the additives and the improved interfacial interactions between the composite components. The COOH functional groups could also be effective in the increase of mechanical traits because they induce the amphiphilic nature into CNTs for better dispersion and to generate the better glass fiber/epoxy (E/G) and carbon fiber/epoxy (E/C) interactions. HCCNT led to the best mechanical properties among all the samples due to its higher carboxyl content. HCCNT also changed the curing peak of epoxy in DSC and improved its thermal stability. For instance, the final residual mass for E/HCCNT was 15.4% at 600 °C compared to 13.92% for the pure epoxy while the values of 17.55 and 16.48% were observed at 500 °C for E/HCCNT and epoxy, respectively. The observed effect of COOH functionality on the void formation within the composite and on the better CNT dispersion in the matrix can be considered as an important observation for investigating the E/C/CNTs nanocomposites.
Keywords: carbon fiber, glass fiber, multi-walled carbon nanotubes, epoxy resin, mechanical properties
Kulcsszavak: szénszál, üvegszál, többfalú szén nanocsövek, epoxi gyanta, mechanikai tulajdonságok

1. Introduction

Multi-component materials, especially polymer composites are usually prepared in order to improve the characteristics of materials or provide samples with unique properties for using in applications such as sensors [1]. Also, these types of composites have present interesting usages in the fields of bio-composites [2-3], recycling [4], and also the laminated materials such as fiber/epoxy composites [5].

Glass fiber composites are one of the layered composites that have industrial applications [6], such as their employment in the airplanes and the radar antennas [7]. Carbon fiber reinforced composites have also been employed in the usages, e.g., railway interior applications [8] and fuel tank of launch vehicles [9]. Nevertheless, the cryogenic aging of the tanks and the micro-cracks grown in the composite matrix due to the difference in the coefficients of thermal expansion of the composite components are from issues that accompany this composite type [10].

Despite the advantages of multi-layer composites, they have exhibited the weakness between layers, i.e., in perpendicular to the fiber direction [11] and also weak interlaminar shear resistance [12]. These mechanical issues can result in the important problems especially in the structural and construction applications. Thus, improve their transverse properties, for example by nano fillers can lead to the important development in these materials [13].

Carbon nanotubes (CNTs) due to their unique traits such as low coefficient of thermal expansion, have been widely used in recent years to strengthen the mechanical properties of various nanocomposites. Nevertheless, CNTs are still of interest for using in the various researches [14], and to improve the characteristics of fibrous composites [15]. Tendency to agglomeration in CNTs could result in unwanted stress concentrations that can be the starting point for failure during loading. The uniform dispersion of CNTs in the polymer matrix can be improved by growing the various functional groups on their surfaces [16]. Moreover, the good dispersion of CNTs into epoxy matrix can strongly affect the matrix-dominated mechanical properties *via* improving the interfacial stress transfer between the composite components by the bridging effect [17].

Incorporating the various nanoparticles into the epoxy resin and/or epoxy/fiber composite to enhance the characteristics of the polymer matrix is the typical method [18]. For example, Kim et al. [19] investigated the enhancement effect of MWCNTs on the crack growth resistance in the CNT/carbon/epoxy nanocomposites at a cryogenic temperature. Hossain et al. employed the XD-grade CNTs for reinforcing E/C composites [20]. Rana et al. developed reinforced E/C composites by adding single-walled CNTs into the epoxy matrix [21]. Taş and Soykok reported a remarkable improvement in the bending strength

by compositing CNTs with carbon fiber-based composites [22]. It is worthy of note that in our previous paper, the dynamic-mechanical properties of the laminar E/C composites were improved by adding the carboxylated CNTs to the E/C matrix [5].

On the basis of this introduction, we incorporated parent-CNT, LCCNT and HCCNT into the E/C and E/G composites separately in order to verify the impact of COOH functionalization and its content on the mechanical behavior of E/C composite in perpendicular to the fiber orientation. The hand laminating and compression molding methods were employed to prepare the E/fiber/CNT nanocomposites.

The present study is important, because strengthen the fiber/epoxy composites is the essential requirement in these materials. Also, studying the effect of COOH content in the CNT nanoparticles on E/C characteristics is a new study that could be developed to other functionalities such as amide, hydroxyl, silane, etc. Also, based on the requirement of polymer engineers to the high modulus but lightweight materials, E/C/HCCNT can be considered as the interesting composite for structural applications.

2. Materials and experiment

2.1 Materials

The unidirectional carbon fiber, UD T200 with the surface area of 200 gr m^{-2} were supplied by PMP Co. (Tehran, Iran). The unidirectional glass fiber (L300E10C-0) with the surface area of 300 gr m^{-2} was purchased from Metyx (Turkey). Bisphenol-A diglycidyl ether (Epikote 828) as the epoxy matrix was supplied by Momentive (USA) with epoxy group content of 5.34 mmol g^{-1}. The dicyandiamide (DICY) curing agent with the melting point of 208-211 °C and average particle size of 150 μm was obtained from AlzChem Co. (Germany). 1-Methylimidazol (DY070) purchased from Huntsman company (Unaited States) was employed as a curing accelrator. Three kinds of MWCNTs as the nano reinforcement filler were supplied by American Elements Company, USA (see *Table 1*). The length and true density of CNTs were 10-30 μm and 2.1 g cm^{-3}, respectively.

Nano particle	Special surface area (m^2/g)	Outer diameter (nm)	COOH (wt%)
Parent-CNT	200	10-20	0
LCCNT	200	10-20	2
HCCNT	500	<8	3.86

Table 1 The specifications of the used MWCNTs derivatives
1. táblázat A használt MWCNT-származékok specifikációi

2.2 Instrumentation

A homogenizer (Polytron, PT6100, Kinematica) was employed to strongly agitate the epoxy/CNT mixtures and achieve the homogeneous dispersion of CNT nanoparticles within the prepared mixtures. The ultrasonic bath (LBS2 series, FALC instruments) was applied for the better dispersion of the CNT nanoparticles in the mixtures. The viscosity determination of the mixtures was accomplished *via* Brookfield viscometer (RVDV-II+Pro model) based on the ASTM D 2196 standard method. For this purpose, a certain quantity of the desired mixture (around 3 to 7 cc) was poured into the chamber of the device and the viscosity of the sample was measured at the desired temperature using Spindle 14. The curing behavior of the epoxy mixtures was analyzed via a differential scanning calorimetry (DSC) by using a NETZSCH DSC 200 F3 instrument. All experiments were conducted under a nitrogen flow of 50 mL min^{-1} at the heating rate of 10 °C min^{-1}. Thermogravimetry analysis (TGA) measurements of the cured epoxy mixtures were carried out on STA thermal analyzer (STA625 model) at the heating rate of 10 °C min^{-1} under a nitrogen atmosphere. The gel time of the uncured epoxy mixtures was recorded on the basis of ASTM D4217 standard test method by using a 15SB-90FA bath (Italy) at three different temperatures of 110, 120 and 140 °C. WEGA/TESCAN scanning electron microscope (*Czech Republic*) was employed to study the morphology of the nanocomposites and the MWCNs dispersion in the matrix. Before performing the microscopy analysis, the ready composites were coated with a thin film of gold under vacuum *via* sputter coater (K450X, EMITECH, England). 20 kV was chosen as a convenient voltage of SEM filament. The tensile tests were accomplished on the basis of the ASTM D3039 standard test method on a universal testing machine (UTM, 150 kN, Santam, Iran). The crosshead speed of the machine was constant at the rate of 2 mm min^{-1}. The three point bending test was done according to ASTM D790-10 standard test method with sample dimensions of 60 × 13 × 3 mm^3 on the universal testing machine (UTM, 150 kN, Santam, Iran). The Izod notched impact test was caried out on the basis of the ASTM D 256 standard test by using Zwick impact tester, model 5102. For investigating the lap shear strength of the prepregs based on the ASTM D1002 standard test, aluminum plates series 5000 were employed with 2 mm thickness and the dimensions of 25 mm ×102 mm. Aluminum surface was treated with sand blasting paper no. 150, degreased with distilled water and acetone and then dried in oven for 2 h in order to better adherence of prepreg to the plate. Then, one ply of prepreg with the dimensions of 25 mm × 17 mm was cut and put on the treated part of aluminum with the overlap region of 13 mm × 25 mm. The samples were cured in a hot press at 140 °C and 25 bar for 45 min after which cooled to room temperature. Finally, the lap shear tests were carried out using a Santam tensile instrument (STM-150) with crosshead speed of 1.3 mm/min and load cell of 2000 kg. The lap shear strength was calculated by dividing the maximum force (to failure the sample) to the overlapping area. The hardness tests were carried out on Shore D hardness tester (GOTECH, GT-GS-MB).

For the fracture toughness measurements, the standard test method of ASTM D5045 was employed for providing the test requirements and the three-point single-edge notch bend (SENB) specimens. An initial crack (6 mm) was machined in the specimens and a natural crack was created by tapping on a fresh razor blade placed in the notch. The tests were accomplished in the flexure mode using a 150 kN Santam UTM instrument at a crosshead rate of 1.5 mm min^{-1} at ambient temperature. The fracture toughness values were computed in the terms of plane strain critical stress intensity factor, K_{IC}, by using the following equation [23]:

$$K_{IC} = \frac{P_Q}{BW^{\frac{1}{2}}} f(x) \quad (1)$$

where B and W are the thickness (cm) and the width (cm) of specimen, respectively, P_Q is the critical load to propagate the crack (kN), and f(x) is a non-dimensional shape factor calculated *via* the following relationship [23]:

$$f(x) = 6\sqrt{x}\frac{1.99-x(1-x)(2.15-3.93x+2.7x^2)}{(1+2x)(1-x)^{\frac{2}{3}}} f(x) \quad (2)$$

where *a* is the crack length (cm) and $x = \frac{a}{W}$.

2.3 Preparation of the pure epoxy sample

A mixture of epoxy resin and the dicyandiamide (DICY) curing agent was obtained by mixing 7 phr of DICY with 100 phr of epoxy resin. Then, the prapared mixture was homogenized at 3000 rpm *via* a homogenizer for 60 min at room temperature. At the last 3 min of the homogenization proccess, 1-methylimidazol (0.6 phr) was added as an curing accelerator to the mixture. The contents of DICY and the 1-methylimidazol in the prepared composites were as the previously used in [5] and [23].

2.4 Preparing the mixtures of epoxy/MWCNT derivatives

DICY (7 phr) and the MWCNT (0.2 phr) were properly mixed with 100 phr of the epoxy resin by using a glass rod and then the sonication at 25 °C in an ultrasonic bath for 15 min. Afterward, the provided mixture was homogenized at 3000 rpm by a homogenizer for 60 min at ambient temperature. Then, 1-methylimidazole (0.6 phr) was added to the mixture and additionally homogenized for 3 minuets at the same rate. This final mixture was sonicated (60 kHz) at 25 °C for 15 min before being used for wetting the carbon fibre in order to providing the desirabale prepregs. The general protocol for preparation of the epoxy/MWCNT mixtures is shown in *Fig. 1*.

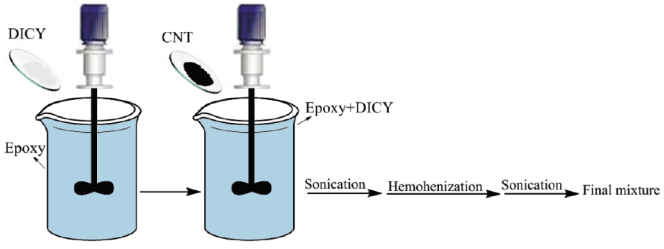

Fig. 1 Schematic representation of the procedure taken for the preparation of E/CNT mixtures
1. ábra Az E/CNT keverékek előállításánál alkalmazott eljárás sematikus ábrázolása

2.5 Preparation of the prepregs

A sample of carbon fiber was impregnated with the pure epoxy resin or the mixture of epoxy/MWCNT, such that the ratio of fiber to resin was kept at 50±2 wt% to assure all the fibers are homogeneously impregnated with the resin mixture. The prepared prepreg (impregnated single layer of the carbon fiber) was provided for the next processing stages of lay-up and curing *via* the hot press to leave the final composite samples. The simmilar protocol was used to providing the glass fiber prepregs.

2.6 Preparing the composite samples

The proper number of the carbon/epoxy prepregs were laid up and the prepared hand lay up laminate was placed between two layers of teflon film in an steel frame with the favoraite thikness. The thickness of the frames used here were on the basis of the corresponding ASTM standard test method for each mechanical test. Then, the compression-molding of the hand lay up sample *via* hot pressing at 140 °C under 30 bar for 1.5 h left the final nanocomposites. After cooling the cured samples to ambient temperature, specimens with the certain dimensions were cut for using in the desired tests. The glass fiber reinforced samples were also prepared by the same methodology as used for the carbon fiber-incorporated composites.

2.7 Resin content of the prepregs and the nanocomposites

Thermal pyrolysis method at the elevated temperature was used to determine the resin content of the glass fibers-based composites. In other words, the difference between the initial and final weights of the nanocomposite after completely burning of epoxy matrix, was designated as the resin content. Due to the thermal dcomposition of carbon fiber at the elevated temperatures higher than 600 °C, acid digestion protocol was applied to evaluating the resin content of the E/C composites. In other words, the given amounts of the composite (initial weight) were soaked in sulphoric acid and after completely dissolving the resin, H_2O_2 was slowly poured into the mixture. At the end, after washing the acid digested sample with deionized water and then drying it, the dried carbon fiber was weighed (final weight) and the difference between the final and initial weights was designated as the resin content.

2.8 Flow test

To determine the epoxy resin flowed from the fiber prepreg under the given pressure, the several samples of the prepreg (with known dimensions) were cut and placed under the hot press at 30 bar and 135 °C for 15 min. Then, after cooling the sample to room temperature, the weight loss of the initial prepreg was defined as the resin flow.

3. Results and discussion

3.1 Viscosity of the epoxy mixtures

The viscosity of the epoxy resin mixtures was obtained at three temperatures and the results were tabulated in *Table 2*. It was found that the MWCNTs and its derivatives led to the increased viscosity in the nanocomposites as compared to the pure epoxy resin. Whereas the significant differences were not observed between the viscosities of the CNT-contained epoxy mixtures.

Sample	Viscosity (cP)		
	30 °C	60 °C	90 °C
E	11660	375	75
E/Parent-CNT	~13300	~460	~112
E/LCCNT	~13400	~470	~114
E/HCCNT	~13450	~480	~115

Table 2 The viscosity results of the epoxy resin and its nanocomposites
2. táblázat Az epoxigyanta és nanokompozitjainak viszkozitási eredményei

3.2 Resin content of the samples

After the resin content determination of the nanocomposites, the values of 45% ± 2 and 40% ± 2 were obtained for E/C and E/G samples, respectively. While, the flow test results showed that ~18% ± 1 of the resin is flowed from the epoxy-wetted carbon and glass prepregs.

3.3 DSC analysis of the uncured epoxy

The DSC results of the different epoxy formulations can be observed in *Fig. 2*. It can be found that the curing peak of epoxy resin has been shifted to the lower temperatures after incorporating CNTs to the epoxy samples. It can be seen that the curing temperature range has decreased from ~120-187 °C for the pure epoxy resin to ~115-176 °C for the CNTs contained nanocomposites. This decrement of the curing temperatures can be related to the accelerating effect of CNT on the epoxy curing process due to its nanoscale size and COOH functional groups. It is worthy of mention that the heat of curing reaction (mJ mg^{-1}) for the nanocomposites were ~1 to 3.7% higher as compared to the pure epoxy showing the promoting effect of CNT on the epoxy curing.

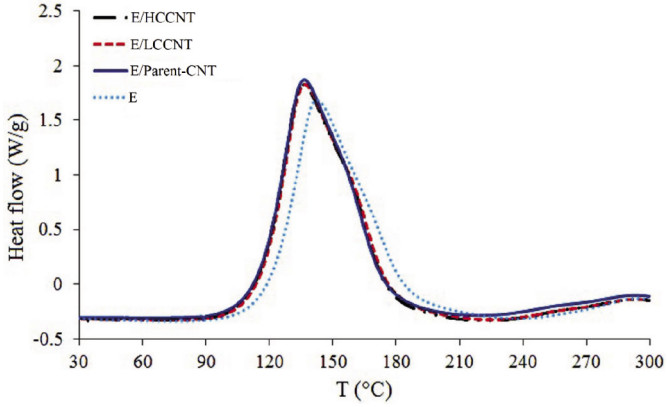

Fig. 2 DSC thermographs of the uncured epoxy resin and its mixtures with MWCNTs
2. ábra A kikeményítetlen epoxigyanta és MWCNT-vel alkotott keverékeinek DSC termográfiája

3.4 Gel time determination of the epoxy resin mixtures

Gel time value is the essential parameter required to evaluating the optimized condition of the prepregs preparation. In other words, at the gel point, the prepregs processing and/or preparation could be difficult. On the other hand, the parameter implies the reactivity of the corresponding accelerator [35]. In this test, during the heating period, the samples were stirred continuously with a glass rod. The resin viscosity was firstly decreased due to the increased molecular movements and then was increased gradually that attributed to the crosslinks created between the epoxy chains. Afterward, it showed an elastic behavior (rubber like) and finally reached the gel state that at this point, the recorded time was designated as a gel time. The gel time of different samples was measured at the temperatures of 100, 120 and 140 °C and the obtained data were tabulated at *Table 3*. It can be found that the gel time of the epoxy/CNTs mixtures is decreased at 100 and 120 °C in comparison to the pure epoxy resin, while all the samples were gelled at ~3 min at 140 °C. This can be attributed to the increasing effect of carbon nanotubes on viscosity and gelling process of epoxy. This reduce of gel time upon increasing temperature, is logical due to increasing the molecular movements after temperature increment.

Sample	Gel time (min)		
	100 °C	120 °C	140 °C
E/C	~37	~12.0	~3
E/C/Parent-CNT	~25	~11.6	~3
E/C/LCCNT	~24	~11.0	~3
E/C/HCCNT	~22	~10.2	~3

Table 3 The gel time values of the epoxy resin mixtures
3. táblázat Az epoxigyantakeverékek gélesedési ideje

3.5 TGA analysis of the cured epoxy mixtures

TGA analysis results for the cured epoxy resin and its nanocomposites with Parent-CNT, LCCNT and HCCNT are shown in *Fig. 3*. It is obvious that CNT derivatives (0.2 phr) have not been caused the observable effect on the thermal degradation temperature of pure epoxy. While, pursuant to the residual content of the samples at various temperatures (e.g., 500 and 600 °C), it can be concluded that the carbon nanotube samples improve thermal stability of pure epoxy resin. On the other word, the solid content of the pure epoxy, E/parent-CNT, E/HCCNT and E/LCCNT were 16.48, 16.44, 16.76 and 17.55% at 500 °C and 13.92, 14.3, 14.3 and 15.44% at 600 °C, respectively. It is clear that HCCNT has been led to the highest thermal stability in the epoxy as compared to other nanoparticles, because it contains the more COOH content (and also the higher polarity) in comparison to other two CNTs.

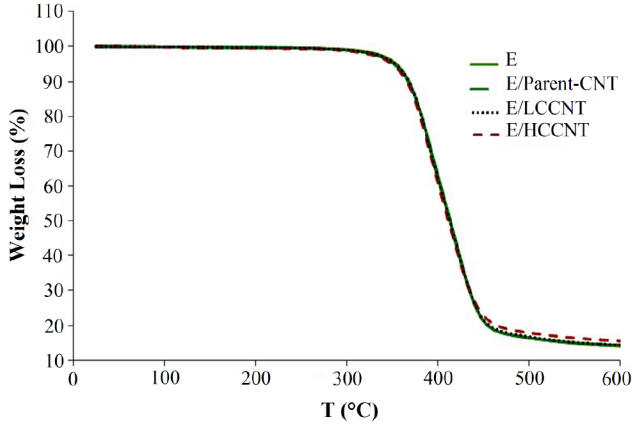

Fig. 3 TGA traces of the cured epoxy resin and its nanocomposites with MWCNTs
3. ábra A kikeményedett epoxigyanta és nanokompozitjainak MWCNT-vel készült TGA nyomai

3.6 SEM microscopy

The SEM micrographs of E/C and its nanocomposites with MWCNT derivatives [9], were explained based on the voids appeared in the sample matrices and on the uniformities of the micrographs, as Seki interpreted the SEM images of polyester/jute fiber/epoxy composites on the basis of the holes observed between the fiber and resin [24]. The large holes in

the micrograph of the pure E/C composite indicate the weaker bondings between the epoxy and the fiber. These voids become even greater when the parent carbon nanotube is added to the E/C composite. The SEM micrographs of the nano-composites contained either LCCNTs or HCCNTs exhibited no remarkable holes/voids in the E/C interface indicating the enhanced bonding between the components. Additionally, the SEM micrograph of E/C/parent-CNT was found to be rougher in the surface than other nanocomposites maybe due to its tendency to agglomeration and inappropriate dispersion in comparison to E/C/LCCNT and E/C/HCCNT. On contrary, the micrographs of E/C/LCCNT and E/C/HCCNT demonstrate the enhanced smoothness and uniformity that can be atrributed to fine dispersion of these CNTs into the polar epoxy matrix. The polar COOH groups remarkably participate in hydrogen bonding and also in dipole-dipole interactions consequently enhance the compatibility of these nanoparticles with epoxy resin. Here, the oxidized MWCNTs can be amphiphilic materials because of presence of the bearing polar COOH groups and the non-polar carbonaceous backbone. This amphiphilic nature allows them to having the π- π and non-polar interactions with the carbon fibers and to create the dipole-dipole interactions in the same time with the polar segment of epoxy. Beside these stacking forces, the carboxylated CNTs can covalently link to the epoxy chains through reaction of epoxy rings with carboxyl groups. Further, the chemical bonding between epoxy and COOH groups can be accelerated by DICY curing agent (*Fig. 4*). Due to these interfacial interactions, LCCNT and HCCNT acquire the better dispersion into epoxy resin causing the smooth appearance and the better mechanical properties. Similar interfacial interactions were previously observed from SEM images by Ma et al., i.e., they demonstrated that silylated-CNTs are dispersed more uniform than pure CNT into epoxy matrix [25].

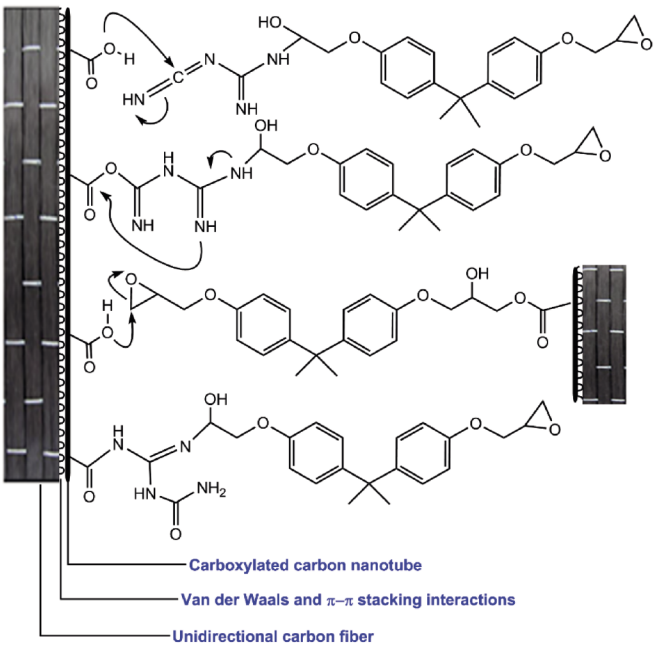

Fig. 4 The expected interactions between carboxylated CNTs and composite components
4. ábra A karboxilezett CNT-k és a kompozit komponensek várható kölcsönhatásai

SEM images for the E/G composites can be seen in *Fig. 5*. It can be seen that the image of the pure E/G composite is smoother and smoother than the prepared nanocomposites. After adding Parent-CNT into the composite bulk, its hydrophobicity could be led to create some voids between the resin and the fibers. As found for the carbon fiber-based nanocomposites, here, LCCNT and HCCNT also were found to be smoother in SEM image and better in dispersion as can be seen in the micrographs. In other words, the uniformity and smoothness of the microscopic images were as the order of HCCNT > LCCNT > Parent-CNT.

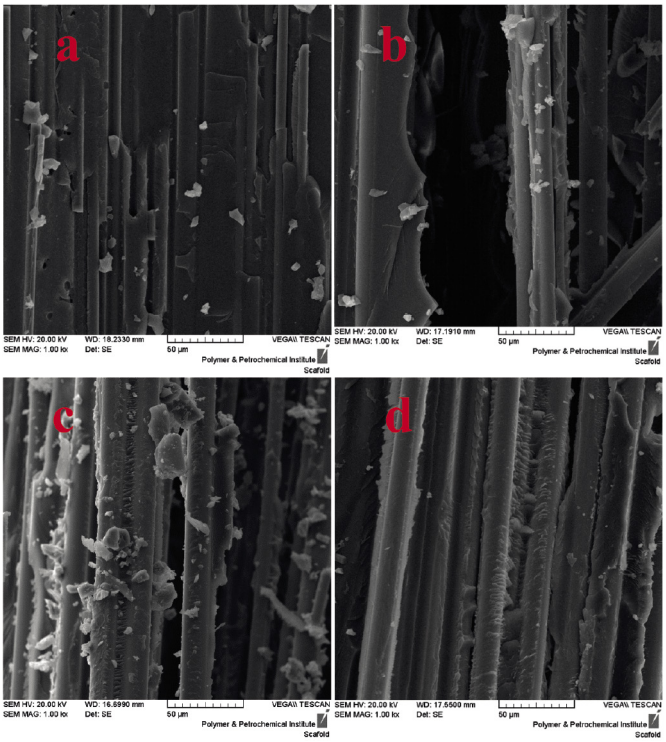

Fig. 5 SEM images of (a) E/G, (b) E/G/Parent-CNT, (c) E/G/LCCNT and (d) E/G/HCCNT
5. ábra (a) E/G, (b) E/G/Parent-CNT, (c) E/G/LCCNT és (d) E/G/HCCNT SEM-képei

3.7 Mechanical properties of E/C/CNT nanocomposites

The order of E/C < E/C/Parent-CNT < E/C/LCCNT < E/C/HCCNT was found for the flexural modolus values of the samples (*Table 4*). Among the samples, HCCNT showed the highest impact on the flexural modolus. It is worthy of note that the rising impact of CNTs on flexural modolus of E/C composite have also reported in [22]. The increasing order was found in the bending strength values similar to the flexural modolus data (*Table 4*). In this case, E/C/HCCNT with bending strength of 85±8 MPa was seen to be the strongest sample in the bending deformation among the samples. In the bending tests perpendicular to the UD fibers, the epoxy/fiber interface intractions are not dominant parameter on the mechanical charcateristics. This can be etributed the fact that the fibers are distinc from each other in this direction, while the epoxy/CNT interactions are dominant and could influence on the mechanical characteristics of the UD fiber-based nanocomposites.

On the basis of the fracture toughness results (*Table 4*), it is obvious that the CNT samples have exhibited the improving effect on the fracture toughness values for the corespounding composites as obsrved in the bending analysis of the samples.

Impact resistance is defined as the material resistance to breaking under a shock loading or the fracture under the applied force at the high speed (low period of time) [26]. The growthing order of E/C < E/C/Parent-CNT < E/C/LCCNT < E/C/HCCNT was observed for the studied samples as apeared for othe mechanical characteristics. The enhancing effect of the pure MWCNT nanoparticles on the fracture toughness of the E/C composites have also been explained in [27] that can be useful for the better realization of the results in the present study.

The hardness of the samples was conducted based on Shore D hardness test. As can be seen in *Table 4*, the CNT samples led to the increasing effect on the hardness of the E/C composite that the maximum values were observed for E/C/HCCNT. It is interesting to mention that the similar Shore D values have been presented by Zakaria et al. [28] for other carbonous material (graphite) as a reinforcing filler.

The results of the lap shear test tabulated in *Table 4*, show the higher lab shear strength for E/C nanocomposites containing CNTs compared to the pure epoxy. This can be atributed to the better missibility/bondings between the nanoparticle and the E/C composites. HCCNT due to its higher polarity exhibited the more increasing effect on the values of the lap shear strength as compared to other two CNT samples. Also, CNTs and COOH functionality can lead to adhesive propertied of the prepregs to the aluminium plates as. For example of the effect of nanopartices on the lap shear srtength, the lab shear strength values of the pure epoxy adhesive and its nancomposites with nanoalumina were found to be in the range of 4.39-6.83 MPa [29].

Generally, the same increasing order observed in all the mechaniccal tests for the samples can be assigned to the inherent reinforcing ability of the CNTs and also to the good interactions between the composite components thereby which the transfer of the impact energy between the phases of the composites can be improved. CNTs can form the interactions in the form of Van der Waals and π – π interactions with the E/C matrix. However, HCCNT and LCCNT can even form the conalant bonds with epoxy chains *via* their COOH functional groups. Moreover, the amphiphilic characteristic of HCCNT (COOHs interact with the epoxy segments, wherase the carbonous parts interact with the carbon fiber) could lead to the improvement effect on the E/C interface cohesion and the better stress transfer from epoxy to fiber and conversely, from fiber to epoxy. Also, the HCCNT polarity can be led to enhance its dispersion in the epoxy matrix (as seen in its uniform and free of void SEM micrograph) that the proper dispersion is very important to reaches the favorite properties. Althought the effects of LCCNT and HCCNT were more than that of Parent-CNT due to their amphiphilic nature and the higher COOH content as compared to the pure CNT. The better performances of LCCNT and HCCNT on comparison to Parent-CNT are expectable owing to their better bondings with the polar epoxy resin due to their COOH functionality. It can clearly that the values of E/C/LCCNT are higher than that of Parent-CNT, however the diameter of LCCNT and parent-CNT is equal to ~10-20 nm. Thus, it is concluded that the effect of COOH content on the fracture toughness values is remarkable and more predominant in comparison to the diameter of CNTs.

3.8 Mechanical properties of E/G/CNT nanocomposites

As shown in *Table 5*, the order of E/G/HCCNT > E/G/LCCNT > E/G/Parent-CNT > E/G was observed for the values of bending strength and flexural modulus of the E/G-based samples. This could be due to the inherent reinforcing properties of carbon nanotubes and different quantities of COOH functional group on the CNTs surfaces. In order to confirm the experimental data, the results were compared with the reported ones in literature, the results of the present study were in accordance to the ones published in literature. For instance, the improvement in modulus and bending strength of E/G composite was developed by adding CNTs into them [30-31].

Based on the results of the fracture toughness test (*Table 5*), Parent-CNT exhibits a higher fracture toughness than the E/C composite, which can be attributed to the small size of the nanoparticles and the intrinsic high modulus of CNTs that inherently strengthen the epoxy resin. While, the better performance of HCCNT and LCCNT than that of Parent-CNT can be due to their better interactions with the composite components. The enhancing effect of CNTs on fracture toughness of E/G composite have also been observed in [30].

Here, the increasing effects were laso found for CNTs on the impact test results of the glass fiber-based nanocomposites similira to other mechanical properties. The imrovment effect CNTs on the impact strength of E/G composites have also been reported by Zulfli et al. [30].

The similar changes were observed in the lap shear strength values of the samples (*Table 5*). This can be assigned to the improving effect of CNTs on the adherence between the glass prepreg and aluminum plates and also to their reinforcing effect on the fiber. The similar alterations were obsrved in the lap shear strength values of the samples (*Table 5*). It should be noted that the increases impacts on lap shear strength of epoxy material by CNTs have been reported in some studies [32-33].

In the hardness tests (*Table 5*), it was observed that Parent-CNT nanoparticles do not have a significant effect on the hardness of E/G composites, while the effects of LCCNT and

Sample	Hardness (Shore D)	Lap Shear Strength (MPa)	Impact Strength (J m^{-2})	Fracture Toughness (MPa m$^{1/2}$)	Bending Strength (MPa)	Flexural Modulus (GPa)
E/C	64±1.2	10.7±0.8	86±1.2	6.4±0.37	45±5.5	5.4±250
E/C/Parent-CNT	65±1.0	11.0±0.8	96±8.0	6.9±0.39	47±6.0	5.8±300
E/C/LCCNT	69±0.7	11.4±0.5	97±5.0	10.9±0.6	70±6.0	6.5±150
E/C/HCCNT	73±1.7	12.0±0.7	100±6	11.1±0.4	85±8.0	8.3±300

Table 4 The mechanical characteristics of the carbon fiber-based samples
4. táblázat A szénszál alapú minták mechanikai jellemzői

Sample	Hardness (Shore D)	Lap Shear Strength (MPa)	Impact Strength (J m^{-2})	Fracture Toughness (MPa m$^{1/2}$)	Bending Strength (MPa)	Flexural Modulus (GPa)
E/G	1.5± 62.3	0.4± 10.5	10± 200	1.0± 19.0	11± 129	0.25± 8.2
E/G/Parent-CNT	1.0± 63.3	0.5± 10.9	11± 205	1.2± 19.4	14± 130	0.23± 8.7
E/G/LCCNT	1.5± 66.0	0.5± 11.4	9.0± 213	1.5± 20.5	10± 133	0.23± 9.1
E/G/HCCNT	2.0± 67.6	0.4± 11.8	14± 267	1.4± 23.6	13± 142	0.27± 9.5

Table 5 The mechanical characteristics of the glass fiber-based samples
5. táblázat Az üvegszál alapú minták mechanikai jellemzői

HCCNT derivatives are more significant. This can be related to the increase of interfacial interactions in the nanocomposite and also to intrinsic reinforcing effect of CNTs. As a comparision with the reported studies, it was found that Mahadevaswamy et al. have also observed an increasing effect of MWCNTs on the hardness of E/G matrix [31].

It is clear that the presence of COOH functionality on the CNTs surface can play an important role on the mechanical properties of the prepared nanocomposites. These observations can be explained through the type of functional groups, the nature of glass fiber and epoxy resin, and the CNT distribution in nanocomposite bulk. It is expected that the COOH-functionalized CNTs exhibit stronger interactions with the fiber (containing SiO_2 units) and epoxy (containing OH and epoxide groups) than the parent-CNT. However, due to their weaker interactions with the composite bulk, the pure-CNT has revealed the less reiforement in the E/G composites compared to the functionalizec-CNTs. The properties can be a function of nanoparticle distribution in the texture of composites, the strength of E/G and nanoparticle/epoxy interactions, and the potential of nanoparticles to agglomerate. In general, fillers can strengthen polymers by four mechanisms, 1- inherent strength of the filler, 2- reducing the movements of polymer strands, 3- improving the interaction between composite ingredients and 4- interlayer stress transfer. Here, parent-CNT cannot create better interactions with epoxy fibers than LCCNT and HCCNT, thereby which the mechanical characteristics of E/G/Parent-CNT was found to be lower than the samples containing functionalized nanoparticles. Moreover,the imaginable accelerating effect of the functionalized CNTs on the curing process of epoxy (represented in *Fig. 4*) can also be occurred and effective in the case of E/G composites. The positive effect of pure carbon nanotubes on these mechanical property can be related to its inherent strength. But in the case of functionalized CNTS, the functionalization can affect on the CNT dispersion and E/G intractions as well as intrinsinc reinforcing effect of CNTs.

4. Conclusions

The multi wall carbon nanotube and its derivatives were successfully incorporated within the E/C and E/G composite separately *via* the hand lay up of the fiber prepregs and then compression moulding by using hot press. The SEM analysis confirmed the good dispersion of HCCNT and LCCNT samples into the epoxy/fiber matrices as compared to the Parent-CNT. The mechanical analyses showed the improveing effects of the carbon nanotube samples on the epoxy/fiber matrices as the order of HCCNT > LCCNT > Parent-CNT. In other words, HCCNT considerablely improves the mechanical characteristics of the nanocomposites in comparision to LCCNT and Parent-CNT. This could be ascribed to its higher COOH content as compared to other CNTs. Undoubtedly, COOH functionality can induce amphiphilic nature into CNT and affcet the CNT dispersion in the epoxy and its iteractions with the composite components.

References

[1] Khater, H. M., El Nagar, A. (2021) Evaluation of chloride resistance of silica fume and glass waste MWCNT-geopolymer composite. Epitoanyag-Journal of Silicate Based & Composite Materials. Vol. 73, No. 2, pp. 44-53. https://doi.org/10.14382/epitoanyag-jsbcm.2021.8

[2] Žižlavský, T., Vyšvařil, M., Rovnaníková, P. (2019) Rheology of natural hydraulic lime pastes modified by non-traditional biopolymeric admixtures. Epitoanyag-Journal of Silicate Based & Composite Materials. Vol. 71, No. 6, pp. 204-209. https://doi.org/10.14382/epitoanyag-jsbcm.2019.36

[3] Nazarpour-Fard, H. (2022) Composites of polyvinylpyrrolidone and polystyrene with rice husk ash as a bio and silica-rich material: thermal characteristics and water vapor absorption ability. Epitoanyag-Journal of Silicate Based & Composite Materials. Vol. 74, No. 6, pp. 229-236. https://doi.org/ 10.14382/epitoanyag-jsbcm.2022.33

[4] Shamsi, R., Asghari, G. H., Mir Mohamad Sadeghi, G., Nazarpour-Fard, H. (2018) The effect of multiwalled carbon nanotube and crosslinking degree on creep–recovery behavior of PET waste originated-polyurethanes and their nanocomposites. Polymer Composites. Vol. 39, No. S2, pp. E1013-E1024. https://doi.org/10.1002/pc.24420

[5] Nazarpour-Fard, H., Rad-Moghadam, K., Shirini, F., Beheshty, M. H., Asghari, G. H. (2018) Reinforcement of epoxy resin/carbon fiber composites by carboxylated carbon nanotubes: a dynamic mechanical study. Polimery. Vol. 63, No. 4, pp. 253-263. https://doi.org/ 10.14314/polimery.2018.4.1

[6] Dasari, S., Lohani, S., Prusty, R. K. (2022) An assessment of mechanical behavior of glass fiber/epoxy composites with secondary short carbon fiber reinforcements. Journal of Applied Polymer Science. Vol. 139, No. 12, pp. 51841. https://doi.org/10.1002/app.51841

[7] Soethe, V. L., Nohara, E. L., Fontana, L. C., Rezende, M. C. (2011) Radar absorbing materials based on titanium thin film obtained by sputtering technique. Journal of Aerospace Technology and Management. Vol. 3, No. 3, pp. 279-286. https://doi.org/10.5028/jatm.2011. 03030511

[8] Jagadeesh, P., Puttegowda, M., Girijappa, Y. G. T., Rangappa, S. M., Siengchin, S. (2022) Carbon fiber reinforced areca/sisal hybrid composites for railway interior applications: Mechanical and morphological properties. Polymer Composites. Vol. 43, No. 1, pp. 160-172. https://doi.org/10.1002/PC.26364

[9] Heydenreich, R. (1998) Cryotanks in future vehicles. Cryogenics. Vol. 38, pp. 125–130. https://doi.org/10.1016/S0011-2275(97)00122-7

[10] Bechel, V. T, Camping, J. D, Kim, R. Y. (2005) Cryogenic/elevated temperature cycling induced leakage paths in PMCs. Composites Part B: Engineering. Vol. 36, No. 2, pp. 171–182. https://doi.org/10.1016/j.compositesb.2004.03.001

[11] Yoshimura, A., Nakao, T., Yashiro, S., Takeda, N. (2008) Improvement on out-of-plane impact resistance of CFRP laminates due to through-the-thickness stitching. Composites Part A: Applied Science and Manufacturing. Vol. 39, No. 9, pp. 1370-1379. https://doi.org/10.1016/j.compositesa.2008.04.019

[12] Ray, B. C. (2006) Temperature effect during humid ageing on interfaces of glass and carbon fibers reinforced epoxy composites.

Journal of Colloid and Interface Science. Vol. 298, No. 1, pp. 111-117. https://doi.org/10.1016/j.jcis.2005.12.023

[13] Rodriguez, A. J., Guzman, M. E., Lim, C. S., Minaie, B. (2011) Mechanical properties of carbon nanofiber/fiber-reinforced hierarchical polymer composites manufactured with multiscale-reinforcement fabrics. Carbon. Vol. 49, No. 3, pp. 937-948. https://doi.org/10.1016/j.carbon.2010.10.057

[14] Vartak, D. A. (2022) Carbon nanotube composites to enhance thermal and electrical properties for space applications-a review. Journal of Environmental Nanotechnology. Vol. 11, No. 3, pp. 11-21. https://doi.org/10.13074/jent.2022.09.223456

[15] Siddiqui, N. A., Khan, S. U., Ma, P. C., Li, C. Y., Kim, J. K. (2011) Manufacturing and characterization of carbon fibre/epoxy composite prepregs containing carbon nanotubes. Composites Part A: Applied Science and Manufacturing. Vol. 42, No. 10, pp.1412-1420. https://doi.org/10.1016/j.compositesa.2011.06.005

[16] Yazid, A. F., Mukhtar, H., Nasir, R., Mohshim, D. F. (2022) Incorporating carbon nanotubes in nanocomposite mixed-matrix membranes for gas separation: a review. Membranes. Vol. 12, No. 6, pp. 589. https://doi.org/10.3390/membranes12060589

[17] Tamayo-Vegas, S., Muhsan, A., Liu, C., Tarfaoui, M., Lafdi, K. (2022) The effect of agglomeration on the electrical and mechanical properties of polymer matrix nanocomposites reinforced with carbon nanotubes. Polymers. Vol. 14, Vol. 9, pp. 1842. https://doi.org/10.3390/polym14091842

[18] Abobo, I. M., Rodriguez, L. D., Salvador, S. D., Siy, H. C., Penaloza. J, D. P. (2021) Effect of organoclay reinforcement on the mechanical and thermal properties of unsaturated polyester resin composites. Epitoanyag-Journal of Silicate Based & Composite Materials. Vol. 73, No. 2, pp. 63-.67. https://doi.org/10.14382/epitoanyag-jsbcm.2021.10

[19] Kim, M. G., Hong, J. S., Kang, S. G., Kim C. G. (2008) Enhancement of the crack growth resistance of a carbon/epoxy composite by adding multi-walled carbon nanotubes at a cryogenic temperature. Composites Part A: Applied Science and Manufacturing. Vol. 39, No. 4, pp. 647-654. https://doi.org/ 10.1016/j.compositesa.2007.07.017

[20] Hossain, M. K., Chowdhury, M. M. R., Salam, M. B. A., Jahan, N., Malone, J., Hosur, M. V., Jeelani, S., Bolden, N. W. (2015) Enhanced mechanical properties of carbon fiber/epoxy composites by incorporating XD-grade carbon nanotube. Journal of Composite Materials. Vol. 49, No. 18, pp. 2251-2263. https://doi.org/ 10.1177/0021998314545186

[21] Rana, S., Alagirusamy, R., Joshi, M. (2011) Single-walled carbon nanotube incorporated novel three phase carbon/epoxy composite with enhanced properties. Journal of Nanoscience and Nanotechnology. Vol. 11, No. 8, pp. 7033-7036. https://doi.org/10.1166/jnn.2011.4226

[22] Taş, H., Soykok, I. F. (2019) Effects of carbon nanotube inclusion into the carbon fiber reinforced laminated composites on flexural stiffness: A numerical and theoretical study. Composites Part B: Engineering. Vol. 159, pp. 44-52. https://doi.org/10.1016/j.compositesb.2018.09.055

[23] Niazi, M., Beheshty, M. H. (2019) A new latent accelerator and study of its effect on physical, mechanical and shelf-life of carbon fiber epoxy prepreg. Iranian Polymer Journal. Vol. 28, pp. 337-346. https://doi.org/10.1007/s13726-019-00704-8

[24] Seki, Y. (2009) Innovative multifunctional siloxane treatment of jute fiber surface and its effect on the mechanical properties of jute/thermoset composites. Materials Science and Engineering A. Vol. 508, No. (1-2), pp. 247-252. https://doi.org/10.1016/j.msea.2009.01.043

[25] Ma, P. C., Kim, J. K., Tang, B. Z. (2007) Effects of silane functionalization on the properties of carbon nanotube/epoxy nanocomposites. Composites Science and Technology. Vol. 67, No. 14, pp. 2965-2972. https://doi.org/10.1016/j.compscitech.2007.05.006

[26] Srinivasa C. V., Bharath, K. N. (2011) Impact and hardness properties of areca fiber-epoxy reinforced composites. Journal of Materials and Environmental Science. Vol. 2, No. 4, pp. 351-356.

[27] Bilisik, K., Erdogan, G., Sapanci, E., Gungor, S. (2019) Fracture toughness (mode-ii) of nanostitched composites. Procedia Structural Integrity. Vol. 21, pp. 146-153. https://doi.org/10.1016/j.prostr.2019.12.096

[28] Zakaria, M. Y., Sulong, A. B., Sahari, J., Suherman, H. (2015) Effect of the addition of milled carbon fiber as a secondary filler on the electrical conductivity of graphite/epoxy composites for electrical conductive material. Composites Part B: Engineering. Vol. 83, pp. 75-80. https://doi.org/10.1016/j.compositesb.2015.08.034

[29] Gupta, S. K., Shukla, D. K., Kaustubh Ravindra, D. (2021) Effect of nanoalumina in epoxy adhesive on lap shear strength and fracture toughness of aluminium joints. Journal of Adhesion. Vol. 97, No. 2, pp. 117-39. https://doi.org/10.1080/00218464.2019.1641088

[30] Zulfli, N. M., Bakar, A. A., Chow, W. S. (2013) Mechanical and water absorption behaviors of carbon nanotube reinforced epoxy/glass fiber laminates. Journal of Reinforced Plastics and Composites. Vol. 32, No. 22, pp.1715-1721. https://doi.org/10.1177/0731684413501926

[31] Mahadevaswamy, M. B., Aradhya, R., Bhattacharya, S., Jagannathan S. R. Effect of hybrid carbon nanofillers at percolation on electrical and mechanical properties of glass fiber reinforced epoxy. Journal of Applied Polymer Science. Vol. 139, No. 26, pp. e52439 (2022). https://doi.org/10.1002/app.52439

[32] Hsiao, K. T., Alms, J., Advani, S. G. (2003) Use of epoxy/multiwalled carbon nanotubes as adhesives to join graphite fibre reinforced polymer composites. Nanotechnology. Vol. 14, No. 7, 791-793. https://doi.org/10.1088/0957-4484/14/7/316

[33] Srivastava, V. K. (2011) Effect of carbon nanotubes on the strength of adhesive lap joints of C/C and C/C–SiC ceramic fibre composites. International Journal of Adhesion and Adhesives. Vol. 31, No. 6, pp.486-489. https://doi.org/10.1016/j.ijadhadh.2011.03.006

Ref.:
Nazarpour-Fard, Hamed – **Beheshty**, Mohammad Hosain: *Reinforcing effect of MWCNT derivatives on glass/epoxy and carbon/epoxy composites perpendicular to the fiber direction*
Építőanyag – Journal of Silicate Based and Composite Materials, Vol. 75, No. 3 (2023), 101–108. p.
https://doi.org/10.14382/epitoanyag-jsbcm.2023.15

The impact of cement type on the correlation between non-destructive testing and the compressive strength of concrete

Ahmed MERAH
Professor, Civil engineering department. Research Professor; Faculty of Civil Engineering and Architecture, Amar Telidji University of Laghouat, Algeria. His research interests include: concrete durability, concrete carbonation, anti-carbonation coating.

Ahmed MERAH ▪ University AmmarTelidji of Laghouat, Faculty of Civil Engineering and Architecture, Research Laboratory of Civil Engineering (LRGC), Laghouat, Algeria ▪ a.merrah@lagh-univ.dz

Érkezett: 2023. 01. 02. ▪ Received: 02. 01. 2023. ▪ https://doi.org/10.14382/epitoanyag-jsbcm.2023.16

Abstract
Buildings' concrete structures are weakened by destructive tests like "coring", which compress cylindrical specimens in the lab to measure the compressive strength of in situ hardened concrete. These tests also produce trash that is hazardous to the environment. Alternative methods to destructive concrete testing include rebound hammering and ultrasonic non-destructive testing of hardened concrete. The first goal of this research is to determine the link between compressive strength, rebound hammer, and ultrasonic pulse velocity tests. The second goal is to investigate the impact of cement type and concrete age on these correlations. In this case, two cement kinds (CEM I 42.5 and CEM II 42.5) and two concrete compositions based on local resources were developed in this context. Simultaneous tests on cubic samples (ultrasonic test, rebound hammer test, compressive strength test) were conducted at ages 7 and 28 days. According to the studies' findings, there is a strong association between compressive strength and the ultrasonic and rebound hammer tests. The compressive strength of concrete can be predicted using these relationships without the requirement for destructive testing. Additionally, the results demonstrate that these correlations are impacted by the type of cement and the age of the concrete, demonstrating that these two parameters have an impact on the outcomes and that it is important to consider them.
Keywords: non-destructive testing, rebound hammer, ultrasonic pulse velocity, compressive strength, cement type
Kulcsszavak: rombolásmentes vizsgálat, Schmidt kalapács, ultrahangos impulzussebesség, nyomószilárdság, cement típus

1. Introduction

The compressive strength of the concrete is a crucial indicator of the quality of this material. This characteristic is often measured using the compressive strength test on concrete samples, that have been prepared in the site. In order to confirm the obtained concrete's compressive strength by using the compression test in the laboratory, the quality of the hardened concrete on the site can be also checked using nondestructive tests, such as the rebound hammer and the ultrasonic pulse velocity test. These types of tests are simpler to carry out and allow for a quick assessment of the concrete's compressive strength to withstand the stresses planned by the engineering design.

In the past few decades, numerous tests on hardened concrete have been developed. These tests are categorized as either completely non-destructive (where there is no damage to the concrete), slightly destructive (where there is slight damage to the concrete), or partially destructive (where there is some damage to the concrete), such as coring.

These two concrete tests have drawbacks that are economic and structural stability because the coring test on the hardened concrete is typically conducted on structural elements by taking sample cores. Moreover, the destructive control methods are divided into two classes, which are: the coring test performed on the actual structure and the compressive strength performed in the laboratory on samples test constructed on site.

However, the coring operations on the concrete are expensive and the concrete structures tested can undergo degradations, which will weaken the concrete structures and minimize their service life. In the same context, the compressive tests made in the laboratory on samples, are not generally representative because they are not made in the same conditions of the site. Moreover, these samples generate significant waste, which has a harmful effect on the environment. To address this concern, the non-destructive methods are coming to remedy to these drawbacks by offering a practical and reliable means to control the concrete without damage.

In this paper, non-destructive techniques based on ultrasonic pulse velocity and the rebound hammer are the focus. The major goal of this research is to establish a correlation between the compressive strength of concrete on cylindrical samples, using a combination of the rebound hammer, ultrasonic pulse velocity, and other techniques without using the destructive tests. The obtained relationship will enable the civil engineer to forecast the compressive strength of structural components without using the destructive tests.

A mathematical model was created in this field to predict the compressive strength of hardened concrete on the site. This model provides a relationship between the compressive strength of the cores taken from the building concrete

and the compressive strength determined by the two non-destructive tests, the ultrasound pulse velocity and the Rebound hammer [1]. Other models based on combined non-destructive test (rebound hammer and ultrasonic velocity) were developed by Revilla-Cuesta V et al. [2], in order to predict the compressive strength of high flowability SCC in real structures. There is a strong correlation between all the models in a linear mathematical relationship between compressive strength and Rebound Number readings using the Minitab 15 program; the correlation ranges from 91% to 98%, indicating a perfect relationship between the concrete compressive strength and the readings of Rebound Hammer Number [3]. Additionally, the destructive compressive test and the rebound hammer test were correlated using MATLAB software, and the three obtained relations (linear, quadratic, and cubic) allowed for the evaluation of the compressive strength of concrete using only the rebound hammer test. These relations were as follows:

Linear relation $f = 1.0501x_1 - 11.8402$ (1)

Quadratic relation $f = -0.0078\ x_1^2 + 1.5979\ x_1 - 21.1986$ (2)

Cubic relation $f = -0.029\ x_1^3 + 0.2975\ x_1^2 - 8.8004x_1 + 94.4267$ (3)

Where x_1 = is the Schmidt hammer rebound strength (MPa), these relationships can be used by engineers to predict the concrete compressive strength [4]. Moreover, the validity of the analytical models that were published in the literature was tested using a destructive and non-destructive test database. This work suggests a fresh, reliable model that can forecast the compressive strength of structures made of Italian reinforced concrete [5]. Similar to this, a study was carried out to evaluate the compressive strength of concrete utilizing ultrasonic pulse velocity and Rebound Hammer testing. The results of this study show that the concrete compressive strength measured via sample smashing, non-destructive tests (ultrasonic pulse velocity and Rebound Hammer), and combination testing are all connected by this relationship. The relationship is:

$fc\ (V, R) = -173.04 + 4.07V^2 + 57.96\ V + 1.31\ R$ [6] (4)

A mixed empirical model using non-destructive techniques is also included (Rebound Hammer and Utrasonic pulse velosity). This model allows for a 10% error in the prediction of concrete compressive strength [7].

In order to evaluate the compressive strength of concrete structures in the cities of Izmit and Istanbul (Turkey), a further combined method test (combination between the concrete core strength and Ultrasonic Pulse Velocity) is also utilized. The linear relationships are as follows:

CCS = 0.544 (UPV) -15.343 with a correlation
$R^2 = 0.8452$ (Cores of Istanbul) (5)

CCS = 0.062 (UPV) -46.497 with a correlation
$R^2 = 0.914$ (Cores of Izmit) (6)

CCS: Concrete Core Strength, UPV = Ultrasonic Pulse Velocity. Since each region has its unique aggregates and cements that affect the results of ultrasonic testing, it is evident from relations (5) and (6) that each region has its own relation, indicating the need to construct a relation for each region [8, 9]. On the other hand, the non-destructive tests used to ascertain the mechanical characteristics of the hardened concrete demonstrate that the evaluation of the strength of the concrete is significantly influenced by the hardness of the particles [10]. Calibration of the obtained compressive strength with the non-destructive methods and the compressive strength of the cylindrical samples (cores) extracted from the same structural elements close to the non-destructive test locations are required due to the variation in the mechanical properties of the concrete tested on site and its relationship with the combined test methods [11]. Studies were conducted on the impact of the components of concrete, the mixture, and the variables related to the effectiveness of non-destructive testing methods for concrete (Rebound Number and Ultrasonic Pulse Velocity) to create a method that combines the two approaches for evaluating the compressive strength of concrete. This study demonstrates that the Rebound Hammer Number increases with concrete compressive strength and that cement kinds, aggregate types, and the presence of voids in concrete have a significant impact on ultrasonic pulse velocity outcomes. Combining the two approaches will address these drawbacks and enable accurate evaluation of concrete compressive strength [12]. The variability of NDT measures can be studied with statistical analyses in order to increase the dependability of the results from non-destructive tests [13]. Additionally, a survey of the non-destructive methods' literature reveals that most of the (NDT) techniques are founded on empirical relationships supplied by the devices' producers. These devices' output findings need to be adjusted utilizing a set of laboratory-conducted correlations [14, 15]. The dependability of the data obtained depends on the type of non-destructive tools used, such as the rebound Hammer [16]. A method for calibrating non-destructive tests on the spot is also needed to enhance the assessment of concrete durability indicators. The study of the in-situ data and the acquisition of the sustainability indicators were the two goals for which this calibration was suggested (porosity and degree of saturation). Compressive strength and water content can both be accurately assessed in the same setting [17, 18]. Non-destructive tests were reviewed, their benefits and drawbacks shown, and a classification of these techniques based on these factors and their applications formed [19]. The accuracy of the concrete compressive strength prediction formulas, which are most frequently employed in Italy, is also examined using the findings of the Rebound Hammer and Ultrasonic pulse velocity. The combined techniques (Rebound Hammer and Ultrasonic Velocity) can increase their accuracy and forecast the compressive strength of concrete [20].

The obtained relationships were the following:

$$f_c = 7.695.10^{-11}.(RI)^{1.4}.(V)^{2.6} \quad (7)$$

$$f_c = 1.2.10^{-9}.(RI)^{1.058}.(V)^{2.446} \quad (8)$$

$$f_c = 0.0286.(RI)^{1.246}.(V)^{1.85} \quad (9)$$

Additionally, relationships between destructive and non-destructive tests were proposed, and these relationships make it possible to combine the two non-destructive tests—ultrasonic pulse velocity and non-destructive test—to estimate the concrete's compressive strength (ultrasonic velocity and Rebound Hammer). These connections also depend on the tested concretes' range of compressive strengths [21, 22]. a connection between the compressive strength of cubes or cylinders, the ultrasonic pulse velocity measurement

method, and the rebound hammer. There is a 20% inaccuracy indicated [23]. The ultrasonic pulse velocity approach is the most effective method for assessing the compressive strength of existing reinforced concrete structures, according to their study [24, 25]. Furthermore, as concrete ages, the compressive strength measured using destructive and non-destructive tests declines [26]. Another option is to estimate how much the old structures are deteriorating using non-destructive approaches [27, 28]. Moreover, the results from these tests are influenced by numerous factors such as the w/c ratio, concrete carbonation, cure and the cement type [29].

The main goal of this work is to investigate and emphasize these impacts because, according to earlier research in the field listed in this one, they have not been studied in relation to non-destructive test findings. The first step in conducting this investigation is to establish a correlation between the compressive strength measured by crushing (a destructive method) and the Rebound Hammer and ultrasonic pulse velocity indices. The readings of the Rebound Hammer and Ultrasonic Pulse Velocity are also influenced by the type of cement used in the creation of concrete. The second portion of this work involved two concrete formulations using two different types of cements (NA 442- CEM I 42.5 R and CEM II/A-L 42.5 R). The findings of this study indicate that the relationship between compressive strength and non-destructive testing is influenced by the kind of cement and the age of the concrete (the Rebound Hammer and Ultrasonic Pulse Velocity). Additionally, without using destructive tests, the results for the two types of cement enable engineers to anticipate the compressive strength of concrete buildings in situ.

2. Materials

2.1 Cements

The two types of cements used in this study (NA 442- CEM I 42.5 R and CEM II/A-L 42.5 R) were made in BISKRA, which is in the southeast of Algeria, and are known as BISKRIA CEMENT. The characteristics with regard to Algerian Standard NA 442 are presented for NA 442- CEM I 42.5 R in the *Tables 1, 2*, and *3* and for CEM II/A-L 42.5 R in the *Tables 4, 5*, and *6*, respectively.

The cements densities are respectively 3.07 g/cm^3 for NA 442- CEM I 42.5 R and 3.13 g/cm^3 for CEM II/A-L 42.5 R.

Elements	Content %	Standards
SO_3	2.30	(NA 237) < 3.5%
CL	0.028	(NA 5080) ≤ 0.1%
P.A.F	2.04	(NA 237) ≤ 5%
C_3S clinker	62	In accordance with Bogue
C_2S clinker	13	In accordance with Bogue
C_3A clinker	1.5	In accordance with Bogue
C_4AF clinker	17	In accordance with Bogue

Table 1 Chemical characteristics of used cement NA 442- CEM I 42.5 R
1. táblázat A felhasznált cement NA 442- CEM I 42.5 R kémiai jellemzői

Designation	Measures	Standards
Specific surface Blaine (cm²/g)	3420	(NA231)
Start of taking (min)	180	(NA233) ≥60 min
Hot expansion (min)	0.5	≤10mm(NA232)
Consistence (%)	25.7	T(NA290)

Table 2 Physics characteristics of used cement NA 442- CEM I 42.5 R
2. táblázat A felhasznált cement NA 442- CEM I 42.5 R fizikai jellemzői

Mechanic proprieties			
Compressive strength (MPa)	2 days	≥10	10
	28 days	62.5≥R≥42.5	40

Table 3 Mechanic characteristics of used cement NA 442- CEM I 42.5 R
3. táblázat A felhasznált cement NA 442- CEM I 42.5 R mechanikai jellemzői

Elements	Content %	Standards NA 442
SO_3	2.00	< 3.5%
CL^-	0.08	≤ 0.1%
C_3S clinker	60	In accordance with Bogue
C_2S clinker	6	In accordance with Bogue

Table 4 Chemical characteristics of used cement CEM II/A-L 42.5 R
4. táblázat A felhasznált cement CEM II/A-L 42,5 R kémiai jellemzői

Designation	Measures	Standards
Specific surface Blaine (cm²/g)	4200	(NA442)
Start of taking (min)	180	(NA442) ≥60 min

Table 5 Physics characteristics of cement CEM II/A-L 42.5 R
5. táblázat A CEM II/A-L 42,5 R cement fizikai jellemzői

Mechanic characteristics		
Compressive strength (MPa)	2 days	≥10
	28 days	62.5≥R≥42.5

Table 6 Mechanic characteristics of cement CEM II 42.5/A-L 42.5 R
6. táblázat A CEM II 42.5/A-L 42.5 R cement mechanikai jellemzői

2.2 Aggregates

- Sand

The alluvial sand utilized in the two concrete formulations originates from the Oued M'zi quarry, which is close to the Algerian city of Laghouat. According to the granulometric analysis curve (*Fig. 1*), this sand has tight granulometry and ranges in fineness from around 2.5 to 5 mm. Its sand equivalent indicates that it is clean sand, and by current standards, it may be utilized to produce high-quality concrete.

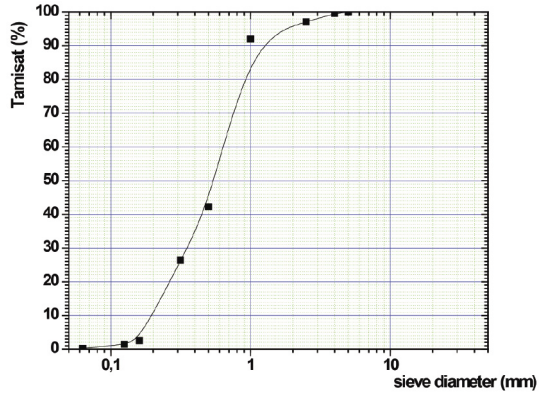

Fig. 1 Curve of granulometric of used sand
1. ábra A használt homok szemcseméret-eloszlása

▪ Gravels

The gravel utilized was limestone crushed gravel, consisting of two granular classes with sizes ranging from 3 to 8 millimeters to 8 to 15 millimeters, and it came from a quarry in Algeria's Laghouat region. The granulomere curves for the two categories of gravel are shown in *Fig. 2*. The physical characteristics of the employed gravels are summarized in *Table 7*.

Physical characteristic of the used gravels and sand	Standard	Aggregates		
		Sand	Gravels	
		0/5	3/8	8/15
Apparent Density (g/cm³)	NF P 18-554	1.564	1.319	1.255
Absolute density (g/cm³)		2.6	2.65	2.65
Absorption Coefficient (%)		1	1.5	1.5

Table 7 Physical characteristic of the used aggregates
7. táblázat A felhasznált aggregátumok fizikai jellemzői

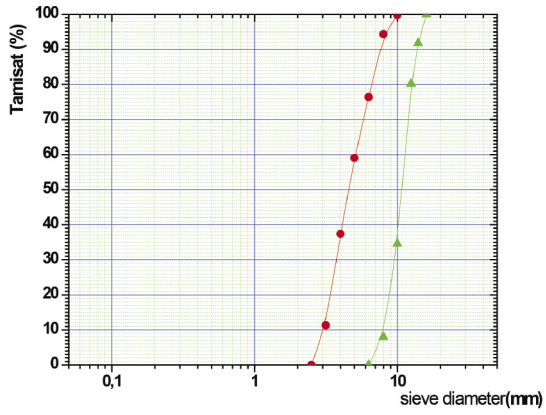

Fig. 2 Granulometric curve of the two classes of gravels size 3-8 mm and 8-15mm
2. ábra A 3-8 mm és a 8-15 mm méretű kavicsok két osztályának szemcseméret-eloszlási görbéje

Fig. 2 show, that the grain size is acceptable for both classes of the used gravel.

▪ Concrete formulations

The DREUX GORISSE method was used to formulate the concrete, and *Table 8* shows the outcomes of various formulations.

Designation of components		Constituent per weights (kg/m³)	Concrete density (kg/m³)	Slump test (cm)
		Biskria Cement E/C=0.6	2270	7.5
Cement	CEM II/A-L 42.5 R	350		
	NA 442- CEM I 42.5 R	350		
Sand 0-5 mm		586,5		
Gravel	3-8mm	174,8		
	8-15mm	943,5		
Water		215,44		

Table 8 Results of the two concretes formulations
8. táblázat A két betonkészítmény eredményei

All of the mixes were combined in a concrete mixer with a vertical axis and a fixed tank with a capacity of 130 litres after washing and drying the used aggregates.

Gravel, cement, and sand were introduced first before the other components. The water is added after one minute of dry mixing, and mixing is continued for at least two minutes to produce a homogeneous slurry. The workability was assessed immediately following each mixing in accordance with standard NF EN 12350-2 using the Abrams cone; the results of the slump test are displayed in *Table 8*.

▪ Preparation and storage of samples

For each type of cement, cubic samples measuring $10 \times 10 \times 10$ cm³ were prepared based on the concrete formulations' results (*Table 9*).

Storage mode	Age (days)	Number of confectioned samples		Water / cement
		CEM II/A-L 42.5 R	NA 442- CEM I 42.5 R	
Controlled humidity chamber	7	50	50	0.6
	28	50	50	

Table 9 Samples for the both concretes formulations
9. táblázat A két betonkészítmény mintái

All types of concrete were made in a laboratory setting. All samples were covered right after preparation to minimize the risk of excessive evaporation and plastic shrinkage. The samples were taken out of the moulds 24 hours later and maintained in the humid chamber (RH = 90%) (*Fig. 3*).

Fig. 3 Samples conserved in laboratory environment
3. ábra Laboratóriumi környezetben tárolt minták

3. Methods

3.1 Materials used for destructive and non-destructive testing

The cubic samples were subjected to destructive and non-destructive tests at ages 7 and 28 days. To get ready for non-destructive tests, the faces of each cubic sample must be sanded with an abrasive stone prior to the start of each test.

The metal molds were used to prepare the 10 x 10 x 10 cm³ concrete cubic samples.

The non-destructive tests were conducted using a Schmidt Rebound Hammer and an ultrasonic pulse velocity instrument; the models of the utilizing devices are as follows:

3.1.1 Schmidt Rebound Hammer (Rebound Hammer)

The Rebound Hammer test entails projecting a load with a fixed initial energy onto the concrete surface. After the shock, some of the energy is absorbed by the concrete and some of it makes the mass bounce back. The impact energy is created by a system of springs, whose recoil movement's amplitude depends on the recoil energy and spring system properties.

A non-destructive method of assessing a concrete's strength is to measure its impact hardness. This approach is intriguing because it is straightforward and enables quick verifications of the consistency of the concrete in a construction.

The method for determining hardness involves measuring the amount of recoil that a spring-controlled mobile device experiences after colliding with a concrete surface. The Schmidt hammer test, also known as the Rebound Hammer test (*Fig. 4*), was created by ERNST SCHMIDT in 1948 and is one of the oldest non-destructive tests still in use today.

Fig. 4 Rebound Hammer type N model C 181
4. ábra C 181 típusú N típusú Schmidt kalapács C 181

- Operating mode of the Rebound Hammer

Before beginning the Rebound Hammer tests, the test pieces were placed between the press plates with the molded faces in contact, ensuring that the direction of compression was perpendicular to the direction of the concrete confection. This was done after the test pieces had undergone an ultrasound pulse velocity test to remove any remaining grease from their faces. According to standard NF EN 12504-2, the sample was maintained between the plates by compression under an initial load of around 15% of the final charge after the loading speed was set to 0.5 MPa/s (i.e., 5 KN/s, which corresponds to the 10 cm cube).

The maintained sample test's two opposite faces were subjected to twelve Rebound Hammer tests, which were conducted in the horizontal compression machine position (*Fig. 5*). The test result for each sample test is then expressed as a whole number in accordance with European Standard NF EN 12504-2 and represents the median value of all readings taken on both sides.

Fig. 5 Measurement of the rebound index with the Rebound Hammer
5. ábra A visszapattanási index mérése a Schmidt kalapáccsal

3.1.2 The ultrasonic device

The Ultrasonic Pulse Velocity is type E 46 with transducers of 50 mm of diameter and 54 kHz of frequency (*Fig. 6*).

Fig. 6 The used device of Ultrasonic Pulse Velocity
6. ábra Az ultrahangos impulzussebesség mérésére használt eszköz

- Operating mode of the ultrasonic Pulse velocity device

The operator must verify that the instrument is functioning correctly by calibrating it using the calibration bar before performing the ultrasonic tests. The direct transmission method was used to conduct the ultrasonic tests, ensuring that the direction of transit time measurement was parallel to the direction of preparation. The two transducers were positioned on the opposing sides of the test tube with a thin coating of grease in between them (*Fig. 7*), and the transit time in microseconds was then recorded. According to standard NF EN 12504-4, the ultrasonic test result for each sample is the median value of two measurements made in both directions. As a result, the determined ultrasonic speed is expressed as 0.01 km/s.

Fig. 7 Transit time measurement with ultrasonic device
7. ábra Átfutási idő mérése ultrahangos eszközzel

3.1.3 Compression machine

The study's damaging test was a straightforward compression test employing a hydraulic press with a 3000 kN capability (*Fig. 8, 9*).

Fig. 8 Hydraulic press with the capacity of 3000 kN
8. ábra 3000 kN kapacitású hidraulikus prés

Fig. 9 Crushing of the cubic samples
9. ábra A kocka alakú minták törése

4. Results and discussions

At the civil engineering research lab, these tests were conducted. Utilizing the hydraulic press described in the section prior, cubic samples were subjected to crushing tests, Rebound Hammer tests were conducted using a calibrated Rebound Hammer, and ultrasonic tests were conducted using a device available in the Laghouat University's Civil Engineering Research Laboratory.

4.1 Relationship between compressive strength (MPa) and the Rebound Hammer (I) in horizontal position

4.1.1 Concrete formulation with NA 442- CEM I 42.5 R at 7 and 28 days

The rebound Hammer index as a function of compressive strength at 7 and 28 days of concrete age is depicted in *Fig. 10*.

The correlations between the compressive strength and the Rebound Number (I) that were discovered from the *Fig. 10* are linear regressions.

For age 7 days CS = 0.33 I +19.278
with the coefficient of correlation $R^2 = 0.79$ (10)

For age 28 days CS = 1.4248 I - 24.44
with the coefficient of correlation $R^2 = 0.78$ (11)

Where CS is the predicted compressive strength of cubic samples in MPa and I is the rebound hammer number. These two relationships allow concretes made with cement type NA 442- CEM I 42.5 R to be estimated to have compressive strength using the reading of the Rebound Hammer Number at a young age (7 days) and at an age (28 days).

Additionally, these relationships demonstrate that the compressive strength of concrete cubic samples at 7 days of age was between 27 and 29 MPa, while at 28 days of age it was between 34 and 41 MPa. These data can be used to forecast the compressive strength of concretes made using NA 442- CEM I 42.5 R cement at the commonly applicable ages (7 days and 28 days) allowing the engineers to assess the concrete construction in-situ using just a nondestructive test (Rebound Hammer). These findings also demonstrate the impact of concrete age on compressive strength measurements made with a rebound hammer.

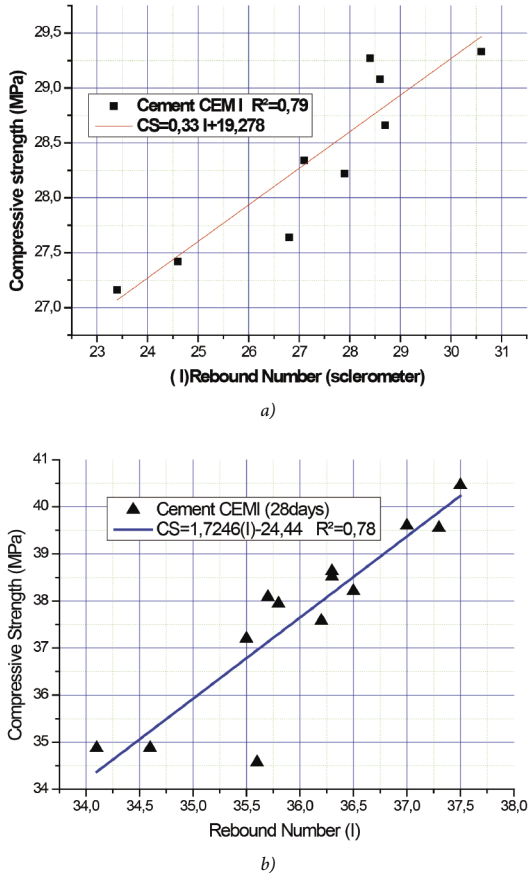

Fig. 10 Rebound Hammer Index as function of the compressive strength at 7 (a) and 28 (b) days age of concrete (NA 442- CEM I 42.5 R)
10. ábra A visszapattanási index a nyomószilárdság függvényében a beton 7 (a) és 28 (b) napos korában (NA 442- CEM I 42,5 R)

4.1.2 Concrete formulation with CEM II/A-L 42.5 R at 7 and 28 days

The compressive strength of concrete at 7 and 28 days old is shown in the *Fig. 11*, along with the rebound number of the Rebound Hammer.

The relationship (12) and (13) between the compressive strength and the Rebound Number(I) that were discovered from the *Fig. 11* are linear regressions.

For 7 days of age CS = 0.8518 I +4.6695
with the coefficient of correlation $R^2 = 0.83$. (12)

For 28 days of age CS = 0586 I + 17.57
with the coefficient of correlation $R^2 = 0.78$. (13)

Where CS: the predict compressive strength in (MPa) on cubic samples; I: Rebound Number.

For concretes that are formed using cement of the CEM II/A-L 42.5 R type, these two relationships (12) and (13) allow for the prediction of the compressive strength as a function of the reading of the Rebound Hammer index at early ages (7 days) and at ages of 28 days.

Additionally, these connections demonstrate that the concrete compressive strength of cubic samples at 7 days of age ranged from 27 MPa to 31 MPa, whereas that at 28 days of age ranged from 36 MPa to 40 MPa.

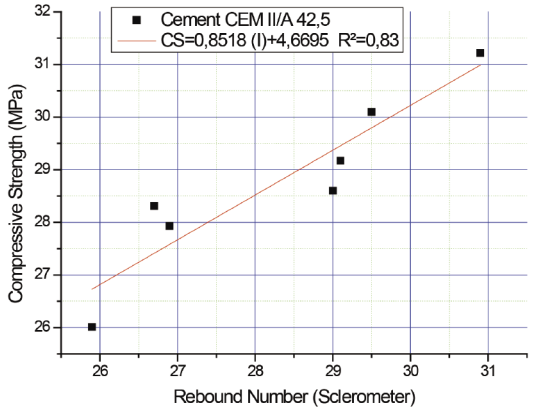

a)

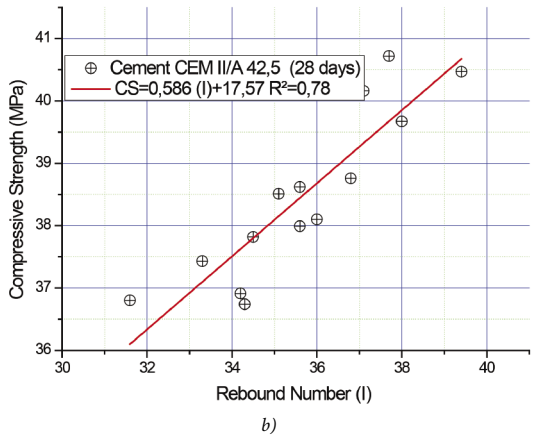

b)

Fig. 11 Rebound Hammer Index as function of the compressive strength at 7 (a) and 28 (b) days age of concrete (CEM II/A-L 42.5 R)

11. ábra A visszapattanási index a nyomószilárdság függvényében a beton 7 (a) és 28 (b) napos korában (CEM II/A-L 42.5 R)

These data can be used to forecast the compressive strength of concretes made using CEM II/A-L 42.5 R cement at the typically useful ages (7 days and 28 days) for the engineers to examine the concrete construction in-situ using just a non-destructive test (Rebound Hammer). Additionally, these data demonstrate that the type of cement has an impact on the outcomes of the rebound Hammer test. These correlations led to the conclusion that the age of the concrete and the kind of cement (NA 442- CEM I 42.5 R and CEM II/A-L 42.5 R) had an impact on the compressive strength of the concrete that can be measured using a non-destructive test (Rebound Hammer).

4.2 Relationship between compressive strength and the Ultrasonic Pulse velocity at 7 and 28 days of age

4.2.1 Concrete formulation using cement type NA 442- CEM I 42.5 R at 7 and 28 days

The ultrasonic pulse velocity at 7 and 28 days of concrete age is shown in *Fig. 12* as a function of compressive strength.

The connections between compressive strength and ultrasonic pulse velocity (V) derived from *Fig. 12* are linear regressions.

For 7 days of age CS = 0.002 V +19.29 with the coefficient of correlation

$R^2 = 0.83$ (14)

For 28 days of age CS = 0.01516 V - 25.328 with the coefficient of correlation

$R^2 = 0.87$ (15)

Where V is the ultrasonic pulse velocity and CS is the predicted compressive strength in MPa for concrete cubic samples. With the aid of these two relationships, compressive strength can be predicted using the Ultrasonic Pulse Velocity reading for both young (7-day-old) concretes and older concretes (28-day-old) made with the NA 442- CEM I 42.5 R cement type. Additionally, these connections demonstrate that the compressive strength of concrete cubic samples at 7 days of age ranged from 26 MPa to 30 MPa, whereas that at 28 days of age it ranged from 36 MPa to 42 MPa.

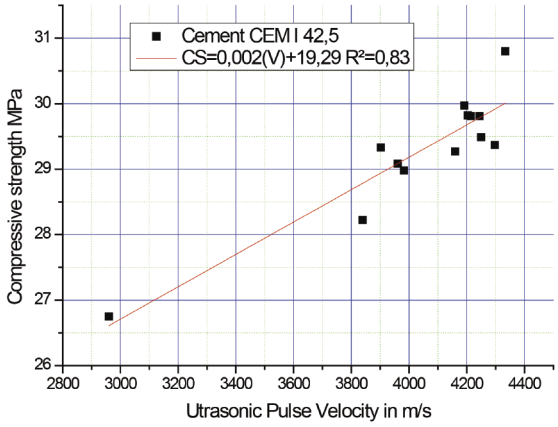

a)

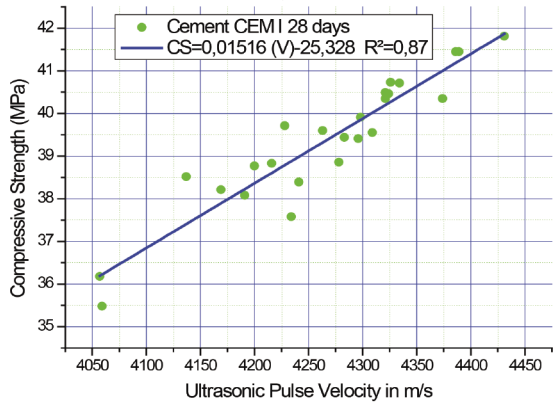

b)

Fig. 12 Ultrasonic Pulse velocity as function of the compressive strength at 7 (a) and 28 (b) days of concrete age (NA 442- CEM I 42.5 R)

12. ábra Ultrahangos impulzussebesség a nyomószilárdság függvényében a beton 7 (a) és 28 (b) napos korában (NA 442- CEM I 42.5 R)

These obtained results can be used in the prediction for the compressive strength of concretes formulated using the NA 442- CEM I 42.5 R cement type at the generally useful age (7 days and 28 days) for the check in-situ by the engineers of the concrete structure using only a non-destructive test (Ultrasonic Pulse Velocity).

These correlations lead to the conclusion that the cement type (NA 442- CEM I 42.5 R and CEM II/A-L 42.5 R) and the age of the concrete have an impact on the results of the non-destructive test for concrete compressive strength (Ultrasonic Pulse velocity).

4.2.2 Concrete formulation using cement type CEM II/A-L 42.5 R at 7 and 28 days of age.

Fig. 16 and *17* depict the relationship between the ultrasonic pulse velocity and the compressive strength of concrete at 7 and 28 days of age.

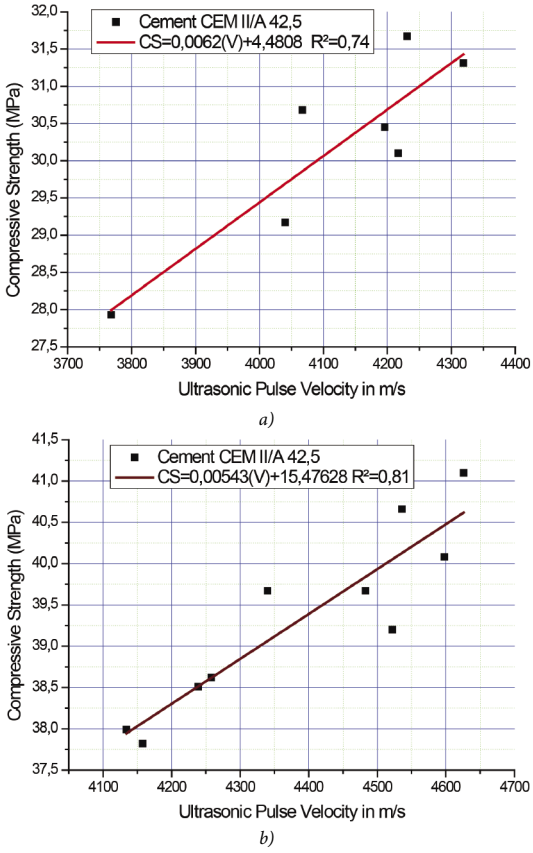

Fig. 13 Ultrasonic Pulse velocity as function of the compressive strength at 7 (a) and 28 (b) days of concrete age (CEM II/A-L 42.5 R)

13. ábra Ultrahangos impulzussebesség a nyomószilárdság függvényében a beton 7 (a) és 28 (b) napos korában (CEM II/A-L 42.5 R)

The connections between compressive strength and ultrasonic pulse velocity (V) derived from *Fig. 13* are linear regressions.

For 7 days of age CS = 0.0062 V + 4.4808
with the coefficient of correlation R^2=0.74 (16)

For 28 days of age CS = 0.00543 V + 15.47628
with the coefficient of correlation R^2=0.81 (17)

Where CS is the anticipated compressive strength of cubic samples in MPa and V is the ultrasonic pulse velocity. The compressive strength can be predicted using the Ultrasonic Pulse Velocity reading for concretes at a young age (7 days) and at an older age of 28 days for concretes made with CEM II/A-L 42.5 R cement type thanks to these two connections.

Furthermore, these connections demonstrate that while the compressive strength of cubic samples at 7 days ranged from 26 MPa to 31 MPa, it varied from 38 MPa to 41 MPa at 28 days. These data can be used to forecast the compressive strength of concretes made using CEM II/A-L 42.5 R cement at the typically usable ages (7 days and 28 days) for the engineers to examine the concrete construction in-situ using only the non-destructive test (Ultrasonic Pulse Velocity).

These correlations lead us to the conclusion that the age of the concrete and the type of cement (CEM I 42.5 and CEM II/A-L 42.5 R) have an impact on the results of the non-destructive test for concrete compressive strength (Ultrasonic Pulse velocity).

5. Conclusions

These relationships were developed for two cement types (CEM I 42.5 and CEM II/A-L 42.5 R), and for two concrete ages, namely 7 and 28 days. In this work, relationships between concrete compressive strength and non-destructive testing (Rebound Hammer and Ultrasonic Pulse Velocity) have been established.

The following conclusions can be summarized from these relationships:

1. Using non-destructive testing tools (Rebound Hammer and Ultrasonic Pulse Velocity), engineers can use the relations to predict the compressive strength of concrete in situ for concrete ages of 7 and 28 days.
2. The age of the concrete affects the results obtained using the non-destructive tests; as a result, engineers must take the age of tested concrete into account when using these relations.
3. The type of cement has an impact on the obtained regression linking the concrete compressive strength and non-destructive tests.
4. Based on these findings, relationships between compressive strength and non-destructive tests for the three most common concrete aging times — 7, 14, and 28 days —need to be established.

References

[1] Kheder GF. (1999) A two stage procedure for assessment of in situ concrete strength using combined non-destructive testing. Mater Struct. Vol. 32. p.410. https://doi.org/10.1007/BF02482712

[2] Revilla-Cuesta V, Skaf M, Serrano-López R, et al. Models for compressive strength estimation through non-destructive testing of highly self-compacting concrete containing recycled concrete aggregate and slag-based binder. Constr Build Mater. 2021 Vol. 280. 122454. https://doi.org/10.1016/j.conbuildmat.2021.122454

[3] Samson D, Omoniyi TM. Correlation between non-destructive testing (NDT) and destructive testing (DT) of compressive strength of concrete. Int J Eng Sci Invent. 2014;3:12–17.

[4] Hajjeh HR. Correlation between destructive and non-destructive strengths of concrete cubes using regression analysis. Contemp Eng Sci. 2012;5:493–509.

[5] Cristofaro MT, Viti S, Tanganelli M. New predictive models to evaluate concrete compressive strength using the SonReb method. J Build Eng. 2020;27:100962.

[6] Shariati M, Ramli-Sulong NH, Arabnejad MM, et al. Assessing the strength of reinforced concrete structures through Ultrasonic Pulse Velocity and Schmidt Rebound Hammer tests. Sci Res Essays. 2011;6:213–220.

[7] Tsioulou O, Lampropoulos A, Paschalis S. Combined non-destructive testing (NDT) method for the evaluation of the mechanical characteristics of ultra high performance fibre reinforced concrete (UHPFRC). Constr Build Mater. 2017;131:66–77.

[8] Jain A, Kathuria A, Kumar A, et al. Combined use of non-destructive tests for assessment of strength of concrete in structure. Procedia Eng. 2013;54:241–251.

[9] Kurtulus C, Bozkurt A. Determination of concrete compressive strength of the structures in Istanbul and Izmit Cities (Turkey) by combination of destructive and non-destructive methods. Int J Phys Sci. 2011;6:4044–4047.

[10] Pucinotti R. The use of multiple combined non destructive testing in the concrete strenght assessent: applications on laboratory specimens. HSNDT Int. 2007;
[11] Pucinotti R. Reinforced concrete structure: Non destructive in situ strength assessment of concrete. Constr Build Mater. 2015;75:331–341.
[12] Jain A, Kathuria A, Kumar A, et al. Combined use of non-destructive tests for assessment of strength of concrete in structure. Procedia Eng. 2013;54:241–251.
[13] Sbartaï Z-M, Breysse D, Larget M, et al. Combining NDT techniques for improved evaluation of concrete properties. Cem Concr Compos. 2012;34:725–733.
[14] Abed M, de Brito J. Evaluation of high-performance self-compacting concrete using alternative materials and exposed to elevated temperatures by non-destructive testing. J Build Eng. 2020;32:101720.
[15] Helal J, Sofi M, Mendis P. Non-destructive testing of concrete: A review of methods. Electron J Struct Eng. 2015;14:97–105.
[16] Kumavat HR, Chandak NR, Patil IT. Factors Influencing the Performance of Rebound Hammer Used for Non-Destructive Testing of Concrete Members: A Review. Case Stud Constr Mater. 2021;e00491.
[17] Ali-Benyahia K, Sbartaï Z-M, Breysse D, et al. Analysis of the single and combined non-destructive test approaches for on-site concrete strength assessment: General statements based on a real case-study. Case Stud Constr Mater. 2017;6:109–119.
[18] Villain G, Garnier V, Sbartaï ZM, et al. Development of a calibration methodology to improve the on-site non-destructive evaluation of concrete durability indicators. Mater Struct. 2018;51:40.
[19] Gholizadeh S. A review of non-destructive testing methods of composite materials. Procedia Struct Integr. 2016;1:50–57.
[20] Nobile L. Prediction of concrete compressive strength by combined non-destructive methods. Meccanica. 2015;50:411–417.
[21] Karahan Ş, Büyüksaraç A, Işık E. The Relationship Between Concrete Strengths Obtained by Destructive and Non-destructive Methods. Iran J Sci Technol Trans Civ Eng. 2020;1–15.
[22] Singh N, Singh SP. Evaluating the performance of self compacting concretes made with recycled coarse and fine aggregates using non destructive testing techniques. Constr Build Mater. 2018;181:73–84.
[23] Lootens D, Schumacher M, Liard M, et al. Continuous strength measurements of cement pastes and concretes by the ultrasonic wave reflection method. Constr Build Mater. 2020;242:117902.
[24] Khan MI. Evaluation of non-destructive testing of high strength concrete incorporating supplementary cementitious composites. Resour Conserv Recycl. 2012;61:125–129.
[25] Poorarbabi A, Ghasemi M, Moghaddam MA. Concrete compressive strength prediction using non-destructive tests through response surface methodology. Ain Shams Eng J. 2020;
[26] Malek J, Kaouther M. Destructive and non-destructive testing of concrete structures. Jordan J Civ Eng. 2014;8:432–441.
[27] Jedidi M, Abroug A, Moalla B, et al. Non-destructive testing for the diagnosis and repair of a reinforced concrete building. Int J Archit Eng Constr. 2017;6:20–28.
[28] Marić MK, Ivanković AM, Vlašić A, et al. Assessment of reinforcement corrosion and concrete damage on bridges using non-destructive testing. Assessment. 2019;3:2018.
[29] Kumavat HR, Chandak NR, Patil IT. Factors influencing the performance of rebound hammer used for non-destructive testing of concrete members: A review. Case Stud Constr Mater. 2021;14:e00491.

Ref.:
Merah, Ahmed: *The impact of cement type on the correlation between non-destructive testing and the compressive strength of concrete*
Építőanyag – Journal of Silicate Based and Composite Materials, Vol. 75, No. 3 (2023), 109–117. p.
https://doi.org/10.14382/epitoanyag-jsbcm.2023.16

Compressive strength, setting time, and flowability of OPC mortar mixtures modified with a composite of Nano carbon and partially de-aluminated metakaolin

Nabil A. ABDULLAH
PhD. Environmental Science (2005), Ain Shams University. Executive Director of Environment and Research / Development. Aluminum Sulphate Co of Egypt.

Hajer ABDULLAH
Teaching assistant in October University for Modern Science and Arts (MSA university).

Nabil A. ABDULLAH ▪ Research & Development Dept. Manager, Aluminum Sulphate of Egypt ▪ nabilxp9@gmail.com
Hajer ABDULLAH ▪ Civil Engineering Dept., MSA University, Egypt ▪ Hnaabdullah@msa.edu.eg

Érkezett: 2023. 04. 19. ▪ Received: 19. 04. 2023. ▪ https://doi.org/10.14382/epitoanyag-jsbcm.2023.17

Abstract
Nano-black carbon (NC) and partially de-aluminated kaolinitic clay (PDK) composite blend was investigated as an additive to mortar fabrication for improving of the compressive strength. PDK was obtained from aluminum sulphate of Egypt (ASCE). PDK was grounded with nano-carbon. PDK achieved a good pozzolanic activity, it reached 120 %. The experimental protocol included chemical and physical properties of the PDK/Nano-carbon (NCPDK) and the produced mortars. The effect of five weight ratios of NCPDK (0, 5, 10, 15 and 20 %) on the properties of the formed OPC mortars was investigated. Each ratio was tested with three contents of Nano-carbon (1, 2 and 3 %) by weight. The accelerating effect of NCPDK was clear on the initial setting time whereas it reduced by about 31 % and the final setting time reduced by 23 % at 10 % NCPDK. The reduction in the initial flowability of OPC mortar reached 2.7 and 6 % for 10 and 20 % replacement respectively of the OPC by NCPDK and After 60 minutes from mixing, the relative flowability loss was 68 % at 10 % NCPDK and 88 % at 0 % replacement. The compressive strength values of the produced mortars ranged between 46.2 and 50.7 MPa (EN 196-1), with a maximum improvement equal to 14.4 % using 10 % NCPDK. There was no significant change in the pH values of the mortar mixtures. According to the obtained results the composite NCPDK can be used as an additive material in mortar fabrication. The structure of the hardened mortar modified with 10% NCPDK was investigated by XRD, FTIR and TGA that assured formation of more CSH. Incorporation of Nano-carbon enhanced the compressive strength.
Key words: nano-carbon, compressive strength, setting time, flowability, dealuminated kaolin, concrete additive
Kulcsszavak: nano-karbon, nyomószilárdság, kötési idő, folyóképesség, dealuminált kaolin, betonadalék

1. Introduction

Meta-kaolinitic clay (MKC) is the reactive phase resulted from heating of kaolinitic clay (KC) at a temperature range of 500 – 750 °C that deteriorate its crystal structure [1]. MKC reacts with sulfuric acid to produce aluminum sulfate solution which is used in the clarification of water. The extraction of aluminum from meta-kaolinitic clay by acid attacking resulted in increasing the silica to alumina ratio, specific surface and the porosity [2]. The accumulation of siliceous solid waste called partially dealuminated metakaolinite clay (PDK), causes negative environmental impacts due to its fine particulates which are easily spread in the surrounding environment [3].

It was reported that the PDK and calcium hydroxide blends using thermal calorimetric experiments, showed considerable cementitious property [4]. The pozzolanic reactivity of the PDK in prepared blends was also confirmed [5]. This reactivity is relatively higher than that of fumed silica and the initial setting duration increased by addition of the nano carbon (NC) and PDK composite denoted (NCPDK). Different ratios of NCPDK were applied to replace certain portion of the normal cement and its effect on consistency, initial and final setting durations of cement and compressive strength of the mortar after the 7 and 28 day were studied.

The rheological characteristics of fresh mortar determine its workability and flowability. The required water for hydration reactions and the physical properties of the hardened mortar depends on the distribution of cement in water. The particle size distribution and mixing intensity affect the rheological properties of the concrete [6]. By application of additive materials to mortar the mechanical properties of mortar/concrete are upgraded such as compressive strength. Referring to the world interest of getting pure and healthy environment and facing the abnormalities in climatic changes, the work for utilization of new nontraditional materials resulted from different industries as a by-product has become necessary. This will improve the environment quality and reduce the negative impacts of the wastes on the public health.

It was known that the manufacturing of traditional Portland cement is highly energy consuming process and significant measures were taken to get cement alternatives. Pozzolana are

known to substitute partially the normal cement in mortar or concrete mixture because it densifies their matrix by closing the pores as well and this enhance the strength growth [7].

ASTM C595, defined pozzolana as a silicate bearing materials which have no binding effect but when they react with lime at normal conditions forming cementing compounds. The majority of pozzolanic materials are a by-product of industrial processes. They are mainly siliceous materials such as fumed silica, flied ash, slag (granulated blast furnace slag of iron smelters), in addition to calcined clays, all of these materials substitute partially the traditional Portland cement.

PDK is an industrial by-product resulted from aluminum sulphate manufacturing. This by-product is a pozzolana has an environmental impact it consists of high silicate and low aluminum content. The pozzolanicity of this by-product was gained as a result of the dehydroxylation process by thermal treatment which removes the OH groups from the tetrahedral silicate and octahedral aluminate sheets of kaolinitic clay changing it to dewatered clay or metakaolin. The sulphuric acid reacts with the calcinated clay extracted aluminum from the structure leaving low aluminum high silicate content by-product. The thermal and acid attack of metakaolin increased the surface area and the porosity yielding amorphous silica [8]. The Brunauer, Emmett and Teller (BET) values that expressing the specific surface area increased as a result of acid attack causing increase of the pore volume and the chemical and physical reactivity such as adsorption and absorption [7].

Carbon black in its pure form is a fine black powder, essentially composed of elemental carbon [9, 10]. It is produced by partial burning and pyrolysis of low-value oil residues at high temperatures under controlled process conditions [11]. Carbon black is mainly used to strengthen rubber in tires, but can also act as a pigment, UV stabilizer, and conductive or insulating agent in a variety of rubber, plastic, ink and coating applications. Apart from tires, other everyday uses of carbon black include hoses, conveyor belts, plastics, printing inks and automotive coat [12].

This study exploited the pozzolanic properties of PDK mixed with Nano-carbon to be used as an additive to mortar replacing a certain proportion of cement ranged between 5 – 20% for improving the compressive strength and the chemical characteristics of the fabricated mortar. The main constituents of PDK are amorphous silica, alumina, and iron oxide; other impurities are reported such as quartz.

2. Materials and experiment

2.1 CEM II 42.5R (EN 197-1)

CEM II 42.5R (EN 197-1) produced by Suez cement company. *Table 1* show the physical properties cement and *Table 2* illustrates the chemical composition of the OPC used.

The properties	Value		Limits
Specific Gravity	2.63		2.50 – 2.75
Bulk density, (kg/m³)	1780		-
The compressive strength for standard mortar (MPa)	2 days	20.8	Not less than 10
	28 days	50.3	Not less than 42.5
Soundness (La Chatelier)	1		Not more than 1
Setting duration (min.)	Initial	135	Not less than 60
	Final	180	-

**ESS 4756-1/ 2013*

*Table 1 The mechanical and physical properties of CEM II 42.5R **
1. táblázat A CEM II 42.5R mechanikai és fizikai tulajdonságai*

Compound	SiO_2	Al_2O_3	Fe_2O_3	CaO	MgO	SO_3	Na_2O	K_2O	Cl^-	LOI	Total
%	22.31	5.40	3.1	62.7	1.4	1.95	0.18	0.16	0.03	2.40	99.28

Table 2 The chemical composition of Ordinary Portland Cement (OPC)
2. táblázat A hagyományos portlandcement (OPC) kémiai összetétele

2.2 Partially dealuminated kaolinitic clay (PDK)

2.2.1 The chemical and mineralogical analysis of PDK

PDK resulted from the reaction of calcined kaolin with sulphuric acid during the manufacturing of aluminum sulphate. The calcination of kaolin at 700 – 800 °C results in dehydroxylation and formation of amorphous structure (metakaolin) easily attacked by sulphuric acid forming aluminum sulphate and amorphous rich silica called dealuminated metakaolin. The acid attack causes that the silica is present in a disordered and non-bonded structure. The surface area of the PDK is high due to the acid treatment in addition to the amorphous nature of metakaolin.

Compound	Amount (weight %)
SiO_2	81
SiO_2 (amorphous)	58 = 0.97 Molar
Al_2O_3	6.7 = 0.066 M
SiO_2/Al_2O_3	14.7
Fe_2O_3	0.7
TiO_2	3.6
MgO	0.09
CaO	0.15
Na_2O	0.03
K_2O	0.05
SO_3	1.2
P_2O_5	0.01
SrO	0.05
Cl	0.06
L.O.I	4.8
Total	98.44

Table 3 The chemical analysis of the PDK
3. táblázat A PDK kémiai elemzése

PDK was collected from aluminum Sulphate factory. It was dried at 105 °C for 3 hours to remove moisture. The chemical composition based on the XRF shows that most of the alumina in the waste is present as part of the unreacted meta-

kaolin (*Table 3*). The amorphous silica is about 58% (*Fig. 1*). The XRD pattern displayed the silicate morphism in 20 – 25 2θ complying with that reported in reference [13].

PDK was first washed carefully in compact filter press unit and dried at 120 °C for three hours then XRF analyzed using an AXIOS, analytical 2005, Wave length Dispersive (WD–XRF) Sequential Spectrometer. *Table 3* shows high content of reactive SiO_2 it averaged 58%; reactive silica represents the fraction of silica able to react in the normal environment with alkalies. The averaged value of Al_2O_3 in PDK was 6.7%.

PDK was analyzed by XRD analysis using a Burkur D8 Advanced Computerized X–Ray Diffractometer apparatus to show its constituting phases. *Fig. 1* displays that its main crystalline phases are quartz and anatase. The presence of aluminum oxide and sulfur oxide in the XRF analysis (*Table 3*) indicate the presence of traces of amorphous aluminum sulfate compound.

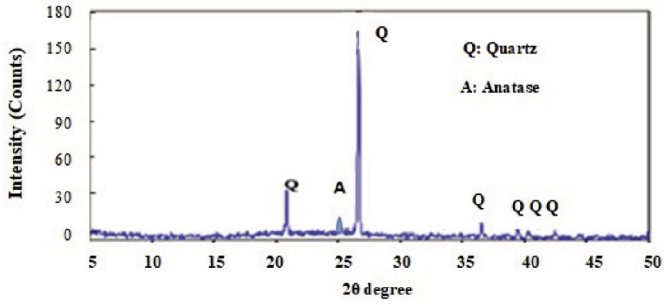

Fig. 1 XRD analysis for PDK
1. ábra A PDK XRD analízise

2.2.2 The grain size-distribution of PDK

The grain size-distribution of the ground PDK by laser granulometry was plotted in *Fig. 2* which shows that the diameter of PDK in cumulative 90% of ~78 μm and 10% of ~ 4.9 μm with an average diameter of ~9.6. BET analysis revealed a high fineness for PDK (20 m^2/g).

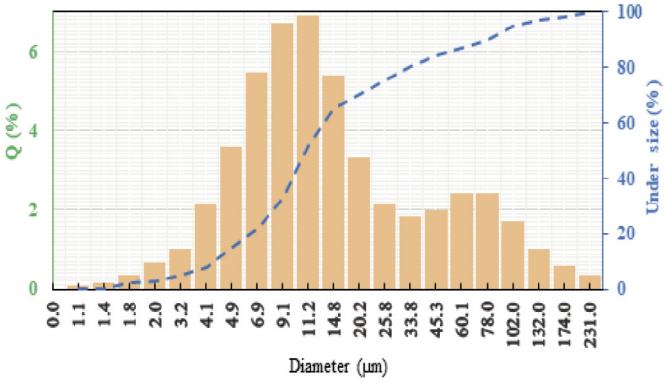

Fig. 2 Grain size distribution of PDK using laser granulometry
2. ábra A PDK lézergranulometriával mért szemcseméret-eloszlása

2.2.3 The pozzolanic testing of PDK

According to ASTM C 618 the pozzolanic materials reacts with portlandite [$Ca(OH)_2$] resulted from the hydration process of OPC and calcium silicate hydrate compound is formed as a cementing material. The pozzolanic reactivity of the samples was determined chemically by mixing of 2 g PDK with 10% lime and 2 drops of water. The free lime of the mixture was measured directly and after 5 days on another sample well covered and stored at 60°C. This chemical method is described in detail elsewhere [14].

Table 4. indicates the pozzolanic activity, specific surface area and the bulk density of PDK. The reactivity test after 5 days recorded 120%.

The parameter	Value
The pozzolanic reactivity	120%
Specific surface area	20 m^2/g
The bulk density	1.35 g/cc

Table 4 The pozzolanic testing of PDK
4. táblázat A PDK puccolán vizsgálata

The surface area was measured by means of BET method which shows the adsorption of nitrogen at liquid nitrogen temperature. The specific density was evaluated using Le Chatelier flask according to ASTM C188-84. The mineralogical composition was monitored by means of X-ray diffraction using an automated diffract meter at a scan range from 10 to 50° (2θ). Positive reaction to pozzolana test (EN 196-4) was given by PDK when blended with CEM I 42.5R. Methylene blue method (UNI EN 933/9) 3.85 g/kg for PDK.

Mixes	NC (g)	PDK (g)	NC/ PDK (%)	NC/OPC (%)	NCPDK / OPC (%)	OPC (%)	Water / binder	Sand / cement
Control 1	0.0	5	0.0	0.0	0.0	100	0.43	2.25
M1	0.0	0.0	0.0	0.0	5	95		
M2	0.05	4.95	1.01	0.0005		95		
M3	0.10	4.90	2.04	0.001	5	95		
M4	0.15	4.85	3.03	0.0015		95		
M5	0.0	10	0.0	0.0	10	90		
M6	0.05	9.95	0.5	0.0005		90		
M7	0.10	9.90	1.01	0.001	10	90		
M8	0.15	9.85	1.52	0.0015		90		
M9	0.0	15	0.0		15	85		
M10	0.05	14.95	0.33	0.0005		85		
M11	0.10	14.90	0.67	0.001	15	85		
M12	0.15	14.85	1.01	0.0015		85		
M13	0.0	20	0.0	0.0	20	80		
M14	0.05	19.95	0.25	0.0005		80		
M15	0.10	19.90	0.50	0.001	20	80		
M16	0.15	19.85	0.76	0.0015		80		

w/b = water/OPC+ weight of NCPDK

Table 5 The mix ratios of mortars ingredients
5. táblázat A habarcs összetevőinek keverési arányai

2.2.4 Thermogravimetry and differential scanning calorimetry of PDK (TG/DSC)

The thermal behavior of the starting PDK is presented in the *Fig. 3*. The main changes revealed by TG and DSC analysis are as follows: The DSC line indicates the removal of absorption

water or free water as demonstrated in the small band at 186.6 °C (water absorbed in pores and on the surface = 1.73%). The thermal degradation occurs between 186.6 and 550 °C is associated with the presence of silicate and the chemical dewatering within the structure. The remaining weight loss at between 550 and 1000 °C can be attributed to more bound water which results from silanol or aluminol. The results show that approximately 6.93% measured over the temperature range of ambient to 988 °C.

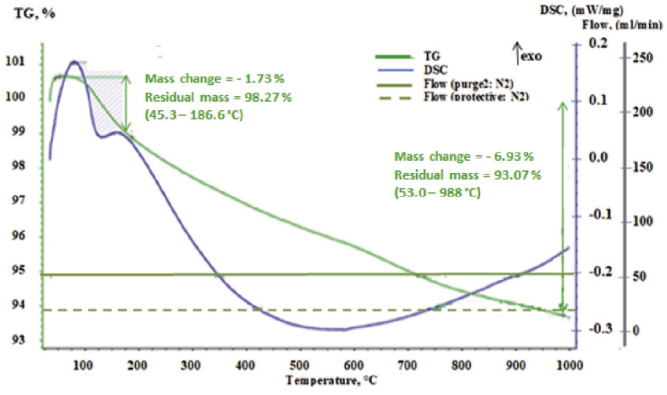

Fig. 3 Thermogravimetry and differential scanning calorimetry of PDK (TG/DSC)
3. ábra A PDK termogravimetriája és differenciális pásztázó kalorimetriája (TG/DSC)

2.3 The fine aggregate

Using sand as a fine aggregate in both mortar and concrete mixtures. Sand tests were carried out according to the standard specifications (EN 1097, EN 933). *Table 6* shows the physical properties of the sand used. *Fig. 4* shows the gradation of sand. The results showed that the specifications of the sand used matched the Egyptian Code for the Design and Implementation of Concrete Structures No. 203 of 2018.

Parameters	The results	The limits ECCS203-2018 Egyptian standard
The specific gravity	2.60	-
The bulk density (ton/m³)	1.60	-
Dust and clay	1.20	Not more than 2.5

Table 6 The physical properties of sand
6. táblázat A homok fizikai tulajdonságai

2.4 Nano carbon

The used Carbon black is a specific kind of the basic carbon which is obtained as colloid particles from incomplete combustion or thermal decomposition of the liquid or gaseous hydrocarbons under controlled conditions. This material can be observed as a fine black powder similar to the materials obtained from the combustion of the hydrocarbons, coal or exhaust soot. Carbon black contains more than 95% of amorphous carbon and a small percentage of oxygen, hydrogen, nitrogen, and others [15, 16].

The addition of nano-carbon black (NC) was made on OPC content weight basis; NC/OPC ratios considered were as follows: 0.0, 0.0005, 0.001 and 0.0015%. The NCPDK mix design/m³ is shown in *Table 5*. The replacement of OPC was made by addition of 5, 10, 15, and 20% NCPDK in cement paste and the mortar mixes. The w/b ratio required to attain the standard consistency of the reference OPC paste was determined using Vicat apparatus according to ASTM C187-92. The initial and final setting times were measured according to ASTM C191-92. The same methods were utilized to investigate the effect of NCPDK on the water demand and the setting behavior of the pastes. The mixing procedures were carried out according to ISO 9597 (1989) and ASTM C305-82.

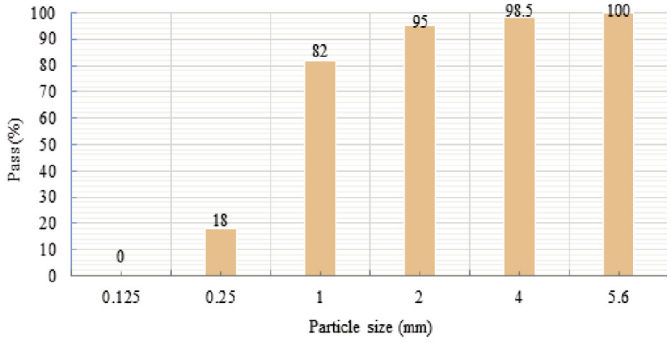

Fig. 4 Graduation of sand
4. ábra A homok szemcsemérete

2.5 The chemical additives

In order to achieve good mixing of the mortar mixtures, a water reducing agent, Master Reobuild 3045, was added, which conforms to ASTM 494 Type G.

2.6 The mixture properties

2.6.1 The pH of mortar slurry

The pH of the mortar slurry was performed as follows by adding 20 g of cement to 100 ml of distilled water (w/b = 5) in glass bottles (ASTM F710-05). The NCPDK was added to the cement as a replacement material with 0, 5, 10, 15 and 20%. The components were mixed manually and the change in the pH- values was recorded by means of a digital pH meter after 0, 30, 60, 90 and 120 minutes.

2.6.2 Flowability testing

The Mortar Flow Table Apparatus (MFTA) was done for determining the flowability and the rate of flowability changing of the OPC and OPC/NCPDK mortars. The MFTA are described in ASTM C230/C230M–14. After mixing; the flowability of the mortar was measured using MFTA, according to the ASTM C109-99. To test the rate of flowability changing during the fresh state of mortar mixes, the flow diameters were determined at different durations from mixing: 0, 30, 60, 90 and 120 min.

The flowability was determined as the ratio between the diameter of the resulting form and that of the original mix:

$$\text{Flowability} = \frac{df - di}{di} \times 100 \quad (1)$$

Where, d_f is the final diameter (mm) and di is the initial diameter (mm).

Casting and compaction of the specimens used in the determination of the compressive and the direct tensile strengths respectively were based on ASTM C109-99. Mixing, casting,

curing, and testing were carried out at normal conditions. The prepared cubic mortars and briquette specimens were covered with plastic for 24 hours, demolded and then immersed in water until testing. The compressive strengths were determined at ages of 7 and 28 days according to ASTM C109-99, the specimens prepared to test the direct tensile strength were tested at the age of 56 days according to ASTM C307-99.

2.6.3 Initial and final setting duration

The initial and final setting tests were done as explained in IS 4031-Part 5. Standard Vicat needle was used in assessing its penetration in a fresh mix. Three specimens were tested each time and the average values were recorded.

2.6.4 Compressive strength testing

The mechanical characteristics of tested mortar specimens fabricated with NCPDK are expressed in compressive strengths**.** According to EN 206, NCPDK can be used as a pozzolanic material. The efficiency of NCPDK as a replacement of portion of OPC has been verified in concrete blends. In all trials the addition were done on dry basis with reference to the sum of cement and additive (c+a).

Superplasticizer was used with an average of 1.6%. The density in the fresh state (EN 12350-6) is 2360 kg/cubic meter; and cubic compressive strength was done according to (EN 12390-3). The samples were immersed in water for 24 hrs, the measurements were done according to the Egyptian specifications ESS 1658-1991.

2.6.5 The mortar mixes preparation and testing

Five mixtures of cement mortar were carried out using five different substitution ratios in the NCPDK mixture of cement to test the compressive strength at the age of seven days for determination of the pozzolanic activity of the mixes, and based on the results, the best substitution ratios were chosen for the test at an age of 28 days. The standard ASTM C1240 was taken into account in determining the basic mixing ratios for cement mortar, where the compressive strength of the mortar was measured at the age of 7 days using the average value of three cubes with dimensions of 70 × 70 × 70 mm using NCPDK mixture substitution ratios of cement (5, 10, 15 and 20% which contain 1, 2 and 3% C for each ratio, respectively) and compared with the control mix that does not contain NCPDK.

2.6.6 Preparing samples and curing

The prepared mortar mixtures were poured into the steel moulds. The mortar mixtures were poured into the moulds in three layers and each layer was compacted using a steel rod. After 24 hours, the mortar specimens were removed from the moulds and cured in water at room temperature until testing.

3. Results and discussion

3.1 The flow of the modified mortars with NCPDK

The initial flowability and the rate of flowabilities loss containing different contents of the NCPDK were tested. The OPC mortar mixes prepared with different ratios of NCPDK were assessed. *Fig. 5* displayed the effect of NCPDK on the flowability of OPC mortars. It is clear from the figure that the incorporation of NCPDK had only a slight effect on the initial flowability of the OPC mortar. The reduction in the initial flowability of OPC mortar reached 2.7 and 6% for 10 and 20% replacement of the OPC by NCPDK. The fineness of PDK and Nano carbon increase the water demand causing reduction of flowability.

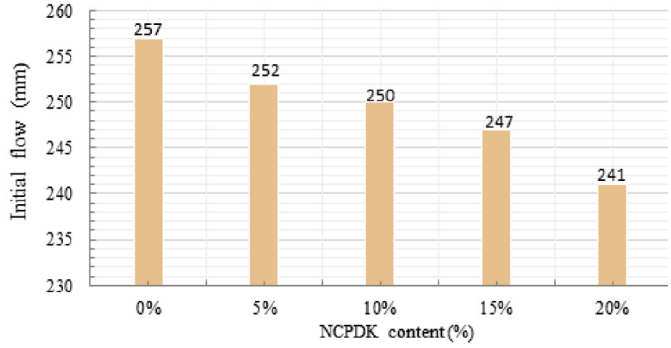

Fig. 5 Flowability of OPC mortar containing different contents of NCPDK
5. ábra Különböző NCPDK-tartalmú OPC habarcsok folyóképessége

The loss rate of flowability of OPC mortar OPC/NCPDK mortars was determined by measuring the instant flowability at different periods of time from mixing namely 0, 30, 60, 90 and 120 min. The relative flowability (instant flowability/ initial flowability) versus time are illustrated in *Fig. 6*. It was found that the relative flowability of the NCPDK modified samples is reducing with increasing time. The flowability loss is decreasing with increasing of as the NCPDK content at a constant time. After 60 minutes from mixing, the relative flowability was 68% at 10% replacement of NCPDK while the OPC mortar was 88 (*Fig. 6*).

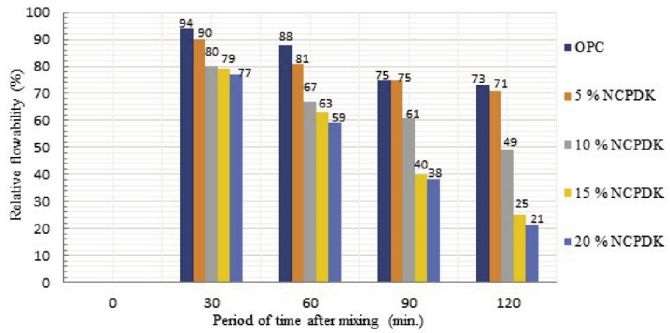

Fig. 6 Flowability loss of OPC mortars containing different contents of NCPDK
6. ábra Különböző NCPDK-tartalmú OPC habarcsok átfolyóképességi vesztesége

3.2 Strength characteristics

The compressive strengths of the twelve mixtures and the control mixture were measured at an age of 7 and 28 days using the average value of three specimens according to the standard specification EN196-1.The mechanical properties of the modified mortar with NCPDK are expressed in terms of compressive and tensile strengths as illustrated in *Fig. 7*. It was found that the compressive strength delayed in the 7 days, but it developed in the 28th day. The 28-days compressive strength of the OPC mortar increases with increasing the replacement ratio of the CPDK in the OPC mix. It achieved a peak value at 10% DK beyond which the compressive strength started to

Design mixes	Cem. (g)	NC/PDK (%)	NCPDK/ OPC (%)	Sand (g)	Flow (mm)	Water (g)	Compressive Strength (MPa)		Increase of compressive strength (%)	Effect of Nano-carbon on compressive strength (%)
							7 days	28 days	28 days	28 days
Control	100	0.0	0.0	225	257	44	36.3	44.3	-	-
M1	95	-	5	225	252	44	34.3	46.2	+4.3	-
M2		1			252		35.4	46.3	+4.5	+0.2
M3	95	2	5	225	252	44	35.6	46.6	+5.2	+0.9
M4		3			252		35.8	46.8	+5.6	+1.3
M5	90	-	-	225	250	44	33.7	50.0	+12.9	-
M6		1		225	250		34.7	50.2	+13.3	+0.4
M7	90	2	10		250	44	35.1	50.5	+14.0	+0.7
M8		3			250		35.8	50.7	+14.4	+1.5
M9	85	-	-	225	247	44	33.6	49.2	+11.0	-
M10		1		225	247		33.5	49.3	+11.3	+0.3
M11	85	2	15		247	44	33.8	49.5	+11.7	+0.7
M12		3			247		34.2	49.7	+12	+1.0
M13	80	-	-	225	241	44	34.0	48.7	+9.9	-
M14		1		225	241		34.2	48.9	+10.3	+0.4
M15	80	2	20		241	44	34.4	49.0	+10.6	+0.7
M16		3			241		35.5	49.2	+11.0	+1.1

Table 7 The mixing ratios and compressive strengths for the mortar mixtures
7. táblázat A habarcskeverékek keverési arányai és nyomószilárdsága

decrease with increasing the NCPDK content. The compressive strength of the OPC mortar specimens made with either 5, 10, 15, and 20% NCPDK (containing 3% of Nano-carbon) are higher than that of pure OPC mortar specimens by about 8.0, 17.0, 15.8 and 4.5%, respectively (*Table 7*, *Fig. 7*). The results show that 3% of Nano-carbon achieved higher strength than 1 and 2%. This behavior attributed to filling concrete pores which causes an increase in the compressive strength. This perfectly lines up with the study conducted by [17].

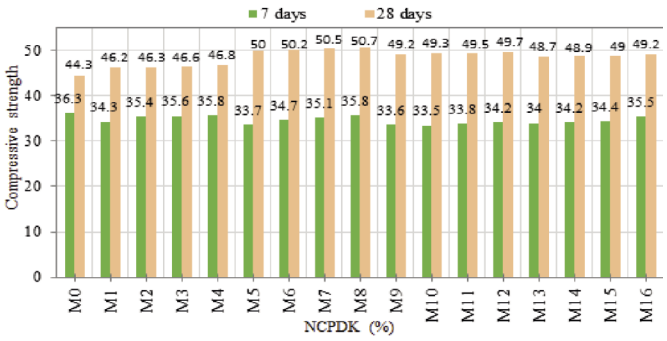

Fig. 7 The compressive strength of cement mortars containing different contents of NCPDK after 7 and 28 days
7. ábra Különböző NCPDK-tartalmú cementhabarcsok nyomószilárdsága 7 és 28 nap után

3.3 The pH change as a result of adding the NCPDK to the cement mixture

As the alkalinity of the mortar medium is of great importance in preserving the mortar from deterioration when the alkalinity decreases below (pH = 11.5), which leads to stresses within the mortar leading to the formation of cracks in it [18]. Therefore, it was necessary to test the effect of replacing a percentage of cement by NCPDK on the pH-value of the cement slurry.

Fig. 8 shows the results of the pH measurements, where a slight decrease in the pH value as a result of the presence of CPDK in the cement mix. It also shows the decrease in alkalinity arising with the increase of NCPDK (15%) due to the presence of a percentage of SO_3 as the pH decreased to 12.4.

Mix No.	OPC (g)	NCPDK (%)	Duration (min)				
			0	30	60	90	120
1	100	0	12.75	12.7	12.64	12.6	12.6
2	95	5	12.7	12.65	12.62	12.6	12.6
3	90	10	12.65	12.62	12.6	12.6	12.6
4	85	15	12.6	12.55	12.5	12.5	12.5
5	80	20	12.54	12.5	12.45	12.42	12.4

Table 8 Effect of NCPDK on the pH values of cement mixes
8. táblázat Az NCPDK hatása a cementkeverékek pH-értékeire

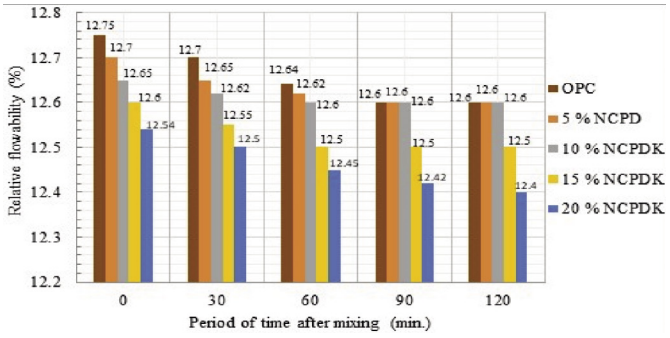

Fig. 8 The pH expressing the alkalinity of the mortar mixtures containing different contents of NCPDK
8. ábra A különböző NCPDK-tartalmú habarcskeverékek lúgosságát kifejező pH-érték

3.4 The paste consistency

Fig. 9 shows the effect of addition of NCPDK on the water/binder ratio (w/b) ratio required for the standard consistency of the replaced OPC. It was found that the w/b ratio increases with increasing the NCPDK ratio.

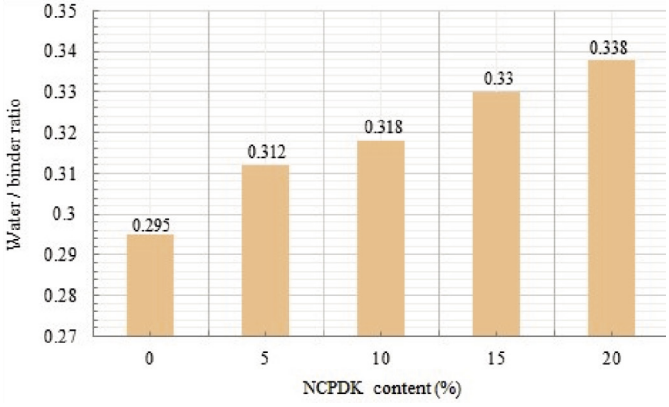

Fig. 9 Effect of NCPDK on the w/b ratio required for standard consistency of OPC pastes
9. ábra Az NCPDK hatása az OPC paszták standard konzisztenciájához szükséges w/b arányra

3.5 Setting duration for the mortar containing NCPDK

The setting time of OPC depends on the phase composition, the concentration of the liquid phase and the pH-value; the amount of alkali and soluble alumina play dominant role in the process. Setting is accelerated by soluble alumina; it is retarded by calcium hydroxide, iron hydroxide, and sulfates. Relative setting delay was noticed due to the presence of Nano carbon particles in NCPDK. *Fig. 10* shows the results of the initial and final setting times of the blends with normal consistency with the NCPDK at different replacement of cement. The setting durations of the fabricated paste without replacement was found to slightly higher than those containing NCPDK and both setting times decrease at higher replacement ratios up to 20%. This means that NCPDK has accelerated the effect especially for the initial setting, i.e. setting time is inversely proportion with the quantity of NCPDK. The initial setting times of the OPC paste without replacement was found to be 122 min. While at replacement ratio of 5% CPDK caused a slight decrease of both setting times and is followed by a steady increase at higher replacement ratios up to 20%. However the reduction of final setting time was referred to the high pozzolana reactivity of NCPDK and high surface areas of NCPDK determined as B.E.T that accelerate hydration of OPC and setting.

The initial setting duration decreased by the added NCPGK, from 118.6 min. at zero addition to 81.7 min at 10%. The final setting duration decreased from 158 min at zero addition down to 121.3 min at 10% addition. Further increasing of NCPDK addition to 15% decrease the initial setting duration to 63.5 min. and the final setting duration to 88.2 min. The accelerating effect of NCPDK was clear on the initial setting time whereas it reduced by about 31% and the final setting time reduced by 23% at the 10% NCPDK. The setting time for the paste fabricated with CPDK/Cement is within the reported range for the normal portland cement mixture (equal or greater than 45 min. and final setting equal or less than 10 hrs.) as recommended by ASTM C 305-82 and ISO 9597(1989).

The pozzolana properties of NCPDK cause increasing of rate and heat of hydration of cement in the fabricated concrete. The specific surface area (BET) active silica and alumina content yield alkali that activates acceleration of hydration process of cement. The addition of NCPDK increases the water requirement due to the fine grained NCPDK. The active hydration, the binding of lime reaction and hydroxide species release heat. The aluminum ions convert to aluminate which react with lime forming hydrated calcium aluminate of weak binding which react with lime sulphate forming ettringite. The presence of lime and active silica hydrated calcium silicate polymer chain. The aluminum content in NCPDK is in the form of metakaolin which has alumina encourage the hydration products and so accelerate hydration and setting duration.

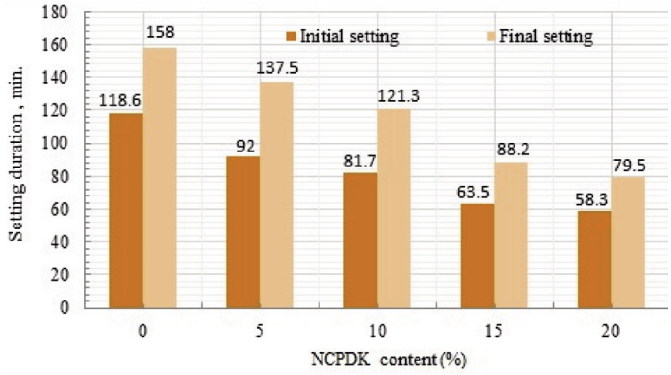

Fig. 10 Effect of NCPDK on the initial and final setting duration of OPC pastes
10. ábra Az NCPDK hatása az OPC paszták kezdeti és végső kötési idejére

3.6 The mineralogical composition of mortar containing 0, 10, 15% of NCPDK

Fig. 11 shows that the XRD for the mixes containing 10 and 15% of NCPDK and the control mix (OPC) after 28 days. It was found that increasing of NCPDK resulted in increasing of calcium silicate hydrate (CSH) and reduction of portlandite ($Ca(OH_2)$).

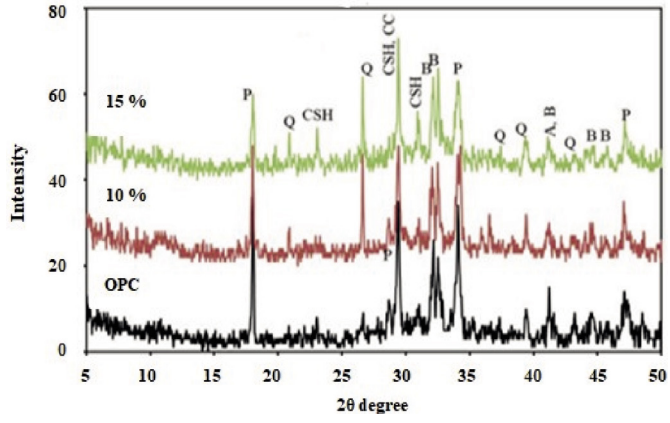

Fig. 11 The XRD analysis for the mortars containing 0, 10, 15% of NCPDK
11. ábra A 0, 10, 15% NCPDK-t tartalmazó habarcsok XRD elemzése

3.7 The thermal properties of cement mixes containing NCPDK (TGA/DTGA)

Fig. 12 shows the appearance of a band before reaching 100 °C it is related to humidity. The thermal absorption band in the thermal range 100 - 200 °C resulting from the presence of hydrated calcium silicate compound. The thermal absorption band in the thermal range 450 - 500°C is due to the removal of the hydroxyl anion of calcium hydroxide. The thermal absorption band at 700°C is due to the formation of calcium carbonate compound as a result of the carbonation of lime with carbon dioxide. It is noted that replacing cement with NCPDK at rates of 5, 10, 15 and 20% increases the formation of CSH compound at the expense of lime. These results are in agreement with previous research studies [19-21].

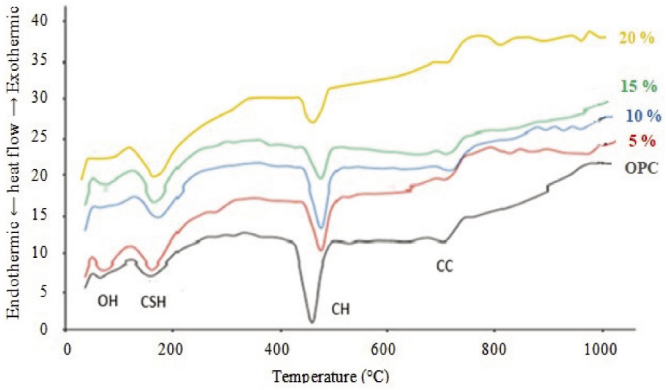

Fig. 12 The thermal analysis of NCPDK-containing cement mixes (TGA/DTA)
12. ábra NCPDK-tartalmú cementkeverékek (TGA/DTA) termikus analízise

3.8 Infrared spectrum analysis (FTIR)

This analysis was carried out to identify the structural state after replacement with NCPDK at 5, 10, 15 and 20% of cement and after 28 days of immersion in water. *Fig. 13* represents the infrared pattern of the reaction products with water after 28 days in the positive range 400-4000 cm^{-1}. The band at 3645 cm^{-1} is due to the tension fluctuation of the OH group of portlandite $Ca(OH)_2$. At 1461 cm^{-1} the band is due to the presence of calcite resulted from the interaction of lime with calcium dioxide. The band in the range 900 - 1000 cm^{-1} indicates the presence of the structure of amorphous calcium silicate. These bands agree with the interpretation of reported in the references [22-24].

The density of the band at 970 cm^{-1} in the aqueous mixtures of NCPDK/OPC increases with increasing of NCPDK up to 15% of the cement. This behavior indicates an increase in the formation of aqueous calcium silicate compound. The density of the band begins to decrease with an increase in NCPDK of more than 15% this is due to the decrease in pozzolanic reactivity.

From the previous experiments conducted on (NCPDK/OPC) mixture, which contains increasing percentages of NCPDK, the manufactured product (5-20% NCPDK/OPC) and after 28 days of curing, to study the behavior of Nano-carbon /partially dealuminated kaolinitic clay as an additive, using DTA /IR shows the following:

NCPDK behaves with cement as a pozzolanic material by interacting with calcium hydroxide resulting from the interaction of cement with water (hydration) forming more (C-S-H) according to the American standard specifications ASTM C618.

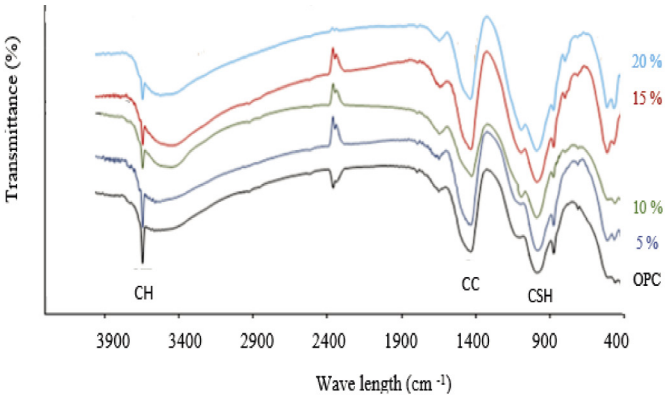

Fig. 13 FTIR analysis of cement mixes containing NCPDK with different substitution ratios
13. ábra Különböző helyettesítési arányú NCPDK-t tartalmazó cementkeverékek FTIR elemzése

Further researches shall be done to investigate the durability of the mortar modified with a composite of Nano-carbon and dealuminated calcined kaolin.

4. Conclusions

- Based on the obtained results it was found that the 10 and 15% replacement ratio of NCPDK achieved 14.4 and 12% respectively improvement in the compressive strength at an age of 28 days compared with the control mix.
- Adding a NC to PDK increased the compressive strength with an average ratio of 1.5% at 10% NCPDK.
- Using of NCPDK with ratios of 5, 10, 15 and 20% resulted in delayed the compressive strength at an age of 7 days compared with the control mix.
- The high surface area of PDK and nano-carbon causes relative reduction of setting duration.
- No significant reduction in the pH of mortar for all mixes.
- The loss rate of flowability Of OPC modified with NCPDK was reported.
- 10% of replacement of OPC with NCPDK is optimum ratio for improving the compressive strength of mortar.

References

[1] Hoda S. Eldin – Nabil, A. Abdullah – Ismail, Mahmoud F. Hashem Ahmed I. (2022) Preparation of meta phase of kaolinite as a precursor for geopolymer adsorbent fabrication, Epitőanyag– Journal of Silicate Based and Composite Materials, Vol. 74, No. 3 pp. 82–87 https://doi.org/10.14382/epitoanyag-jsbcm.2022.13.

[2] Macedo, J.C.D., Mota, C.J.A., Menezes, S.M.C., Camorin, V. (1994) NMR and acidity studies of de-aluminated metakaolin and their correlation with cumene cracking, Appl. Clay Sci. Vol. 8 No. 5 pp. 321-330.

[3] Nabil A. Abdullah, El-Sokkary, T. M. – Gharieb, Mahmoud (2022) Synthesis of geopolymer binder from the partially de-aluminatedmetakaolinite by-product resulted from alum industry, Epitőanyag– Journal of Silicate Based and Composite Materials, Vol. 74, No. 5 pp. 166–174. https://doi.org/10.14382/epitoanyag-jsbcm.2022.25.

[4] Mostafa, N.Y., El-Hemaly, S.A.S., Al-Wakeel, E.I., El-Korashy, S.A., Brown, P.W. (2001), Activity of silica fume and Dealuminated kaolin at different temperatures, Cem. Conc. Res. Vol. 31 pp. 905-911. https://doi.org/10.1016/S0008-8846(00)00485-3.

[5] Mostafa, N.Y., Brown, S.A., (2005) Heat of Hydration of high reactive pozzolana in blended cements: Isothermal conduction calorimetry Termochimica Acta Vol. 435, pp. 162-167. https://doi.org/10.1016/j.tca.2005.05.014

[6] Hela R. and Máršalová, J. (2009) Study of metakaolin influence on rheological properties of cement mortars» Annual Transactions of the Nordic Rheological Society, Vol. 17, pp. 1 – 4.

[7] Aderemi B.O., Edomwonyi O.L. and. Adefila S.S. (2009) A new approach to metakaolin dealumination» Australian Journal of Basic and Applied Sciences, Vol. 3 No. 3, pp. 2243-2245.

[8] Salwa A., Mohamed A., Tantawy A., Abdallah E.M., Qassim M.I. (2015) Characterization and application of kaolinite clay as solid phase extractor for removal of copper ions from environmental water samples" International Journal of Advanced Research, Vol. 3, pp. 1 – 3.

[9] Padma Priya B., Mrs. K. (2016) Pandeeswari Experimental Investigation on the Properties of Concrete with Carbon Black and PET International Journal of Advanced Research, Volume 4, Issue 4, pp. 1082-1088. https://doi.org/10.21474/IJAR01/277

[10] Rezania, M. Panahandeh, S. Razavi and F. Berto (2019) Experimental study of the simultaneous effect of nano-silica and nano-carbon black on permeability and mechanical properties of the concrete Theoretical and Applied Fracture Mechanics. Vol. 104, 102391. https://doi.org/10.1016/j.tafmec.2019.102391

[11] Taylor R. and Carbon Blacks (1997) Production, properties and applications. Ch. 4 in Marsh H, Heintz EA, Rodriguez-Reinoso F, editors. Introduction to Carbon Technologies, University of Alicante, 1997, pp. 167-210.

[12] «Market Study (2013) Carbon Black. Ceresana. Retrieved 2013-04-26.

[13] Ajayi, A.O., Atta, A.Y., Aderemi, B.O. and Adefila, S.S. (2010) Novel method of metakaolin dealumination -preliminary investigation» Journal of Applied Sciences Research, Vol. 6 No.10, pp. 1539-1541.

[14] Javellana, M. P. and Jawed, I. (1982) Extraction of the free lime in Portland Cement and Clinker by Ethylene Glycol, Cement and Concrete Research, Vol. 12, pp. 309-403. https://doi.org/10.1016/0008-8846(82)90088-6

[15] Real, S. and A. Bogas (2017) Oxygen permeability of structural lightweight aggregate concrete, Constr. Build. Mater. 137, 2017, pp. 21–34. https://doi.org/10.1016/j.conbuildmat.2017.01.075

[16] Boğa, A. R. and I.B. Topçu (2012) Influence of fly ash on corrosion resistance and chloride ion permeability of concrete, Constr. Build. Mater. Vol. 31, pp. 258–264. https://doi.org/10.1016/j.conbuildmat.2011.12.106

[17] Monteiro, A. O., P.B. Cachim, and P.M.F.J. Costa (2017) Self-sensing piezoresistive cement composite loaded with carbon black particles, Cem. Concr. Compos. Vol. 81, pp. 59–65. https://doi.org/10.1016/j.cemconcomp.2017.04.009

[18] Gouda, V. K., R. Sh. Mikhail, W.E. Mourad (1974) Hardened portland blast-furnace slag cement pastes: I. Effects of additives on surface area and on pore structure, Cement and Concrete Research, Vol. 4 No. 5, pp. 807-820. https://doi.org/10.1016/0008-8846(74)90052-0

[19] Palomo, A., Blanco-Varela, M.T., Granizo, M.L., Puertas, F., Vazquez, T., and Grutzeck, M.W., (1999) Chemical Stability of Cementitious Materials Based on Metakaolin, Cement and Concrete Research, Vol. 29, pp. 997. http://dx.doi.org/10.1016/S0008-8846(99)00074-5

[20] Mlinarik, L. and Kopecsko, K., (2013) Impact of Metakaolin – A New Supplementary Material- on the Hydration of Cements, ActaTechnica Napocensis: Civil Engineering & Architecture, Vol. 56, pp. 100.

[21] Juenger, M.C.G. and Siddique, R., (2015) Recent Advances in Understanding the Role of Supplementary Cementitious Materials in Concrete, Cement and Concrete Research, Vol. 78, pp. 71. https://doi.org/10.1016/j.cemconres.2015.03.018

[22] Saikia, N.J., Sengupta, P., Gogoi, P.K and Borthakur, P.C., (2002) Cementitious Properties of Metakaolin – Normal Portland Cement Mixture in the Presence of Petroleum Effluent Treatment Plant Sludge" Cement and Concrete Research, Vol. 32, pp. 1717. https://doi.org/10.1016/S0008-8846(02)00865-7

[23] Trezza, M.A. and Lavat, A.E, (2001) Analysis of the System 2 CaO-Al_2O_3-$CaSO_4$. $2H_2O$-$CaCO_3$- H_2O By FTIR Spectroscopy, Cem. Concr. Res., Vol. 31, pp. 869. https://doi.org/10.1016/S0008-8846(01)00502-6

[24] Taylor, M.F.W. (1997) Cement Chemistry 2nd ed., Thomas Telford, London, 190 p. http://dx.doi.org/10.1680/cc.25929

Ref.:
Abdullah, Nabil A. – **Abdullah**, Hajer: *Compressive strength, setting time, and flowability of OPC mortar mixtures modified with a composite of Nano carbon and partially de-aluminated metakaolin* Építőanyag – Journal of Silicate Based and Composite Materials, Vol. 75, No. 3 (2023), 118–126. p. https://doi.org/10.14382/epitoanyag-jsbcm.2023.17

GUIDELINE FOR AUTHORS

The manuscript must contain the followings: title; author's name, workplace, e-mail address; abstract, keywords; main text; acknowledgement (optional)**; references; figures, photos with notes; tables with notes; short biography** (information on the scientific works of the authors).

The full manuscript should not be more than 6 pages including figures, photos and tables. Settings of the word document are: 3 cm margin up and down, 2,5 cm margin left and right. Paper size: A4. Letter size 10 pt, type: Times New Roman. Lines: simple, justified.

TITLE, AUTHOR

The title of the article should be short and objective.

Under the title the name of the author(s), workplace, e-mail address.

If the text originally was a presentation or poster at a conference, it should be marked.

ABSTRACT, KEYWORDS

The abstract is a short summary of the manuscript, about a half page size. The author should give keywords to the text, which are the most important elements of the article.

MAIN TEXT

Contains: materials and experimental procedure (or something similar), results and discussion (or something similar), conclusions.

REFERENCES

References are marked with numbers, e.g. [6], and a bibliography is made by the reference's order. References should be provided together with the DOI if available.

Examples:

Journals:

[6] Mohamed, K. R. – El-Rashidy, Z. M. – Salama, A. A.: In vitro properties of nano-hydroxyapatite/chitosan biocomposites. *Ceramics International.* 37(8), December 2011, pp. 3265–3271, http://doi.org/10.1016/j.ceramint.2011.05.121

Books:

[6] Mehta, P. K. – Monteiro, P. J. M.: Concrete. Microstructure, properties, and materials. *McGraw-Hill*, 2006, 659 p.

FIGURES, TABLES

All drawings, diagrams and photos are figures. The **text should contain references to all figures and tables**. This shows the place of the figure in the text. Please send all the figures in attached files, and not as a part of the text. **All figures and tables should have a title**.

Authors are asked to submit color figures by submission. Black and white figures are suggested to be avoided, however, acceptable.

The figures should be: tiff, jpg or eps files, 300 dpi at least, photos are 600 dpi at least.

BIOGRAPHY

Max. 500 character size professional biography of the author(s).

CHECKING

The editing board checks the articles and informs the authors about suggested modifications. Since the author is responsible for the content of the article, the author is not liable to accept them.

CONTACT

Please send the manuscript in electronic format to the following e-mail address: femgomze@uni-miskolc.hu and epitoanyag@szte.org.hu or by post: Scientific Society of the Silicate Industry, Budapest, Bécsi út 122–124., H-1034, HUNGARY

We kindly ask the authors to give their e-mail address and phone number on behalf of the quick conciliation.

Építőanyag – *Journal of Silicate Based and Composite Materials*, Quarterly peer-reviewed periodical of the Hungarian Scientific Society of the Silicate Industry, SZTE.
http://epitoanyag.org.hu